T.R.
ONDOKUZ MAYIS UNIVERSITY
INSTITUTE OF GRADUATE STUDIES
DEPARTMENT OF NANOSCIENCE AND NANOTECHNOLOGY

BIOCOMPATIBLE POLYMER COATING WITH HERBAL EXTRACTS ON DENTAL METALLIC MATERIALS

Ph.D. Thesis

Arife Kübra YONTAR

Supervisor

Assist. Prof. Dr. Sinem ÇEVİK

SAMSUN
2023

T.R.
ONDOKUZ MAYIS UNIVERSITY
INSTITUTE OF GRADUATE STUDIES
DEPARTMENT OF NANOSCIENCE AND NANOTECHNOLOGY

BIOCOMPATIBLE POLYMER COATING WITH HERBAL EXTRACTS ON DENTAL METALLIC MATERIALS

Ph.D. Thesis

Arife Kübra YONTAR

Supervisor

Assist. Prof. Dr. Sinem ÇEVİK

This thesis was supported by Ondokuz Mayıs University with project number PYO.MUH.1908.21.001, PYO.MUH.1908.22.024 and PYO.MUH.1904.22.028.

SAMSUN
2023

DECLARATION OF COMPLIANCE WITH SCIENTIFIC ETHIC

I hereby declare and undertake that I complied with scientific ethics and academic rules in all stages of my Ph. D. Thesis , that I have referred to each quotation that I use directly or indirectly in the study and that the works I have used consist of those shown in the sources, that it was written in accordance with the institute writing guide and that the situations stated in the article 3, section 9 of the Regulation for TÜBİTAK Research and Publication Ethics Board were not violated.

Is Ethics Committee Necessary?

Yes ☐

No ☒

08/06/2023
Arife Kübra YONTAR

DECLARATION OF THE THESIS STUDY ORIGINALITY REPORT

Thesis Title: BIOCOMPATIBLE POLYMER COATING WITH HERBAL EXTRACTS ON DENTAL METALLIC MATERIALS

As a result of the originality report taken by me from the plagiarism detection program on 18/04/2023 for the thesis titled above;

Similarity ratio : % 6

Single resource rate : % 1 has been released.

08/06/2023
Assistant Prof. Dr. Sinem ÇEVİK

ÖZET

DENTAL METALİK MALZEMELERİN BİTKİ ÖZÜTÜ KATKILI BİYO UYUMLU POLİMERLER İLE KAPLANMASI

Arife Kübra YONTAR
Ondokuz Mayıs Üniversitesi
Lisansütü Eğitim Enstitüsü
Nanobilim ve Nanoteknoloji Anabilim Dalı
Doktora, Haziran, 2023
Danışman: Dr. Öğr. Üyesi Sinem ÇEVİK

Bu çalışma, diş hekimliğinde kullanılan metalik biyomateryallerin bitki özleri içeren polimer materyallerle kaplanması için tasarlanmıştır. Yeşil sentezlenmiş nanopartiküller, bitki özleri ve Polivinil Alkol (PVA) ile üretilen mikrometre ölçeğindeki kaplamaları oluşturmak için düşük maliyetli ve pratik bir yöntem olan elektrosprey biriktirme (ESD) tekniği kullanıldı. Kenevir tohumu, Sarı Kantaron, Biberiye ve Kiraz Defne Yaprağı ekstraktları kullanılarak üretilen nanoparçacıkların ve polimer kompozit kaplama malzemelerinin özellikleri araştırılmış ve farklı konsantrasyonlar ve bitki grupları ile karşılaştırılmıştır. Üretim tekniğinin ve başlangıç bileşiminin nanokompozit kaplamaların morfolojisi, termal, mekanik ve kimyasal davranışları üzerindeki etkileri araştırılmış ve tartışılmıştır.

Taramalı Elektron Mikroskobu (SEM) analizi, yeşil sentezlenmiş nano gümüşlerin homojen bir boyut ve dağılımla ortalama 34 nm boyutunda üretildiğini göstermiştir. Dinamik mekanik analiz, %0,3(D) ve %0,5(E) nano gümüş modifikasyonu ile üretilen numunelerin kaplama sonrası termal ve mekanik dayanımı en yüksek numuneler olduğunu göstermiştir. Antibakteriyel testler, nano gümüş katkılı tüm kaplamaların bakteri üremesini 100 kata kadar azalttığını ve en yüksek antibakteriyel etkiye sahip numunenin %0,5 nano gümüş modifiye E numunesi olduğunu ortaya koydu. Kaplama mekanik özelliklerini belirlemek için uygulanan çizilme testi, kaplama yüzeyleri içerisinde en sert numunelerin %0,1(C), %0,3(D) ve %0,5(E) olduğunu göstermiştir. Ayrıca bitki ekstraktlarının PVA'ya modifikasyonu ile kaplamaların mekanik dayanımlarının saf kaplamalara göre en az 2 kat arttığı tespit edilmiştir. Nano gümüş modifiyeli C, D ve E numunelerinin 37 °C sudaki kimyasal ve mekanik stabilitelerinin diğer numunelere göre daha yüksek olduğu belirlendi. Toksisite testleri, kaplamalarda 62 µg/mL ve altındaki konsantrasyonların kullanılmasıyla yeşil sentezlenen nano gümüşlerin HaCaT canlı hücreleri ve A549 akciğer kanseri hücreleri üzerinde toksik etki göstermediğini doğruladı.

Bu çalışma, sağlık alanında bitki özleri ve nano-gümüş modifiye polimer nanokompozit kaplama uygulamalarının araştırılması için bir çerçeve sunmuştur. Elde edilen ampirik bulgular ışığında bu çalışma, bitki özleri kullanılarak metalik biyomalzemelerin antibakteriyel ve biyouyumlu üretimi için yeni bir anlayış sunmaktadır. Ayrıca, düşük hammadde ve üretim maliyetli, kolay üretilebilir, insan sağlığı ve çevreye dost üretim yöntemiyle denklerine kıyasla yüksek termomekanik dayanıma ve düşük toksik etkiye sahip olmaları sayesinde bu biyokompozit malzemelerin bilimsel ve biyomedikal çevreler için geniş bir kullanım alanına sahip olacağı düşünülmektedir.

Anahtar Kelimeler: Biyomalzeme, yeşil sentez, bitki özleri, elektrospray biriktirme, nanokompozit film, nano gümüş.

ABSTRACT

BIOCOMPATIBLE POLYMER COATING WITH HERBAL EXTRACTS ON DENTAL METALLIC MATERIALS

Arife Kübra YONTAR
Ondokuz Mayıs University
Institute of Graduate Studies
Department of Nanoscience and Nanotechnology
Ph.D., June 2023
Supervisor: Assist. Prof. Dr. Sinem ÇEVİK

The present study was designed to applicate the coating of metallic biomaterials used in dentistry with polymer materials containing plant extracts. The electrospray deposition (ESD) technique, which is a low-cost and practical method, was used to form micrometer-scale coatings produced with nanoparticles produced by green synthesis, plant extracts, and Polyvinyl Alcohol (PVA). The properties of nanoparticles and polymer composite coating materials produced using Hemp seeds, St. John's Wort, Rosemary and Cherry Laurel Leaf extracts were investigated and compared with different concentrations and plant groups. The effects of fabrication technique and initial composition on the morphology, thermal, mechanical, and chemical behavior of nanocomposite coatings are investigated and discussed.

Scanning Electron Microscope (SEM) analysis showed that green synthesized nanosilver was produced with an average size of 34 nm and homogeneous size and distribution. Dynamic mechanical analyses showed that the samples produced with 0.3% (D) and 0.5% (E) nanosilver modifications were the ones with the highest thermal and mechanical strength after coating. Antibacterial tests revealed that all nanosilver-added coatings reduced bacterial growth up to 100 times, and the sample with the highest antibacterial effect was the 0.5% nanosilver-modified E sample. The scratch test applied to determine the coating's mechanical properties showed that the hardest samples among the coating surfaces were 0.1% (C), 0.3% (D), and 0.5% (E). In addition, it was determined that the mechanical strength of the coatings increased at least two times with the modification of plant extracts to PVA compared to the pure coatings. It was determined that the chemical and mechanical stability of nanosilver-modified C, D, and E samples in water at 37 °C were higher than the other samples. Toxicity tests confirmed that the green synthesized nanosilver did not show toxic effects on HaCaT live cells and A549 lung cancer cells with concentrations at 62 µg/mL and below in coatings. The present study has offered a framework for the exploration of plant extracts and nano-silver-modified polymer nanocomposite coating applications in the health field.

This study provided a framework for investigating plant extracts and nano-silver-modified polymer nanocomposite coating applications in the healthcare field. In light of the empirical findings obtained, this study offers a new understanding of the antibacterial and biocompatible production of metallic biomaterials using plant extracts. In addition, it is thought that these biocomposite materials will have a wide range of uses in scientific and biomedical environments thanks to their low raw material and production costs, easy production, human health-friendly and environmentally friendly production methods, high thermomechanical strength, and low toxic effect compared to their equivalents.

Keywords: Biomaterials, green synthesis, plant extracts, electrospray deposition, nanocomposite film, nanosilver.

ACKNOWLEDGMENTS

A special thanks to my esteemed advisor and friend Asst.Prof. Dr. Sinem ÇEVİK, who always provided me with her knowledge, experience, and unending support at every stage of my doctoral studies, whose ideas and opinions I highly value, and from whom I learned a lot not only about academia but also about life.

I would like to thank my thesis monitoring committee members, Prof. Dr. Engin BURGAZ and Asst.Prof. Dr. Emrah DÖLEKÇEKİÇ, for their guidance and support.

I would like to thank my colleagues Asst.Prof. Dr. Suna AVCIOĞLU, Asst.Prof. Dr. Tuğba MUTUK, Dr. Mehmet KURU, PhD., and Assoc.Prof.Dr. Mevlüt GÜRBÜZ who assisted me with my experimental studies, as well as all of my friends for their encouragement.

I'm also grateful for the financial support from the Ondokuz Mayıs University under the contract numbers of PYO.MUH.1908.21.001, PYO.MUH.1908.22.024 and PYO.MUH.1904.22.028.

I would like to express my endless love and gratitude to all my family members, especially my dear, my beloved husband Asst. Prof. Dr. Onur YONTAR, who has never spared me their love and support and also who assisted me with my experimental studies.

Arife Kübra YONTAR

CONTENTS

SYMBOLS AND ABBREVIATIONS

t	: Time
T	: Temperature
XRD	: X-Ray Diffractometer
SEM	: Scanning Electron Microscopy
EDS	: Energy Dispersive X-Ray Spectroscopy
DSC	: Differential Scanning Calorimetry
FT-IR	: Fourier Transform-Infrared
MTT	: Metiltiazoledfenil-tetrazolyum bromür
PVA	: Polyvinyl Alcohol
ESD	: Electrospray Deposition
AgNPs	: Silver Nanoparticles
DMA	: Dynamic Mechanical Analysis
AFM	: Atomic Force Microscopy
Ti	: Titanium
V	: Vanadium
Al	: Aluminium
mL	: Milliliter

FIGURES LEGENDS

TABLES LEGENDS

1. INTRODUCTION

Metals are widely used in biomaterial manufacturing because of their superior mechanical strength and corrosion-resistant properties (Neoh and Kang, 2011). Prosthetic components, including abutment screws, cylinders, abutments, prosthetic screws, clasps, and various attachments are all made of metallic materials. Gold, chromium-cobalt alloys, stainless steel, zirconium, commercially pure titanium, tantalum and titanium alloys are the most commonly used metallic materials in dentistry (Sykaras et al., 2000). Among the metals mentioned, titanium and its alloys are the most commonly used metallic materials in the manufacture of implants due to their superior properties. Infection and unsuccessful osseointegration may occur as a result of the excess of toxic contents used in the production of metallic nanoparticles added to give antibacterial properties to metallic materials used in the health field and the failure of metallic parts to exhibit sufficient biocompatibility properties. The coating is the addition of material/agent of various thicknesses superficially on the surface of core material and a type of surface treatment of dental implants. The coating techniques contribute to important positive effects of dental implant application (Jemat et al., 2015). Polymer coatings continue to be used in evermore increasingly diverse applications and sectors. With the polymer coating, the material can gain different properties from the original properties in the field of biomedicine, such properties include wear resistance, improved mechanical strength, corrosion protection, enhanced biocompatibility, electrical conductivity and tailored surface chemistry (Smith and Lamprou, 2014). Various types of polymer coatings are used to make the implants antibacterial, show high corrosion resistance and improve osseointegration. Multiple biological, synthetic and hybrid polymers are used for multiple medical applications. One of the most important and simple methods used in coating applications of metallic biomaterials is the electrospray deposition method (ESD). ESD is an effective technique for producing submicron size miniature droplets by applying an electric field to the metal substrate surface. The resulting droplets then wing towards the counter electrodes or the collector connected to the ground and accumulate on the metal substrate. It is also applied to prepare thin polymeric nanomaterials through encapsulation and other carrier-mediated systems (Kurakula and Raghavendra Naveen 2021). With the electrospray deposition method, many different types of coating materials can be coated on metallic substrates (Buga et al.

2021; Buga et al. 2019; Levana et al. 2022; Pei et al. 2021). With this method, antibacterial and biocompatible coatings of metallic implants can be realized (Chen et al. 2023).

The increase in toxic components used in the world and the decrease in raw materials have increased the orientation towards green energy and production methods and products with clean content (Sudha et al. 2020; Reinhold 2007; Sealy 2020; Zhang et al. 2022). It is of great importance to reduce toxic substances used in the fields of energy, health, food, cosmetics and construction and in the production of products, and to increase natural products and energy. For this reason, more natural products have started to be produced for many different areas, especially by using plants (He et al. 2019; Tan et al. 2022; Ahmad and Mirza 2017). These areas include applications such as nanoparticle production by green synthesis, energy generation, adhesive plasters and coatings for health, cosmetics and food packaging. Studies on the synthesis of metallic nanoparticles with plant extracts have recently increased (Anchan et al. 2019; Angel Ezhilarasi et al. 2018; Arularasu et al. 2018; Bibi et al. 2019; Shume et al. 2020; Li et al. 2019b; Eskandari Azar et al. 2020; Hairom et al. 2015).

The methods used in the production of nanoparticles in which harmful chemicals and high energy are used such as chemical and physical vapour deposition, flame pyrolysis, sol-gel process, thermal plasma synthesis, inert gas condensation and laser prolysis (Brayner et al. 2013). As an indicator of a new era, green synthesis approaches/ methods have become one of the current R&D topics in materials science and nanotechnology. Green synthesis has got lots of advantages (Gour and Jain 2019). There are many physical and chemical synthesis approaches (Oza et al. 2020; Thompson et al. 2020; Shin et al. 2022). These have a negative impact on both humans and marine life. In contrast, the green synthesis of metallic nanoparticles is a one-step, environmentally friendly bio-reduction method (Jadoun et al. 2021; Ostovan et al. 2018). Also, relatively low energy is required to initiate the reaction. This method also provides an extra advantage with its low cost (Dikshit et al. 2021). Plant extracts provide the green synthesis of nanoparticles with various hydroxyl group (OH) (carboxy, hydroxy, ortho-dihydroxy, amino-, catechol) biomolecules (Ahmad, 2017; Anchan et al., 2019b). Biomolecules such as terpenoids, phenolic acids, amino acids, alkaloids, flavonoids, polyphenols, enzymes, tannins, carbohydrates, phenols, saponins, or proteins in plant extracts stabilize and reduce metal ions (M^{+}) to (M^{0}).

These secondary metabolites generally work as both reductants and stabilizers. Thus, they prevent the aggregation of the synthesized metallic NPs. Bioreduction of metal NPs from plant extracts occurs in 3 stages. The first stage involves reduction and nucleation of metal ions. In the second stage, small nuclei are brought together by increasing the thermodynamic stability of NPs. Finally, after the growth phase, NPs form their own shape. As a result of reduction of metal ions with active metabolites, NPs are centrifuged and collected from the solution as precipitate. Concentrations of plant extracts, pH of solutions, temperature, pressure, metallic ion concentration and amount of light are important factors that determine the sizes, distributions and amounts of green synthesized nanoparticles. (Amini and Akbari, 2019; Bassie Gelaw et al., 2021; Csakvari et al., 2021; Martínez-Cabanas et al., 2021). Alharbi et al., (2022) explained in their study that the (OH) groups from plant extracts are bonded with carbon atoms in aromatic rings and this reaction provides the reduction of metal nanoparticles. In this way, nanoparticles with less threat to the more minor environment and human health can be produced without using toxic chemicals and at a lower cost (Chand et al., 2020; Khan et al., 2020; Mali et al., 2020; Yontar et al., 2022). The usage areas of these nanoparticles are quite wide and one of them is the production of antibacterial materials. In general, silver is the most widely used antimicrobial metal due to its broad spectrum anti-pathogen activity. AgNPs can kill more than 650 types of pathogenic microbes such as bacteria, fungi and viruses. Silver nanoparticles (AgNPs) act by multiple mechanisms that include oxidative stress induction, metal ion release, and non-oxidative processes. The gradual release of free silver ions from the AgNPs solution inhibits the proliferation of bacterial cells. The bacteria-killing mechanism of nano silver is explained by the electrostatic interaction between bacterial cells (-) and silver ions (+), due to the rupture of the cell wall, leaking of the inner cell contents and eventual death of the bacteria (Park et al. 2021). In addition, plant extracts have positive effects on health with the minerals of elements such as K, P, Mn and Ca. It is known that the harmful effects of polymer materials used in the production of band-aids, coatings, packaging and biomaterials, which have been produced recently, on health and the environment are tried to be reduced (Abhilash et al., 2019; Jain et al., 2020; Koe et al., 2020; Narayan, 2010; Zare et al., 2019; Yontar and Çevik, 2023). The plant extracts used in the study were obtained from Hemp seeds, St. John's Wort, Rosemary and Cherry Laurel plants that are rich in many minerals, have benefits for human health, are very easy to grow and are

renewable. Apart from this, cost-effective–production and reduction of energy consumption are also important issues in order to protect environment. In this direction, one of the materials experiencing a growing use in the mentioned areas, is Polyvinyl Alcohol (PVA). The reason for this can be shown as features such as being economical, biocompatibility, easy production, not harming the environment and human health and not showing toxicity (Pervez et al., 2020; Sharmin et al., 2020). The studies on PVA are still in continue because apart from being biocompatible and harmless to the environment, it has superior properties with the added ingredients. This improves the properties of nanocomposites based on PVA.

In the thesis study, coating of dental metallic materials with plant extract modified Polivinil Alcohol (PVA) nanocomposite thin films was carried out using electrospray deposition (ESD) method. For the production and characterization of the coating material, polymer nanocomposite thin films were produced and developed using the solvent casting method. Nano silver, which is used in the production of these films and provides antibacterial properties and mechanical strength to the coating, was produced by the green synthesis method. The microstructural characterization and chemical mapping of samples were observed by a Scanning Electron Microscope (SEM) with an Energy Dispersive X-Ray Spectroscopy (EDS) attachment. X-Ray Diffractometer (XRD) analyzes of the films prepared in all compositions and contents determined for coating applications were carried out separately and the presence of silver nanoparticles was investigated. To characterize the influence of plant extracts and silver nanoparticles on the chemical structure PVA matrix, Fourier Transform-Infrared (FT-IR) analysis was performed. Dynamic mechanical analysis (DMA) and Shore-D hardness tests were performed to investigate the mechanical properties of coating films. Finally, bacteria killing effects were determined using antibacterial test methods. The surface characterizations after coating were performed with (SEM) and (EDS) analysis. Also AFM analyses were conducted to evaluate the surface topography of the selected coated subtrates and analysize the surface roughness by atomic force microscopy. The mechanical strength of the coatings was determined by the Scratch Test. The aqueous and high temperature performance tests of the coatings were carried out in the incubator. In addition, toxicity tests of nano silvers produced by green synthesis were also carried out.

2.LITERATURE RESEARCH

2.1. Titanium and Its Alloys as Dental Metallic Material

Metallic biomaterials are engineered systems designed to provide internal support to biological tissues. They are being used highly in joint replacements, dental implants, orthopaedic fixations and stents (Prasad et al. 2015). Many of the metals and alloys (gold, stainless steel, cobalt-chromium) are use as dental materials. Titanium and its alloys have become popular for endosseous parts of currently available dental implants. Prosthetic components, including abutment screws, abutments, cylinders, prosthetic screws, and various attachments, are still made from gold alloys, stainless steel, and cobalt-chromium and nickel-chromium alloys (Sykaras et al. 2000). Titanium was discovered in 1798 by the Reverend William Gregor. It is almost the ninth most abundant element in the lithosphere, as it is a component of all crystalline rocks. Titanium is extremely difficult to produce pure titanium due to its high reactivity, so it was not more widely used until the second half of the twentieth century (van Noort 1987). Depending on their microstructure, titanium alloys are divided into 4 groups as a alloys, alloys close to a, a-b alloys and b alloys. Titanium is superior to stainless steels and cobalt-chromium alloys in terms of specific strength, but lower in terms of tribological properties. As biomaterials, the use of titanium and its alloys is higher as they have comparatively lower modulus, superior biocompatibility and improved corrosion resistance (Chen and Thouas 2015).

The most interested forms of titanium are commercially pure form of titanium (Ti-160) and Ti-6% Al-4% Va (Ti-318). Commercially pure titanium is an alloy of titanium and oxygen. This alloy has a close packed hexagonal structure. When aluminium and vanadium are added to titanium in only small quantities the strength of the alloy increased over that of commercially pure titanium. Ti-6% A1-4% V has a two phase structure of alpha (aluminium) and beta (vanadium) grains (van Noort 1987). In dentistry devices fitanium and its alloys are generally used such as implants, crowns, bridges, overdentures, and dental implant prosthesis components. Commercially pure titanium is used preferentially for endosseous dental implant applications (Elias et al. 2008). The types of dental implants produced from titanium alloys are shown in Figure 2.1.

Figure 0.1 Different types of titanium dental implants (Elias et al. 2008).

Al and V released from Ti–6Al–4V alloy are both of them found to be linked to long-term health problems, such as Alzheimer's disease, other neuropathies and osteomalacia (Nag et al, 2005). Ti–6Al–7Nb and Ti–5Al–2.5Fe alloys have therefore been developed for vanadium-free applications. Both alloy are metallurgically similar to Ti–6Al–4V. For femoral prosthesis stems, fracture fixation plates, spinal components, nails, rods, fasteners, screws and wires Ti–6Al–7Nb alloy has been used. Because of Ti–5Al–2.5V has excellent cold formability and tensile properties, it is used mainly for tubing and intramedullary nails (Chen and Thouas 2015). Comparison of α, near α, α–β and β titanium alloys properties and applications shown in Table 2.1.

Table 0.1 Comparison of α, near α, α–β and β titanium alloys (Chen and Thouas 2015).

Ti-alloys	Advantages	Disadvantages	Medical applications
CP-Ti	1. High corrosion resistance 2. Excellent biocompatibility 3. High weldability	1.Cannot be significantly strengthened by heat treatment 2. Poor forgeability especially below β transus due to HCP structure 3. Having a narrow forging temperature range 4. Low strength at ambient temperature	For non-load-bearing, corrosion resistant applications: e.g. 1. Pace-maker case 2. Housings for ventricular-assist devices 3. Implantable fusion drug pump 4. Dental implants 5. Maxillofacial and craniofacial implants 6. Screws and staple for spinal surgery
α or near α microstructure	As above	As above	Not yet
α–β microstructure	1. Can be strengthened by heat treatment		Ti–6Al–4V and Ti–6Al–4V ELI 1. Total joint replacement arthroplasty (hips and knees). Ti–6Al–7Nb 2. Femoral hip stems 3. Fracture fixation plates 4. Spinal components 5. Fasteners, nails, rods, screws, and wires Ti–3Al–2.5V Tubing and intramedullary nails
β microstructure	1. High hardenability 2. Good ductility and toughness, excellent forgeability and good cold rolling capability (formability) at the solution-treated condition 3. Good fractural toughness	1. High density 2. Low creep strength 3. Low tensile ductility in the aged state 4. Low resistance to wearing	

2.2. Osseointegration And Biocompatibility

Osseointegration is a direct structural and functional connection between ordered, living bone and the surface of a load-bearing implant (Listgarten et al. 1991). Because the fragment ends become united by bone without intermediate fibrous tissue or fibrocartilage formation osseointegration can be compared with direct fracture healing (Schenk and Buser 1998). The various stages of osseointegration process are shown diagramatically in Figure 2.2 and can be listed as follows:

Stage 1: Once the implant is placed in living tissue, it is not fully compatible with the bone. The grooves on the implant surface allow the bone to grow inward, thus allowing the implant to attach to the bone. There is hematoma in the recesses of the screw threads and bone layer damaged as a result of thermal and mechanical trauma during the operation.

Stage 2: During healing the haematoma is gradually transformed into new bone and the damaged bone also heals by a process of revascularization and deand re-mineralization.

Stage 2: During healing the haematoma is gradually transformed into new bone and the damaged bone also heals by a process of revascularization and deand re-mineralization.

Stage 3: When the healing has completed, new bone is in virtual direct contact with the implant without any intermediate layer of fibrous tissue (Brånemark 1983).

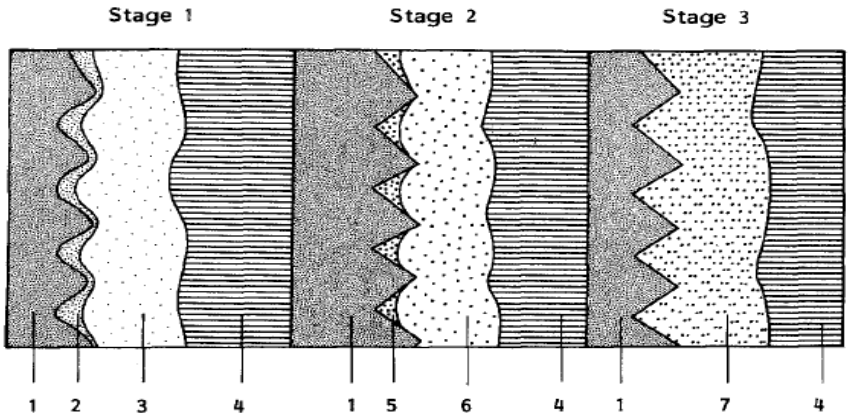

Figure 0.2 Representation of the process of osseointegration adapted where the numbers denote (1) Titanium implant, (2) Haematoma, (3) Damaged bone, (4) Healthy bone, (5) Haematoma transforming into new bone, (6) Damaged bone healing itself by de- and re-mineralization, (7) New healthy bone (Brånemark 1983).

For an implant to integrate well with the surrounding bone, it is essential that it has a biocompatible surface. Surface chemistry, surface topography, surface roughness are important factors to consider for good osseo-integration. Surface modification of implants is one of the most common strategies to enhance surface biocompatibility (Chen and Thouas 2015). Addition of surface roughness and porosity stimulates cell attachment and osseointegration. Traditional methods range from sandblasting to acid etching to laser ablation. For instance, sandblasting of titanium with large grit acid can be used to create roughness over the implant surface, providing micro-level topography for growth and attachment of cells (Prasad et al. 2015).

Metals may be widely distribute when entered the body. The distribution of a metallic element is critical since they have ability to cause systemic toxicity. When elements in the alloy ionize corrosion of alloys occurs. Thus, the elements that are initially uncharged inside the alloy lose electrons and become positively charged ions as they are released into solution. Corrosion is a chemical process that has unfavorable consequences for other alloy properties, such as esthetics, strength, and biocompatibility. It is important to understand the interaction between the biomaterialand the biological system, to understand biocompatibility. These interactions are usually seen on a molecular level in an interface zone of about 1 nm (Prasad et al. 2015). Biocompatibility of an alloy importantly depends on corrosion because the release of elements from the alloy is nearly always necessary for adverse biologic effects such as toxicity, allergy, or mutagenicity (Wataha 2000).

Bioinert or bioactive materials can achieve osseointegration as long as certain guidelines are respected. Commercially pure titanium is recognized today as a biomaterial of choice, since it is not only characterized by excellent biological properties but also good has goog mechanical properties (Schenk and Buser 1998). Titanium and its alloys have a proven quality as biomedical implants due to their excellent biocompatibility. This is related to the presence of an oxide layer that is typically present on the surface of the material in an oxidising environment. As much as commericial pure titanium and Ti6AI4V have a number of advantages, they have some disadvantages as far as implant applications are concerned in that they both have low wear resistance properties. Since the vanadium contained in the Ti-64 alloy is cytotoxic this alloy is limited to certain appropriate applications and devices. New titanium alloy compositions have been developed for biomedical applications. The

first generation of these biomedical implant alloys have included Ti-6Al-7Nb and Ti-5Al-2.5Fe, two alloys with properties similar to Ti6AI4V that were developed to address concerns relating vanadium's cytotoxicity (Sidambe 2014).

2.3. Surface Modification Methods Of Biometals

A biomaterial is a non-viable material used in medical devices intended to interact with biological systems in order to evaluate, treat, augment or replace any tissue, organ or function of the body in their original form. There are numerous metallic biomaterials that can be used in the human body, such as stainless steel, cobalt alloys and titanium alloys. Among these metallic materials, titanium (Ti) and titanium alloys are considered to be some of the most significant biomaterials, due to their resistance to body fluid effects, great tensile strength, flexibility and high corrosion resistance and this specific combination of strength and biocompatibility makes them suitable for medical and dental applications. Materials implanted in body contact with extracellular body fluids such as blood and interstitial fluid. Body fluids contain amino acids and proteins that tend to accelerate corrosion of implant materials. Body fluids also act as a buffer solution and accordingly, their pH changes little. If metallic materials are corroded by body fluid and if metallic ions of implants are released into the fluid for a long time, ions combine with biomolecules such as proteins and enzymes and that cause toxicity and allergy. Thus, corrosion resistance of metallic biomaterials in body is important (Hanawa 1999).

For increasing corrosion resistance and related properties of biomaterial surfaces, surface modification techniques are the most viable methods. With surface modification superior corrosion behavior, improved wear resistance, better osseointegration rate, high biocompatibility and enhanced aesthetics are most important characteristics which can be attained. Some examples of surface modification technics which can be employed to improve the corrosion behavior and other desirable properties of implant materials are: physical and chemical vapor deposition, laser cladding, thermal oxidation and thermal spraying, plasma spray, ion implantation, micro-arc oxidation, sandblasting and electrochemical treatment (Mohammed et al. 2014).

2.3.1. Electrospray Deposition Coating

The electrospray deposition method is the technique of producing submicron-sized miniature droplets by applying an electric field to a metal substrate, and the resulting droplets are then winged towards the counter electrodes or the ground-connected collector pad and deposited on the substrate. The application of electrospray technology is used in a variety of research areas, particularly to formulate micro/nanoparticular cargo carriers for a variety of biomedical applications, including biomedical imaging, implant coatings, drug delivery, and tissue engineering (Kurakula and Raghavendra Naveen 2021). Electrospray deposition, a coating technique based on the electrospray process, is one of the effective methods for coating or modeling nano/microparticles. Electrospray deposition is generally equipment consisting of a metal capillary syringe, a syringe pump, a voltage generator, and a metal collector that provides coating of electrospray particles over the entire surface area of the metal collector. For locally patterned precipitation of electrosprayed particles, it may be necessary to model nano/microparticles, use additional components such as a mask or an additional power supply in the basic electrospray deposition configuration (Lee et al. 2020). In addition, ESD is a low-cost method with high coverage, requiring no expensive equipment or vacuum generation. The microstructure and mechanical properties of ESD-deposited films depend on deposition parameters such as substrate temperature, flow rate, distance from nozzle to substrate, and deposition time, which affect the heated substrate and the size of the droplets. On the other hand, mainly the physico-chemical properties of the precursor solution, including the chemical composition of the coatings, the nature of the solvent and precursors, also affect the quality of the deposited films (Müller et al. 2021).

The application of electrical charge to the polymer solution is the basic mechanism of the electrospraying process, and the use of high electrical voltage deforms the droplet interface, producing micro- or nanometer-sized droplets depending on the process parameters. The known mechanism is that by applying the electric field to a liquid droplet an electrostatic force is created in the droplet, called the Coulomb force, which competes with the cohesive force in the droplet. When the applied coulomb force overcomes the cohesive force of the droplet, the surface tension is released and the formation of micro or nanodroplets takes place (Kurakula and Raghavendra Naveen 2021). The reason why ESD is popular is that multilayer thin

film growth is superior to spin coating, dip coating and screen printing, because the bottom organic layer solvent cannot be avoided during top layer growth (Ahmadi et al. 2014).

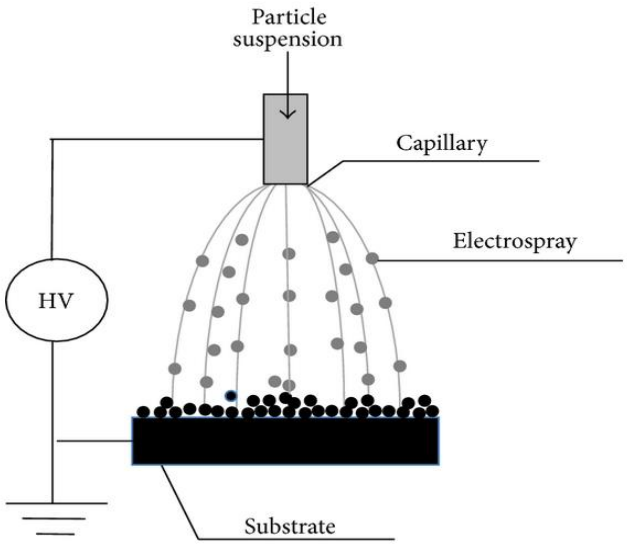

Figure 0.3 Schematic of electrospray deposition device (Ahmadi et al. 2014).

2.4. Polymer Nanocomposites And Their Applications

Significant scientific and technological interest has focused on polymer nanocomposites (PNCs) over the last two decades. Nanocomposites in general are the two-phase materials in which one of the phases has at least one dimension in the nanometer range (1–100 nm). It possesses many vital properties than that of microcomposites due to their large surface area and greater aspect ratio. The advantages of nanocomposite materials when compared with conventional composites are in their superior thermal, mechanical, and barrier properties at low reinforcement levels as well as their better recyclability, transparency and low weight (Bari et al. 2016). Fillers play important roles in modifying the desirable properties of polymers and reducing the cost of their composites. In conventional polymer composites, many inorganic filers with dimensions in the micrometer range, e.g. calcium carbonate, glass beads and talc have been used extensively to enhance the mechanical properties of polymers (Tjong 2006).

Polymer nanocomposites incorporate a new spectrum of fillers that extend the function and utility of polymers while main taining the manufacturing and proc essing flexibility inherent to plastics, thermosets, and resins. In particular, polymer nanocomposites have been successful with regard to overcoming traditionally antagonistic combinations of properties (Winey and Vaia 2007). Polymer nanocomposites represent a new alternative to conventionally filled polymers. Because of their nanometer sizes, filler dispersion nanocomposites exhibit marked improved properties when compared to pure polymers or their traditional composites. These include; (1) outstanding barrier properties, (2) increased modulus and strength, (3) improved solvent and heat resistance, (4) decreased flammability, (5) variation in Tg values of the polymer, (6) novel optical properties, (7) overall changes in physico-chemical properties, (8) enhanced biocompatibility, and (9) raised bactericidal activity. In recent years, there has been an increasing interest in and studies on biodegradable polymeric materials for biomedical purposes. There is a large literature on the conducted and performed studies in the field of bionanocomposites. Table 5.1 highlights some of the achievements and trends in this area combining soft biopolymer components with hard inorganic particles (Dwivedi et al. 2013).

2.4.1. Polymer Nanocomposites In Antibacterial Medicine

The potential for using a variety of polymer nanocomposites, including those based on chitosan (CS), poly(N-vinyl-2pyrrolidone) (PVP), poly(vinyl chloride) (PVC), and poly(vinyl alcohol) (PVA), as antibacterial goods is being investigated. In several polymer nanocomposites with antibacterial activity, Ag or its salts are utilized as fillers in addition to other nanoparticles. Aqueous acetic solution containing CS, poly (ethylene oxide), and $AgNO_3$ was added. Electrospinning this polymer nanocomposite produced nanofibrous mats exhibiting antibacterial activity against Staphylococcus aureus and E. coli, with a larger inhibition zone for extract-exposed mats against the latter. To reduce Ag nanoparticle agglomeration, the biopolymer polyhydroxyalkanoat was utilized as a capping and stabilizing agent (22–43 nm). This polymer's antimicrobial activity demonstrated an inhibitory impact on the Gram-negative E. coli XLIB strain and the Lysini bacillus fusiformis strain (Grampositive).

By decreasing poly(sodium 4-styrene sulfonate) (PSS), it was possible to make effective use of the ordered packing of polyelectrolyte multilayers on planar substrates

with horizontally oriented Ag nanoparticles. Ag nanoparticles with exposed low-energy crystal faces have strong antibacterial properties. The production of horizontally oriented Ag nanoparticles is caused by the confinement of Ag atom and nanoparticle diffusion caused by the interaction of reduced Ag atoms and Ag nanoparticles with the $-SO_3$ and $-SO_3H$ groups in PSS. This study sheds light on the connection between Ag nanoparticle properties and antibacterial function. By redox interactions between $Ag^{(1)}$ and catechol functional groups of polyurethane (PU) containing tannin, a variety of polymer nanocomposite coatings were created (TA). Catechol groups had two functions: they caused the reduction of $Ag^{(1)}$ to $Ag^{(0)}$ and gave PU antimicrobial properties. The poly(ethylene glycol) (PEG)/TA/nano Ag coatings were 100% resistant to Gram-positive and Gram-negative bacteria at 37 °C after 12 hours of incubation with a ratio of catechol: $Ag^{(1)}$ 2:1. Dual responsive semi-interpenetrating polymer network hydrogels/Ag nanocomposites based on sodium alginate and poly (acrylamide-co-N-vinyl caprolactone-co-acrylamidoglycolic acid) shown outstanding antibacterial properties toward E. coli and Bacilli. Under static circumstances, as well as by the antibacterial activity against Staphylococcus aureus, the silver release from PVP/Ag nanocomposite was verified. The nanocomposite continued to have 20% of its original Ag content after 25 days. An efficient antibacterial system with outstanding activity against E. coli and adequate activity against Staphylococcus aureus has been demonstrated using medical grade PVC reinforced with Ag nanoparticles and semiconducting ZnO micro particles. Many antibacterial polymer nanocomposites also include polyolefins like polyethylene (PE) or polypropylene (PP). The cytotoxicity of PP/PVP/Ag nanoparticles for mammalian cells was demonstrated by a PP/PVP/Ag nanoparticles film, although they did have an antibacterial impact on Gram-negative E.Coli and Gram-positive Staphilococcus aureus. The bacterial pathogen Enterococcus fecalis has been reported to be preferentially inhibited by the poly(4-allyloxy-2H-chromen2-one)/Ag nanocomposite, with minimal inhibitor concentrations of 50 and 32 g mL^{-1}, respectively. Moreover, the combination of poly(lactic acid) (PLA) and ZnO (3%) nanoparticles is antimicrobial. High levels of the nanofiller's dispersion encouraged nanocomposite photocatalysis and produced HO radicals with significant bacterial activity. Moreover, a certain Zn_2C ion concentration has some effect on the polymer nanocomposite's antibacterial activity. An outstanding mechanically performing PLA/nano ZnO/Cu chlorophyll acid (CCA) polymer nanocomposite was made. It was demonstrated to

have a 99.9% antibacterial rate (R) against E. coli, however the addition of tolylene diisocyanate did not significantly reduce the antibacterial rate (R) (TDI). Research demonstrated that the PLA/ZnO/CCA/TDI polymer composite exhibited a potent antibacterial activity against E. coli that was over 99% effective. Together with other enhancements, adding graphene nanoplatelets to PLA that included PEG and epoxidized palm oil increased the antibacterial efficacy against E. coli. Staphylococcus aureus, Salmonella typhimurium, and Listeria, monocytogenes. Antimicrobial activity was proved also in the case of PP/ Cu polymer nanocomposite (Feldman 2016).

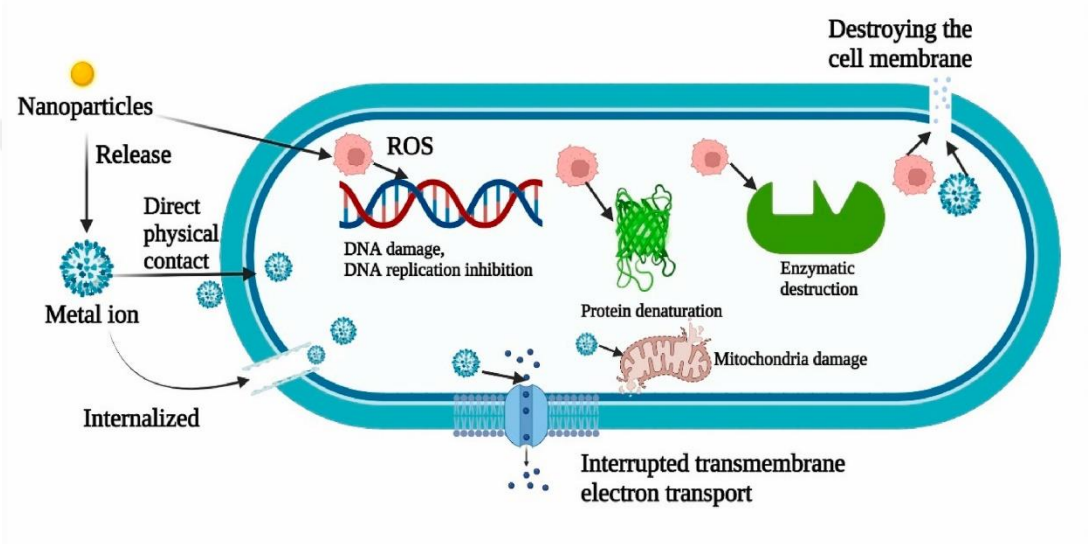

Figure 0.4 Mechanisms for antimicrobial behavior of metal nanoparticles (Jiang et al. 2022).

2.4.2. Polymer Nanocomposites And Tissue Engineering

Polymer nanocomposites play an important role in TE and regenerative medicine. They can be used for producing scaffolds providing a 3D framework on which cells can proliferate and differentiate, secret extracellular matrix (ECM) and form functional tissue. The knowledge of cell biology, materials science and bioengineering provides the basics for TE that ai to regenerate different body tissues with specific properties and versatility. The design and fabrication of bioinspired nanomaterials for tissue engineering applications requires a fundamental understanding between polymer nanocomposites and cells. The use of polymer nanocomposite scaffolds for TE is rapidly expanding. Aspects relating to chemistry, biochemistry, materials science, orthopedics, and surgery are taken into account while designing a scaffold. The extracellular matrix or basement membrane of a particular

intended tissue must meet the mechanical, chemical, surface, and electrical properties of synthetic scaffolds. The four main tissues that make up the human body-nerve, muscle, epithelium, and connective can have a wide range of these features. In order to accurately replicate the extracellular matrix seen in living things, polymer films are converted into fibrous matrices with a decreasing fiber-size scale and an increasing porosity. High porosity and pore sizes that are conducive to cell development are a few of additional parameters for designing scaffolds. For instance, holes must have a specific size for bone cells (osteoblasts), which need them to proliferate and deposit new tissue. Conductive polymers (like PANi) have been demonstrated in the biological sector to be friendly to biological molecules and cells. Such polymers have a wide range of uses as biomaterial components that successfully transmit electrical impulses to the planted cells from an external source. Cardiomyocytes, neurons, and osteoblasts are just a few examples of cells that respond to electrical impulses by becoming more functional. A few polymer nanocomposites for TE also included hydroxyapatite (HAp), tricalcium phosphate (TCP), bioactive glass (BG), and other nanofillers including magnetic particles. A macromolecular magnetic scaffold consisting of PCL and magnetite (10 wt%) was the study's main focus. In this instance, the researchers were able to produce a magnetic polymer sponge with a high degree of porosity and magnetic filler dispersion. These features were verified by magnetic measurements, scanning electron microscopy (SEM) analysis, and X-ray computed tomography (m-CAT). In order to enhance the mechanical and tribological characteristics of ultra-high molecular weight PE, bioceramic HAp was added to it. The bioceramic adds to the polymer by offering bioactive spots on its surface that can be occupied by osteoblast cells and subsequently bioresorb and be replaced by genuine bone cells. Applications for collagen nanocomposite with intercalated lamellar structure in hard tissue regeneration are also possible. Biomaterials made of natural or synthetic polymers aid in the organization of cells into functional tissues, but a patch's capacity to contract strongly as a unit is constrained by its weak conductivity. Gold nanowires with a 30 nm diameter were integrated into an alginate matrix and used as a scaffold material to deliver electrical stimuli to promote the contractibility of the heart cells. After adsorption, au nanoparticles can assist proteins in maintaining their biological function. Such nanoparticles have been widely employed in the creation of electrochemical sensors and biosensors due to their enormous surface area and strong electrical characteristics. A PVA/waterborne-PU composite reinforced with TEMPO-

oxidized cellulose nanofibers would be a desirable option for a material for tissue scaffolding, a filter, or a wound dressing (Feldman 2016). In tissue engineering, scaffolds aid in cell metabolite and nutrition transfer as well as cell adhesion, proliferation, and differentiation. While nanocomposite hydrogels can serve as scaffolds for tissue regeneration, they are unusable and weak mechanically. The addition of various nanoparticles, including carbon nanotubes and clay, can enhance the mechanical and functional qualities needed for tissue engineering. For instance, a nanocomposite hydrogel made of sodium alginate and carbon nanotubes demonstrated biocompatibility, an inflammatory response, and noncytotoxicity. Because of its improved qualities, nanocomposite hydrogel makes for ideal scaffolding materials (Kawaguchi et al. 2006).

2.4.3. Polymer Nanocomposite For Drug Delivery System

In order to absorb a lot of water, cross-linked hydrophilic polymers containing acidic, basic, or neutral monomers are known as nanocomposite hydrogels. Since they are biocompatible and biodegradable, many kinds of nanocomposite hydrogels have been employed in a variety of biological applications. In medical procedures, biotechnology, agricultural, and pharmaceutical applications, nanocomposite hydrogels are utilized as bioabsorbent materials for the delivery of pharmaceuticals as distinctive carriers (Yoshida et al. 1993). Inorganic components including silver, iron oxide, clay, gold, carbon nanotubes, hydroxyapatite, and tricalcium phosphate are found in nanocomposite hydrogels. Drug stability and slower, continuous drug release are both provided by the addition of nanoparticles to nanocomposite hydrogels, which also minimizes the effect of burst release (Satarkar and Zach Hilt 2008). They can be effective carriers to load and transport pharmaceuticals due to the regulated swelling ratio, mesh size, and diffusion coefficient of nanocomposite hydrogel. Nanocomposite hydrogels can store drug molecules for drug delivery thanks to interactions between the drug and the nanofiller. Drug release from the nanocomposite matrix is aided by variations in external stimuli such the magnetic field, electric field, temperature, and pH (Zhang et al. 2010).

2.4.4. Polymer Nanocomposite For Wound Dressing

Inflammation, granulation tissue development, matrix remodeling, and re-epithelialization are the four stages of the biological and biochemical process of wound healing (Baskovich et al. 2008). Wound dressings' primary purpose is to promote optimal healing and quicken the natural healing process (Rezayan et al. 2017). The presence of an acceptable level of moisture in the wound region has a significant impact on how quickly the lesion may heal. This creates a desired biological environment that offers the prerequisites for the intricate processes of wound healing. Each cell's and the tissue's metabolic activity can be increased, which is not possible in dry tissue (Hebeish and Sharaf 2015). By incorporating useful nanoparticles into the hydrogel matrix, nanocomposite hydrogels improve their ability to treat wounds. In order to halt bleeding, ease pain, and guard against infection, wounds are typically dressed using nanocomposite hydrogels. Nanocomposite hydrogels are great wound-dressing materials with unique qualities including good swelling, tensile strength, and biocompatibility. Wound-dressing materials include foams, pastes, and films (Varshney 2007). Hydrogels made of poly(vinyl alcohol) nanocomposites are biocompatible, non-toxic, and have a high water absorption capacity without dissolving. Poly(vinyl alcohol) nanocomposite hydrogels are superior choices for dressing applications because to all these characteristics. Due to their excellent biocompatibility, cellulosic fibers have received the majority of interest for biomedical applications. When cellulosic materials are hydrolyzed with powerful acids (such as sulfuric or hydrochloric acid), crystalline rod-like nanoparticles known as "cellulose nanowhiskers" are created (Li et al. 2011). Three different kinds of hydrogels with excellent mechanical strength include topological gel, nanocomposite gel, and double network gel. Brown seaweed's natural polysaccharide, sodium alginate, has been employed as a new material in the treatment of wounds. Gels and foams that promote "wet healing" can be created using sodium alginate. Due to ionic crosslinking with calcium bridges between mannuronic acid and guluronic acid, sodium alginate may produce nanocomposite hydrogel in the presence of divalent (Ca^{2+}) cation (Sun et al. 2012).

2.5. Fabrication of Polymer Nanocomposite Films

Polymer nanotechnology fundamentally involves the creation of polymer nanocomposites. The creation of nanocomposites is based on the assembly and interactions of molecular or polymeric species with inorganic nano-substrates. The procedures are as follows: (1) choosing and modifying a polymer for the matrix (continuous phase); (2) selecting a biocompatible nanostructured reinforced material; and (3) dispersing the discontinuous material inside the continuous phase. The in situ formation of the nanoparticles in the polymer matrix can be accomplished in one of two ways: by mixing the nano-precursor with the polymer matrix, or by using the "breath in and breath out technique," which causes the particles to form separately before being reinforced in the polymer matrix. The nanoparticles are successfully stabilized by the chemical and physical interactions between the particulate and polymeric phases, which also inhibit clustering or agglomeration. Both top-down and bottom-up methods can be used to fabricate objects at the nanoscale. Chemical reduction, reverse micellar synthesis, sol-gel process, microemulsion, co-precipitation, decomposition of organometallic compounds, hydrothermal routes, solution evaporation process, sonochemical ultrasonication, synthesis of bi-metallic nanoparticles in micellar medium at room temperature, gas condensation, laser pyrolysis are all discussed in a wide range of articles. Nanometer-sized particles have been created from various organic-inorganic particles to improve the characteristics of composite materials. Metal (Al, Fe, Au, Ag, etc.); metal oxide (ZnO, Al_2O_3, $CaCO_3$, TiO_2, etc.); non-metal oxide (SiO_2); and other particles have been utilized to form polymer/inorganic particle nanocomposites (SiC). The nanoparticles used are chosen based on the desired qualities and application of the nanocomposites (Dwivedi et al. 2013).

2.5.1. Solvent Casting Method

Among the various polymer composite film production techniques, the solvent casting method is applicable, preferable and undoubtedly a widely used method; It is highly preferred because of its simple production process and low processing cost. The production procedure and parameters of thin composite films by solvent casting method are shown in Figure 2.5 (Akiyode and Boateng 2018). In solvent casting method water soluble polymers are dissolved in water and the drug along with other

excipients is dissolved in suitable solvent then both the solutions are mixed and stirred and finally casted in to the petri plate and dried (Luchina et al. 1975).

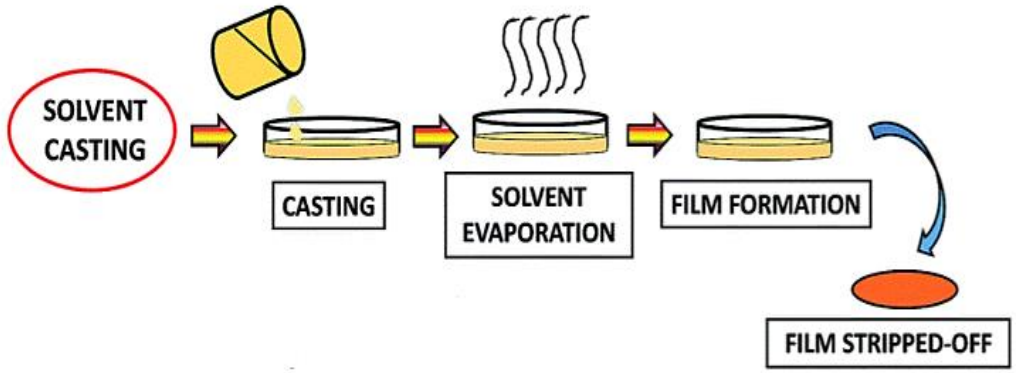

Figure 0.5 Schematic diagram of solvent casting process (Khan et.al., 2018).

As they affect the drying rate, the thickness of the film, the morphology as well as the material uniformity of the films, the rheological properties of the polymeric mixture should be taken into account. The mixing method may unintentionally introduce air bubbles into the liquid; de-aeration is therefore a prerequisite for obtaining a homogeneous substance. They are left to dry after casting the solution onto an appropriate substrate to allow the solvent to evaporate, leaving a polymeric film with a drug on it. Based on the required dosage of the shaped strip, it is cut into the necessary shape and size following the full drying of the film. In certain cases, before cutting, the strips are rolled and held for a certain amount of time, which in an industry is known as 'rollstock'. However, because a film is susceptible to damage, it should not be exposed for too long. If necessary, in order to preserve its stability, it should be cut and wrapped directly after preparation. The film obtained by solvent casting has many benefits, such as improved physical properties, simple and low-cost manufacturing and excellent thickness uniformity (Karki et al. 2016).

2.5.2. Green Synthesis Of Metallic Nanoparticles

Environmental pollution and climate change have become insurmountable with the use of toxic wastes and raw materials, non-recyclable polymer packaging waste, and ingredients harmful to nature and human health. With the depletion of natural resources and the increase in the amount of pollution, the crisis that arose around the world led governments to create regulatory and preventive regulations. The European

Union (EU) is leading the way as the largest community that takes the biggest steps in this regard and fights the climate crisis. In this direction, the European Commission has initiated studies on protecting the ecosystem and diversity, the use of recyclable and natural-content polymer packaging, and sustainable raw materials with the Green Deal Action Plan (Bernstein et al. 2022; Fayet et al. 2022; Miłek et al. 2022). Similarly, research institutions and various communities contribute to the creation of a greener and cleaner environment by starting studies on the climate crisis, the increase of toxic poisoning, and the production and use of renewable resources. Promoting the use and reproduction of products produced with green production methods and clean ingredients is one of these studies. Green production is an approach that does not show toxic properties, is environmentally friendly, prevents waste generation, and does not pose a threat to human and animal health. This approach, which is realized by using plant extracts, natural ingredients, antioxidants, animal-based raw materials, provides economic products, ease of production, low energy consumption and the use of renewable energy sources.

Green synthesized metallic nanoparticles suitable for many industrial applications along the lines of antibacterial coatings (Huq et al. 2022; Martorana et al. 2022; Ahmed et al. 2022b), bandages (Senthamarai Kannan et al. 2022), textiles (Tahir et al. 2022; Sadeghi-Kiakhani et al. 2022), wallpapers (Elangovan et al. 2022), biomaterials (Subha et al. 2022; Nicolae-Maranciuc et al. 2022; Selvamani et al. 2022) and packaging (Martínez-Molina et al. 2022; Srichiangsa et al. 2022). As another industrial application, Yontar et al. (Yontar et al. 2022) have shown that polymer nanocomposite films produced by modification of plant extracts to PVA exhibit photocatalytic properties and provide dye removal from water.

Plant extracts have been the most preferred natural ingredients in green production (Jouyandeh et al. 2022; Moshood et al. 2022a, 2022b; Torricelli et al. 2022; Vidal et al. 2022; Yontar et al. 2022). Plant extracts provide the green synthesis of metallic (gold, copper and silver) nanoparticles with their polyphenols, alcoholic compounds, terpenoids, quinones, antioxidants, glutathiones, organic acid, alkaloids (-OH) groups and minerals (Alharbi et al. 2022a; Lomelí-Rosales et al. 2022; Nieto-Maldonado et al. 2022; Oves et al. 2022; Parmar and Sanyal 2022). Apart from this, they can also be used in the production of polymer nanocomposites exhibiting photocatalytic properties (Yontar et al. 2022). The fact that they have natural, cheap

and renewable properties has made plant extracts one of the important raw materials in green production methods. The green synthesis method allows metallic nanoparticles to be synthesized from metal salts without the use of any toxic chemicals or alcohol. Schematic draw of green synthesis of nano metal particles using extracts from different parts of plants is shown in Figure 2.6. Since the green synthesis method does not require the use of expensive raw materials, it has low production costs and energy consumption. Thanks to this method, antibacterial materials that do not harm the environment and human health can be easily produced (Oves et al. 2022; Parmar and Sanyal 2022). One of the important types of metallic nanoparticles synthesized naturally using plant extracts is silver. Silver nanoparticles show good antibacterial, catalytic, antifungal, and antioxidant properties and exhibit various applications in synthesis, drug delivery, anti-cancer, bio-detection, biomedical applications, as well as in environmental remediation (Garg et al. 2022; Balachandar et al. 2022). While nano silver exhibits toxic properties on bacteria, it does not cause toxic effects in humans. Although the antibacterial action mechanism of nano silver has not been fully proven in the literature, it has been explained that two different bacteriostatic interactions occur. Silver oxidizes on the surface of AgNPs and generates superoxide radicals and other reactive oxygen species, inducing the production of reactive oxygen species (ROS) and killing bacteria. Oxidative stress and Ag^+ release caused by AgNPs are the main theories that are effective in the functioning of the antibacterial effect mechanism (Zhao et al. 2022). Another mechanism is the application of antimicrobial activities through a bactericidal mechanism where AgNPs adhere to the cell wall and react with membrane proteins. It has been stated in various studies that AgNPs attack the DNA mechanism in the cells as well as the respiratory chain, that their direct contact with bacteria causes cell damage, and that Ag^+ released by AgNPs can cause cytotoxicity and lead to the death of bacteria (Ong and Nyam 2022; Zhao et al. 2022; Bapat et al. 2022; Garg et al. 2022).

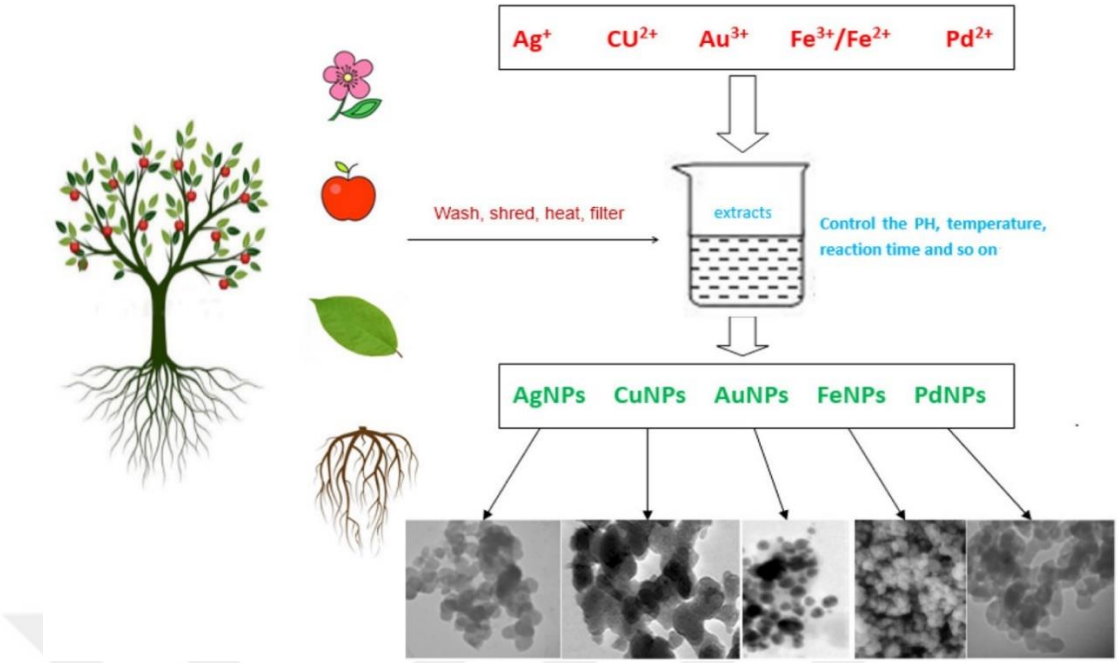

Figure 0.6 Green synthesis of nano metal particles using extracts from different parts of plants (Ying et al. 2022).

2.5.3. Applications of Nanomaterials and Particles in Dentistry

The use of nanoparticles (NP) for the treatment and prevention of dental infections and illnesses is currently being investigated. There are several forms of NPs, which are generically classed as inorganic and organic NPs. Semiconductors (ZnO, ZnS, quantum dots), metallic NPs (gold, silver, copper, aluminum, platinum), and magnetic NPs (cobalt, iron, nickel, iron oxide) are examples of inorganic NPs; organic NPs include carbon (fullerenes, carbon nanotubes) and polymeric (chitosan, liposomes) NPs. As illustrated in Figure 2.7, all of these nanoparticles are effective in a variety of experimental dental and oral applications. These nanoparticles are used to prevent and treat oral disorders such as restorative, prosthetic, endodontic, periodontal, and dental caries through treatments and implants (Zare and Shabani 2016; Rafique et al. 2017; Makvandi et al. 2021).

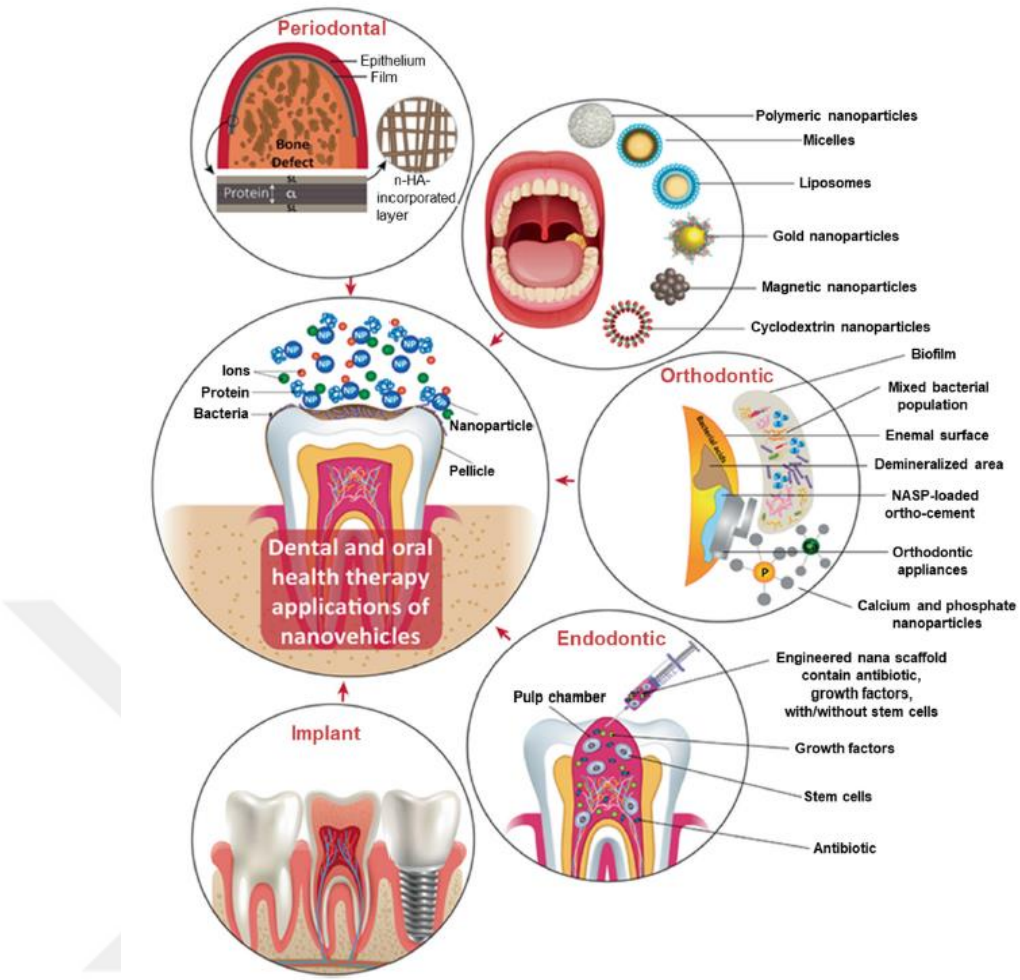

Figure 0.7 Applications of organic and inorganic nanomaterials in dental treatment and care (Ahmed et al. 2022a).

2.5.4. The Role of AgNPs in Dental Treatments

AgNPs are used in various fields of dentistry (restorative, prosthetic, endodontics, implantology and periodontology) to prevent caries, infections and to treat oral cancers. When AgNPs are modified into composite resins, they do not alter the inherent mechanical and biological properties and impart significant antimicrobial properties to the nanocomposite material even when low AgNP concentrations are used. It is also known that AgNPs can reduce microleakage in the root canal system and can be used instead of sodium hypochlorite (NaOCl) as canal irrigation. AgNP-based irrigation solution has a similar effect with NaOCl in the elimination of E. Faecalis. Although the two solutions are effective for their antibacterial activity, irrigants with AgNP have the added benefit of removing the smear layer, which can enhance the ability of AgNPs to interact with bacteria. By using AgNPs with

antimicrobial properties and nanocomposites containing restorative agents, the incidence or recurrence of caries due to microleakage can be reduced. AgNPs, which can stimulate the regeneration of mammalian cells, can also eradicate periodontal diseases.

AgNPs do not exhibit significant cytotoxicity when immobilized on sand-blasted, coarse-grained and acid-etched titanium surfaces, but inhibit the growth of S. aureus and F. nucleatum. These results showed that by coating the titanium implants with AgNPs, the implants can be equipped with balanced antibacterial and osteogenic functions, which bodes well for safe and long-term clinical applications. Commercially produced AgNPs (Nano-world Company, Kolkata, India) have a Minimum Inhibitory Concentration (between 2.82 and 90 μg/mL) against S. mutans, Streptococcus oralis, C. albicans, L. acidophilus and Lactobacillus fermentum. MIC) value. The amount of AgNPs required to inhibit bacterial growth is similar to that of conventional antimicrobial agents such as CHX, SDF and 70% isopropanol. The effects of silver particles were not diminished when formulated into dental products such as toothpaste. Toothpaste containing AgNP (TruCareNanosilver) had the highest antibacterial activity against S. mutans compared to those containing chitosan (Conybio Plus Chitosan Dental) and fluoride (Oral B Pro Health). This validates the efficacy of AgNP-based dental formulations for plaque control and prevention of dental caries or infections, achieving significant clinical effects with less bystander toxicity (Chien et al. 2018; Rani et al. 2015).

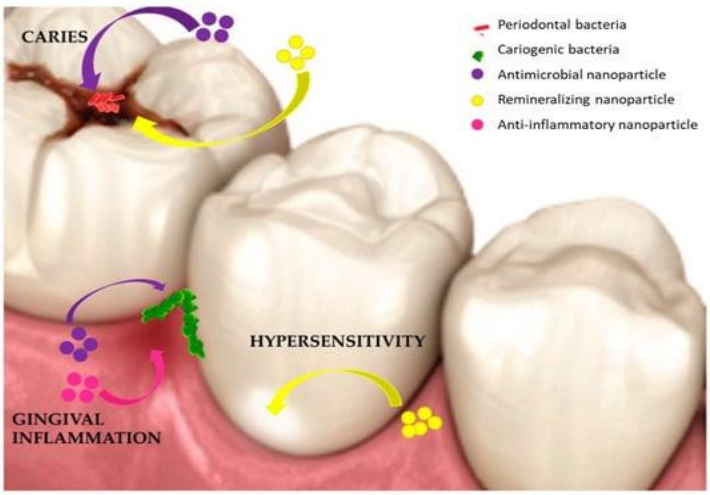

Figure 0.8 Application of nanoparticles (NPs) contained in oral care products (Carrouel et al.2020).

3. MATERIALS AND METHOD

3.1. Starting Materials

3.1.1. Chemicals

PVA average molecular weight Mw = 95.000 g/mol, 99% hydrolyzed purchased from Sigma–Aldrich Germany were used without further treatment or purification. Silver nitrate ($AgNO_3$) and plant extracts were used in the synthesis of silver nanoparticles. Silver nitrate ($AgNO_3$) salt (99%) was acquired from Sigma Aldrich. For the fabrication of colloidal solutions propanol solvent was also supplied from Merck KGaA, Germany. All the starting materials are analytic grade and used without further purification.

3.1.3. Plant Types and Extract Preparation

For the production and characterization of polymer coating material containing plant extracts, polymer nanocomposite films were produced by solvent casting method. For the production of nano silver particles, which are also used for films to have antibacterial properties, with green synthesis, production was carried out with two different plant groups. Similarly, films were produced using two different plant extract groups. In this way, the effects of plants on the properties of the films and the properties of green synthesized nano silvers were compared. Production was made with Hemp Seed/St. St. John's Wort and Rosemary/Cherry Laurel plant groups. According to the results obtained, it has been determined that the best properties will be obtained by using Hemp Seeds/St. John's Wort plant extracts in the solution to be produced for coating. Hemp seeds, St. John's Wort and rosemary were collected from the local market, the Cherry Laurel leaves were collected from wild nature and all plants were washed adequately with DI water. After cleaning, Cherry Laurel was cut into fine pieces and dried in the oven. There are different organic acids, phenolic and hydroxyl groups in each different plant (Alharbi et al. 2022b; Martínez-Cabanas et al. 2021). Hydroxyl groups are simple structures consisting of two lone pairs bonded to a hydrogen atom and an oxygen atom. They easily combine into hydrogen bonds to form an ion with a net positive or negative charge. This group can also participate in chemical reactions to link molecules together and form chains of sugars or fatty acids. The addition of a hydroxyl group converts many organic compounds to alcohols, increasing the solubility of the structure in water (Ivanets et al. 2021; Li et al. 2019a).

Hemp seeds contain carboxylic acids (cannabigerolic acid and cannabidiolic acid), antioxidants, flavonoids and canniprene (Csakvari et al. 2021b), St. John's Wort contains flavonoids, antioxidants, hypericins, hyperforins, mono- and polysaccharides, phenolic acids (Alahmad et al. 2021b), Rosemary polyphenolic acids (e.g., flarosmarinic acid). e.g., apigenin and luteolin), and triterpenes (e.g., ursolic and betulinic acid) contain caffeic acids (Lešnik et al. 2021a), while Cherry Laurel contains chlorogenic acid, o-coumaric acid, Apigenin 7-glucoside, quercetin 3-glucoside, naringenin (Karabegović et al. 2014).

To prepare the plant extracts, 20 g of each plant species, were added to 150 mL of DI water, and after heating at 90 ˚C for 60 minutes, the plant extract mixture was filtered to remove coarse particles. For the production of each film sample, 10 mL of the plant extract mixture, which continued to be mixed homogeneously, was used. In this way, the highest homogeneous concentrations of plant extracts were modified for each individual film sample. The properties, names and applications of plants types used in study are shown in Figure 3.1. The prepared plant extract solutions are shown in Figure 3.2.

Figure 3.1 Plants used in polymer nanocomposite films, their properties and applications.

Figure 3.2 Plant extracts for production.

3.1.1. Substrates

The produced polymer nanocomposites were coated by electrospray deposition method on Ti6Al4V alloy, which is widely used in the production of dental metallic biomaterials. The chemical composition of Ti-6Al-4V substrates are given in Table 3.1. Square substrates of 2 mm thickness and 1.5x1.5 mm width were cut by laser cutting device in order to cover 4 substrates at the same time to fit on the table of the electrospray deposition device. Firstly, the surfaces of the cutted substrates were sanded and then was roughened by etching with an etching solution. In this way, the surface was made ready for the coating process. The solution used for etching the surfaces was prepared with 10 mL of water, 5 mL of nitric acid and 5 mL of sulfuric acid. Surface images of metal substrates before and after etching are shown in Figure 3.3.

Table 3.1 Chemical composition of Ti-6Al-4V.

Element	**Weight (%)**
Ti	Remaining main part
AI	5.5-6.5
V	3.5-4.5
Fe	0.25
C	0.08
N	0.05
H	0.012
O	0.13

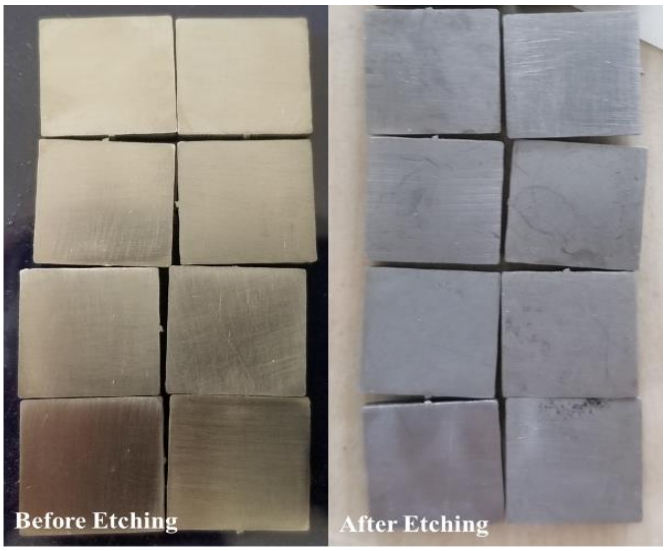

Figure 3.3 Ti6Al4V substrates before and after etching process.

3.2 Coating Fabrication

3.2.1. Green Synthesize Of Silver Nanoparticles

Production of nano silvers was executed with green synthesis method. Nano silver synthesis was carried out considering the synthesis parameters used in the studies in the literature (Ahmed and Mustafa 2020; Jalilian et al. 2020; Varadavenkatesan et al. 2019). In order to prepare the plant extracts, 20 g of dried herbs was added in 150 mL of DI water and heated for about 30 minutes at a temperate of 90 ˚C and then filtered. As the first step in nano silver synthesis 0.1 mM $AgNO_3$ solution was prepared. 0.1 mM concentration of $AgNO_3$ was prepared (0.6 g of $AgNO_3$ salt was added in 36 mL DI water) and stirred magnetically at room temperature until a homogeneous solution was obtained. 4 mL of plant extracts were added to each separated two different $AgNO_3$ solutions and mixing was continued until the the color of the reaction mixture turns transparent to dark brown. After 5 minutes the solutions were almost black in color which preliminarily indicates the formation of AgNPs and then mixing was stopped. The solution was filtered and the nano silver powders were ultrasonically washed in distilled water. The nano silver particles obtained from the last filtered solutions after drying in an oven at 35 ˚C for 2 h. The impact of plant extract on the fabrication of AgNPs was also observed by varying the type of plants. Figure 3.4 shows the process of obtaining nano silver powders from plant extracts. The color changes of the solutions are clearly visible in the photos.

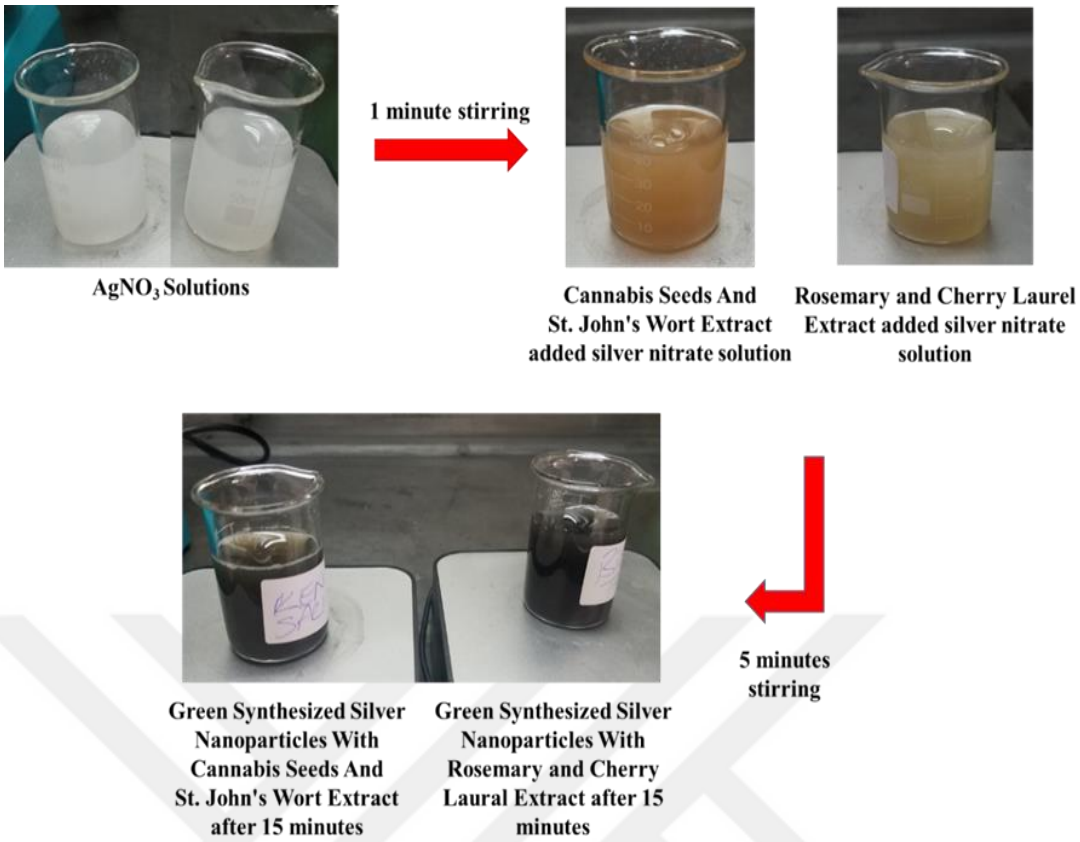

Figure 3.4 The process of synthesized nano silver particles from plant extracts.

3.2.2. Production of Plant Extract and Silver Nanoparticle Modified PVA nanocomposite films

Among the various polymer composite film production techniques, the solvent casting method is the easiest applicable, cost- effective, preferable and undoubtedly a widely used method. In solvent casting method, water soluble polymers are dissolved in water and the other additives is dissolved in suitable solvent then both the solutions are mixed and stirred and finally casted in to the petri dishes and dried (Salević et al. 2022). The production of biopolymer nano-composite material containing plant extracts (Hemp Seeds, St. John's Wort, rosemary and Cherry Laurel leaves) was carried out by solvent casting method. In the preparation of polymer nanocomposite films, the PVA ratio was prepared with reference to the study of Yontar et al. (Yontar et al. 2022) The rate of silver nanoparticle modification used in the films was determined as 1% based on similar studies (Srikhao et al. 2021; Bulla et al. 2021; Aljohny et al. 2021; Ragab and Rajeh 2020; Htwe and Mariatti 2020; 2020; 2020). These mixing ratios belong to the films showing the most optimum properties. The

produced composite films were producted in groups with and without AgNPs modification. In total 4 groups of polymer composite films were manufactured. The film groups and their ingredients in percentage by weights are given in Table 3.2. Group A and B polymer composite films do not contain AgNPs. Plant extracts used in group A were hemp seeds and St. John's Wort. In group B, rosemary and Cherry Laurel leaf extracts were used. The ingredients of PVA composite films with AgNPs modified are are hemp seeds and St. John's Wort extract in group C films, and rosemary and Cherry Laurel leaf extracts in group D films. AgNPs were used with the same ratios in both plant extract modified sample groups. Neat sample also produced for comparisons with other modified sample groups.

Table 3.2 The film groups and their ingredient in percentage by weight.

Neat	**A**	**B**	**C**	**D**
PVA (4 g)	Hemp Seeds (5 mL)	Rosemary(5 mL)	Hemp Seeds (5 mL)	Rosemary (5 mL)
DI water (40 mL)	St. John's Wort (5 mL)	Cherry Laurel Leaves (5 mL)	St. John's Wort (5 mL)	Cherry Laurel Leaves (5 mL)
	PVA (4 g)	PVA (4 g)	AgNPs (0.05 g)	AgNPs (0.05 g)
	DI water (30 mL)	DI water (30 mL)	PVA (4 g)	PVA (4 g)
			DI water (30 mL)	DI water (30 mL)

The first step in the production of polymer nanocomposite films was to prepare the PVA solution. 4 g of PVA powder was dissolved in 40 mL DI water in a beaker at 90 ˚C for 1 h by constant stirring to form homogeneous solution. After the PVA was dissolved in water, 10 mL of plant extracts (Hemp seeds-*St. John's Wort* and *Cherry Laurel*-Rosemary) and 0.5 g AgNPs were added separately with 40 mL PVA solutions and the resulting mixture was stirred for 1 h at 90 ˚C. Stirring was continued for 1 hour under 90˚C temperature until all the combined ingredients were homogeneous.

After perapering the solutions, the polymer mixtures were poured into petri dishes to form as a thin films and kept in an oven at 40 ˚C for 24 hours**.** Figure 3.5 shows the production process of polymer nanocomposite films and their images. These films are termed as plant extract-PVA/AgNPs nanocomposite films. The neat sample, seen as the lightest color in Figure 3.6, is the PVA thin film without any additives or modifications. In the Figure 3.6, the yellow and light brown films are polymer

composite film containing plant extracts. The black colored samples are AgNPs and plant excract modified PVA nanocomposite films. The thickness of the produced nanocomposite films was measured as 1 mm. Polymer nanocomposites, which are successfully produced using plant extracts, nano silver and PVA by using solvent casting method, have many uses such as health, water purification, coating, photocatalytic applications. The areas where the produced films can be used are shown in Figure 3.7 with a schematic drawing.

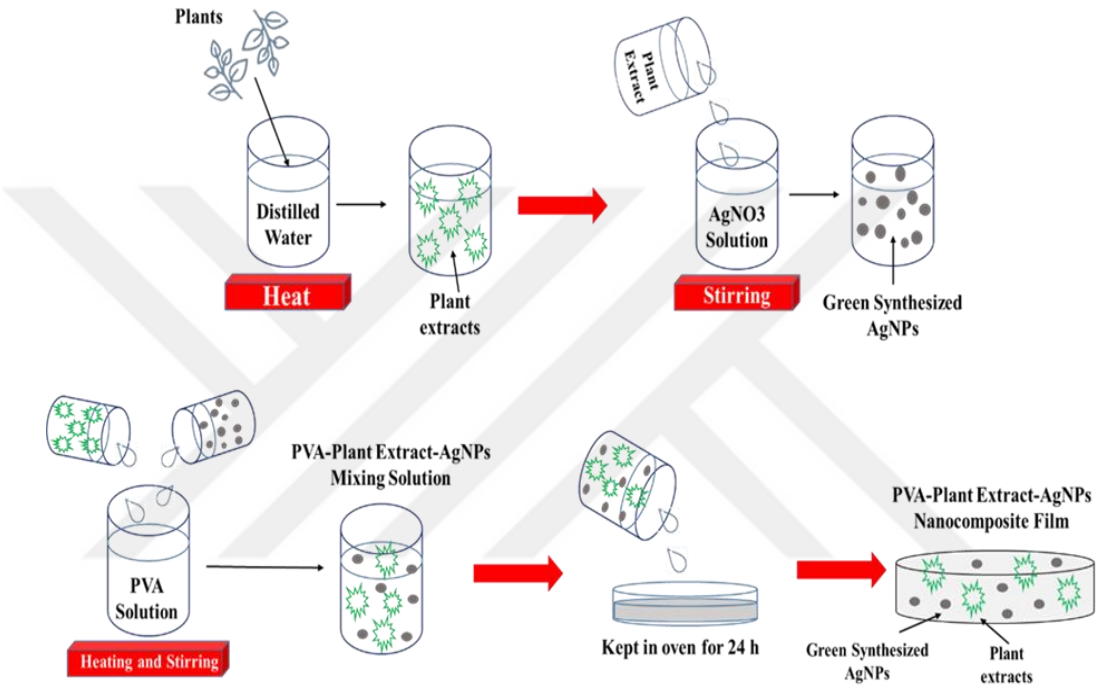

Figure 3.5 Polymer nanocomposite films production process.

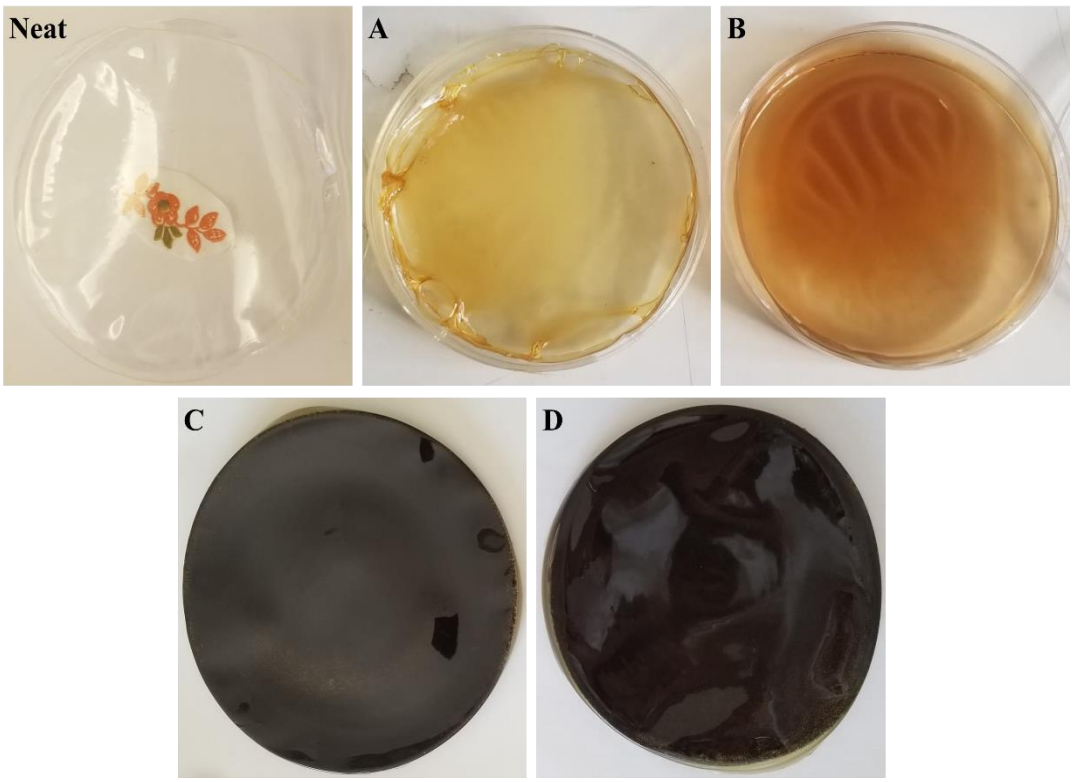

Figure 3.6 Polymer nanocomposite films produced by solvent casting method.

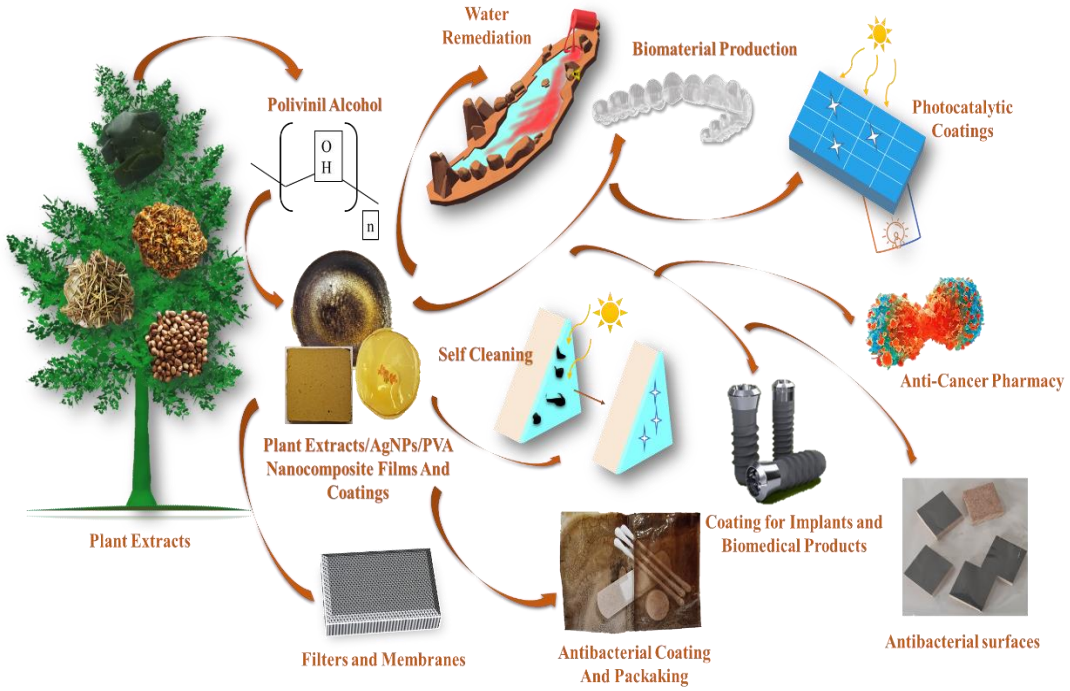

Figure 3.7 Various usage areas of polymer nanocomposites produced with plant extracts, nano silver and PVA.

3.2.3. Electrospray Deposition

After surface preparation processes were completed, substrates were placed on the electropray device panel and coating processes were carried out. The mixture of Hemp seeds and St. John's Wort extracts has been the plant group used in the coating material, since the polymer films it is modified show photocatalytic properties, increase the mechanical strength, increase the water absorption capacity, and enable nano silvers to be produced in smaller sizes by green synthesis. The solution groups prepared for the coating process and their contents are given in Table 3.3. When the literature is examined (Alcudia et al. 2022), there is no toxic effect when the nano silver ratio used in the material is kept at 0.4%. Therefore, coating solutions were prepared within the framework of this ratio. 0.05%, 0.1, 0.3 and 0.5% nano silver were used in the prepared solutions. In the study, coating processes made with 10% PVA solutions were unsuccessful. The coating surfaces appeared rough and inhomogeneous. Failed coating attempts and surfaces are shown in Figure 3.8. For this reason, the ratio of PVA used in coating solutions was determined as 8% and also taking into account the previous studies. Isopropyl alcohol was added to each solution so that the prepared polymer solutions could be mixed homogeneously and sprayed from the needle without precipitation during electrospray coating. Coating processes were carried out with a speed of 0.020 mL/min and a power of 15 V for 35 minutes with 5 mL solutions. As the coating time increased, the coating solution was kept at 5 mL and the coating time for 35 minutes due to the roughening of the coating surfaces and the non-homogeneous spraying of the nanoparticles on the substrates. The coating process was carried out by spraying the solutions on the metal base from the syringe. The electrospray device used for coating is shown in Figure 3.9. Surface images of the successfully coated substrates with %8 PVA mixing solutions are shown in Figure 3.10.

Green synthesized nano silver and plant extracts (Hemps seeds and St. John's Wort) modified polymer nanocomposite material produced and developed in the thesis study were successfully coated on Ti6Al4V alloy substrates by electrospray method. Coating thicknesses were measured by SEM analysis as an average of 27 μm.

Table 3.3 Coating solution groups and their contents.

SAMPLE NAMES	INGREDIENTS				
	PVA	**DI water**	**Isopropyl Alcohol**	**Hemp Seeds And St. John's Wort Extract**	**AgNPs**
Neat	%8	4 mL	1 mL	-	-
A	%8	1.5 mL	1 mL	2.5 mL	-
B	%8	1.5 mL	1 mL	2.5 mL	%0.05
C	%8	1.5 mL	1 mL	2.5 mL	%0.1
D	%8	1.5 mL	1 mL	2.5 mL	%0.3
E	%8	1.5 mL	1 mL	2.5 mL	%0.5

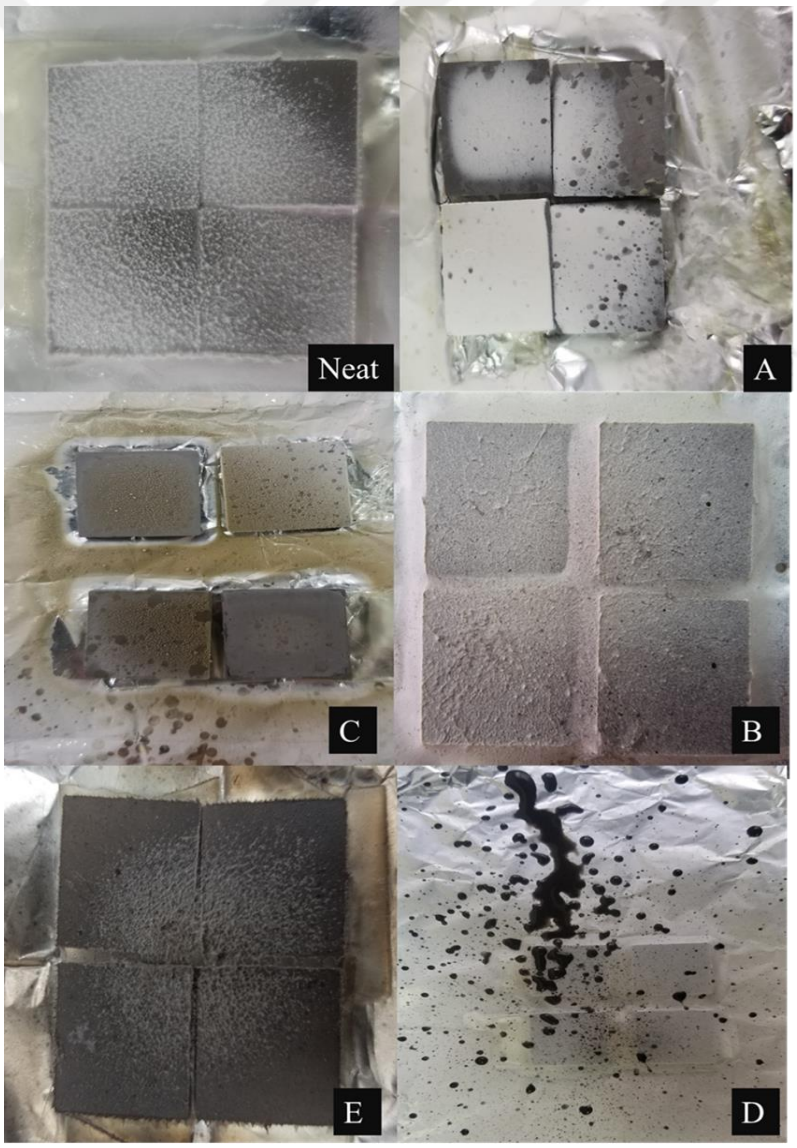

Figure 3.8 Unsuccessful coating preliminary trials made with 10% PVA solutions.

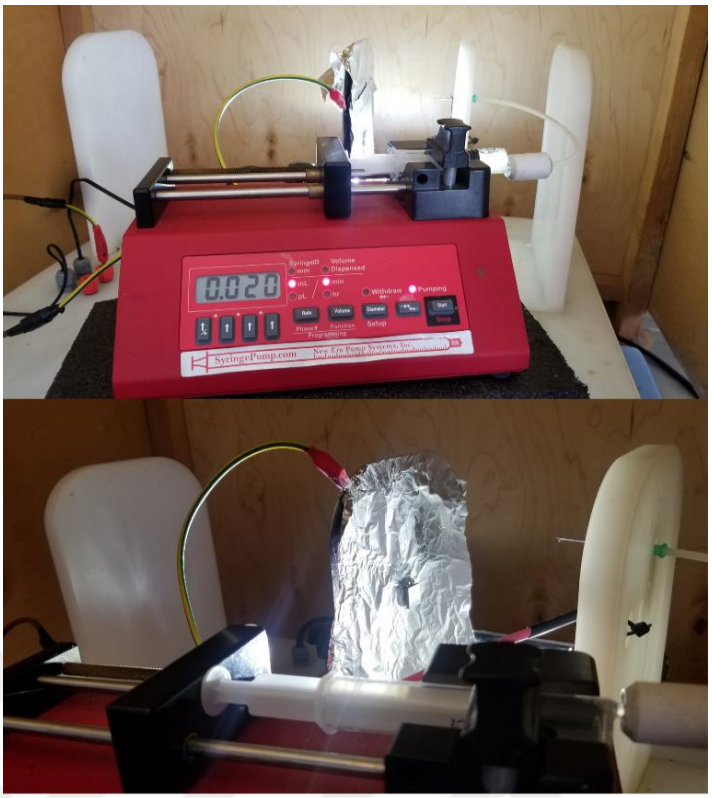

Figure 3.9 Electrospray deposition system.

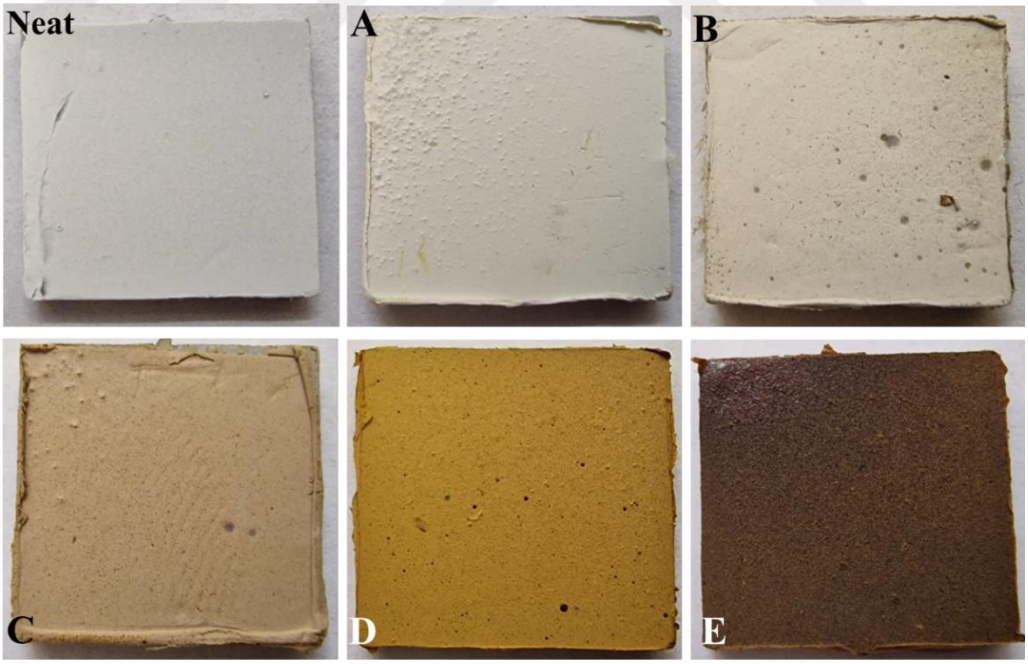

Figure 3.10 Ti6Al4V substrates coated with the electrospray method, Neat, (A) Plant extract modified, (B) Plant extract and 0.05% AgNPs modified, (C) Plant extract and 0.1% AgNPs modified, (D) Plant extract and 0.3% AgNPs modified and (E) Plant extract and 0.5% AgNPs modified PVA.

4. RESULTS AND DISCUSSION

4.1. Characterizations of Polymer Nanocomposite Coating Films

4.1.1. Microstructural Analysis

The determination of the minerals that come from the elements in plant extracts was carried out by EDS analysis. EDS was performed for each plant extract group separately and the elemental contents were obtained by spectrum analysis. It was seen from the EDS spectrum results given in Figure 4.1 that all plant types used in the study contained minerals of K, Mg, Ca and P elements. Mineral types found in plant extracts (Hemp Seeds, *St.John's Wort*, Rosemary and *Cherry Laurel*) have also been determined by previous studies, and similar minerals have been found (Farinon et al. 2020; García-Galdeano et al. 2020; Macit 2021; Zvezdanović et al. 2021).

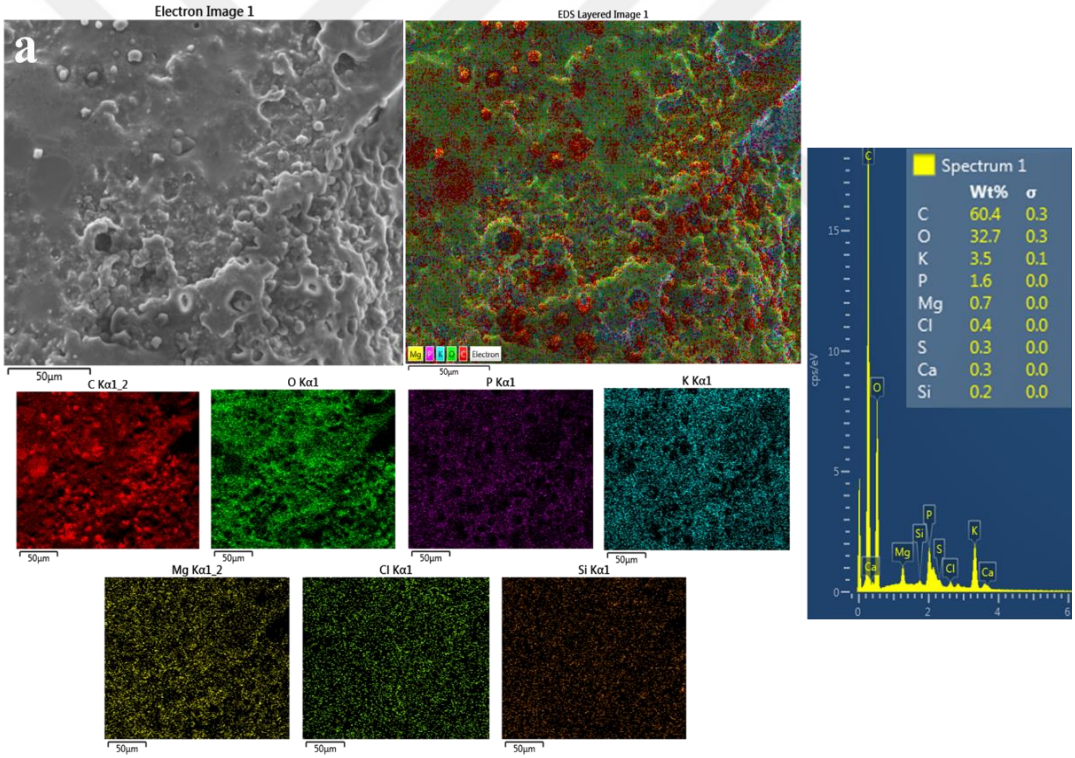

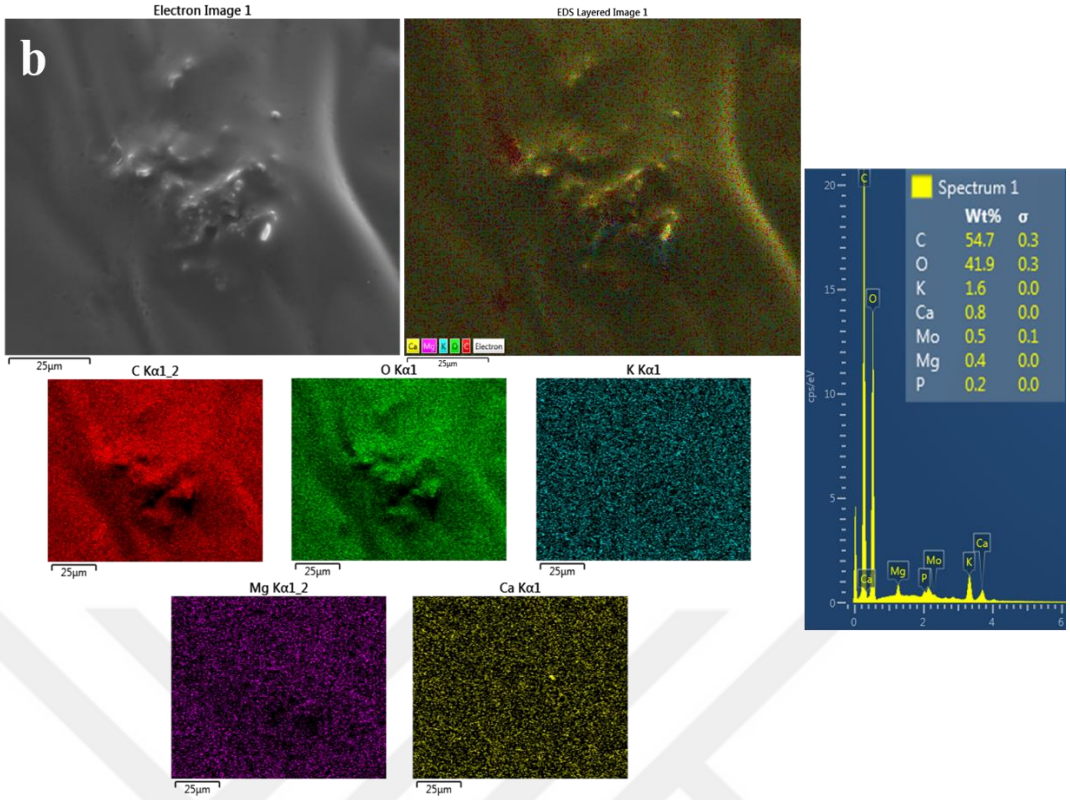
b
Electron Image 1
EDS Layered Image 1
C Kα1_2
O Kα1
K Kα1
Mg Kα1_2
Ca Kα1
25µm
Spectrum 1
Wt% σ
C 54.7 0.3
O 41.9 0.3
K 1.6 0.0
Ca 0.8 0.0
Mo 0.5 0.1
Mg 0.4 0.0
P 0.2 0.0
cps/eV

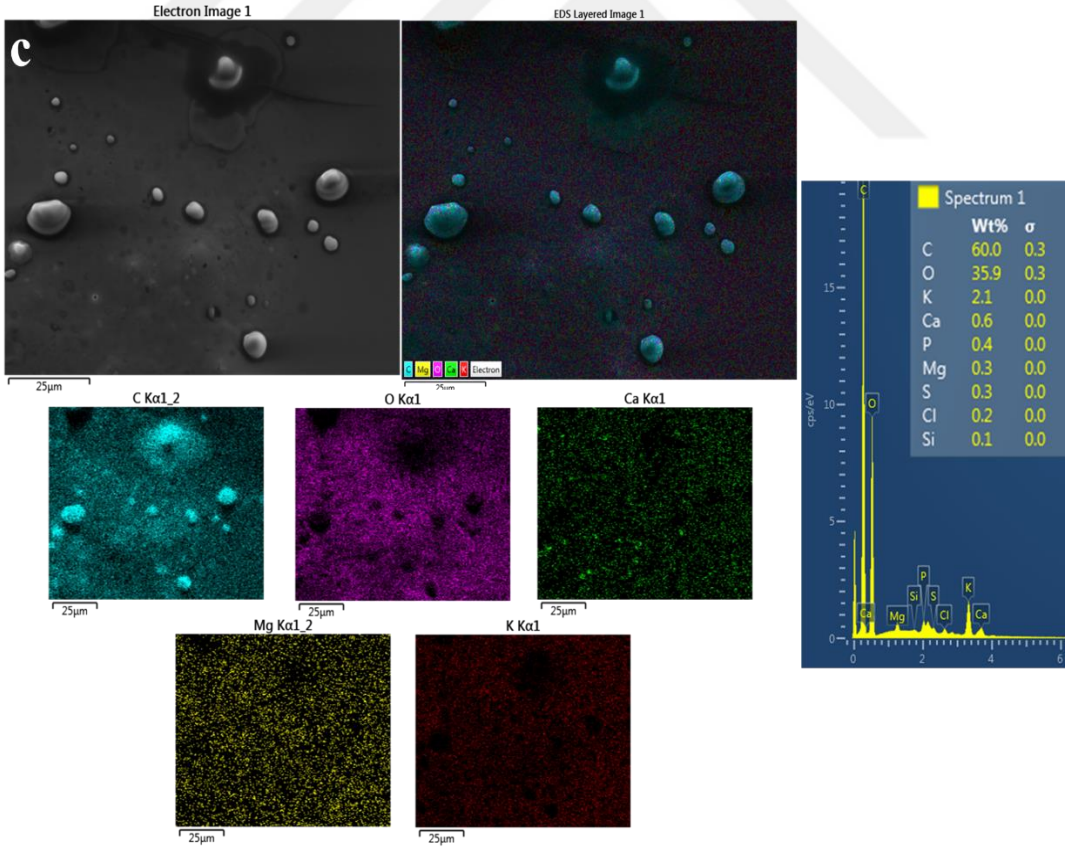
c
Electron Image 1
EDS Layered Image 1
C Kα1_2
O Kα1
Ca Kα1
Mg Kα1_2
K Kα1
25µm
Spectrum 1
Wt% σ
C 60.0 0.3
O 35.9 0.3
K 2.1 0.0
Ca 0.6 0.0
P 0.4 0.0
Mg 0.3 0.0
S 0.3 0.0
Cl 0.2 0.0
Si 0.1 0.0
cps/eV

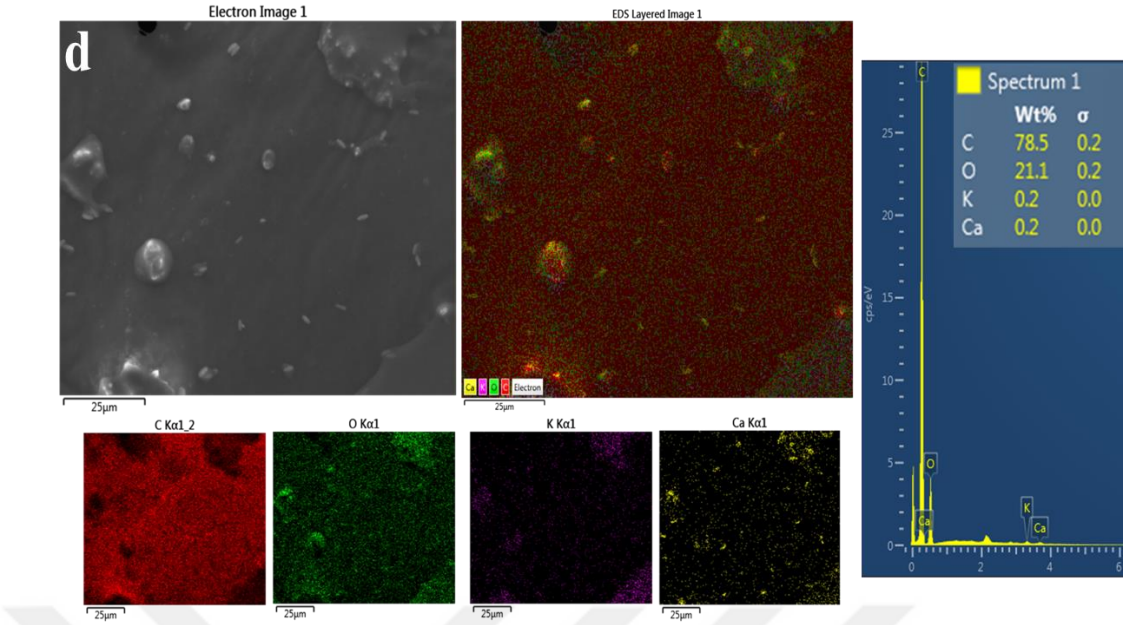

Figure 4.1 SEM images and EDS results of of a) Hemp Seeds, b) St.John's Wort, c) Rosemary and d) Cherry Laurel extracts.

The microstructural characterization and EDS chemical mapping of samples were observed by a JEOL 7001F Field Emission (FE) Scanning Electron Microscope with an EDS attachment which has an 80 mm^2 X-MAX detector. SEM analysis was performed on all the polymer nanocomposite films and examined the size and distribution of green synthesized silver nanoparticles by two different plant groups. SEM images were examined and the effect of plant groups on nano silver production with green synthesis was compared. Semi quantitative chemical analysis on samples was performed by energy dispersive spectroscopy (EDS). The compositions of nanocomposite films were determined from EDS spectrum and map analysis. The presence of Ag elements on the surface of the prepared composite film samples were determined by EDS.

Nanocomposite films and neat film were cut into 1x1mm squares and examined by SEM. The effects of the plant extract types used in the green synthesis process on the sizes and shapes of the synthesized silver nanoparticles were investigated with SEM images. The SEM image of the neat sample reveals that the film was produced smoothly and homogeneously, without any additives and as can be seen it is colorless. When A and B samples were examined, it was observed that the particles come from plant extracts were homogeneously dispersed in the polymer matrix. Green synthesized AgNPs were clearly detected in SEM images and are shown in Figure 4.2.

The spherical and white colored particles seen in Figure 4.2 were AgNPs. AgNPs synthesized with Hemp/St.John's Wort were more rounded and homogeneous, while AgNPs synthesized with Rosemary/Cherry Laurel were more irregular in shape. As can be seen clearly in Figure 4.2(c)-(d), green synthesized AgNPs with Hemps Seeds and *St.John's Wort* extracts are smaller in size than the synthesized with Rosemary/Cherry Laurel and in both samples AgNPs were distributed homogeneously in the matrix. Table 4.2 also shows this differences in crystallite sizes with the Debye-Scherer's calculation and found for C and D samples respectively, 12 nm and 21 nm. The sizes of nano silvers were found to be similar to the nanoparticle sizes bio-synthesized by Uzunoğlu et.al.,(2020). Differences in the sizes of green-synthesized AgNPs according to plant extracts may occur due to many factors, as mentioned in M. Prakash et.al's study. Parameters such as concentration, pH, timing, and temperature of the plant extract and metal salt solution influence the size, shape and purity of the synthesized nanoparticles. Since it changes the shape, structure and yield of nanoparticles by affecting the structure of metal ions, one of the most effective parameters is the pH of the reaction medium (Prakash et al. 2022). Aldeen T.S. et.al. explained the nanoparticle synthesis mechanism with through the interaction of positively charged metal ions with polyphenols and OH^- groups that comes from plant extracts (Aldeen et al. 2022). The electrochemical potential difference that occurs in the solution is the main reason behind the interaction of ionic silver and secondary metabolite components. Secondary metabolites include flavonoids, tannins, polyphenols, and gallic acid contains high concentrations of –OH groups. The hydroxyl groups present in polyphenols are oxidized and release electrons. These electrons are involved in the reduction of Ag^+. After atomic silver Ag^0 formation, NPs are formed by agglomerations and these reactions are called nucleation. Polyphenols complexing with metallic silver and binding with biomolecules provide stabilization of nanoparticles (Perveen et al. 2021). Since Hemp Seeds and St. John's Wort (Alahmad et al. 2021a; Csakvari et al. 2021a) are quite rich in flavonoids compared to Rosemary and Cherry Laurel (Csakvari et al. 2021a; Lešnik et al. 2021b), AgNPs sizes are smaller and properly shaped, since they perform the reduction and stabilization of silver ions more effectively. Apart from secondary metabolites, another important factor effective in green synthesis was pH. It has been shown that when the solution pH is more basic, it enables the synthesis of nanoparticles in smaller sizes compared to acidic environments and prevents their agglomeration (Drummer et al. 2021;

Chandhru et al. 2022). While the pH value of AgNPs solution synthesized with Hemp seeds and St. John's Wort extracts was 5.5, the pH value of AgNPs solution synthesized with Rosemary and Cherry Laurel extracts was found to be 4.7. The size, morphology and agglomeration differences of AgNPs synthesized with Hemp seed-St. St. John's Wort and Rosemary-Cherry Laurel plant groups used in the study can be explained by the reasons mentioned. It has been revealed that nanoparticles synthesized with Hemp seeds- St John's Wort plant extracts are clearly more homogeneous, have smaller dimensions, and undergo less agglomeration.

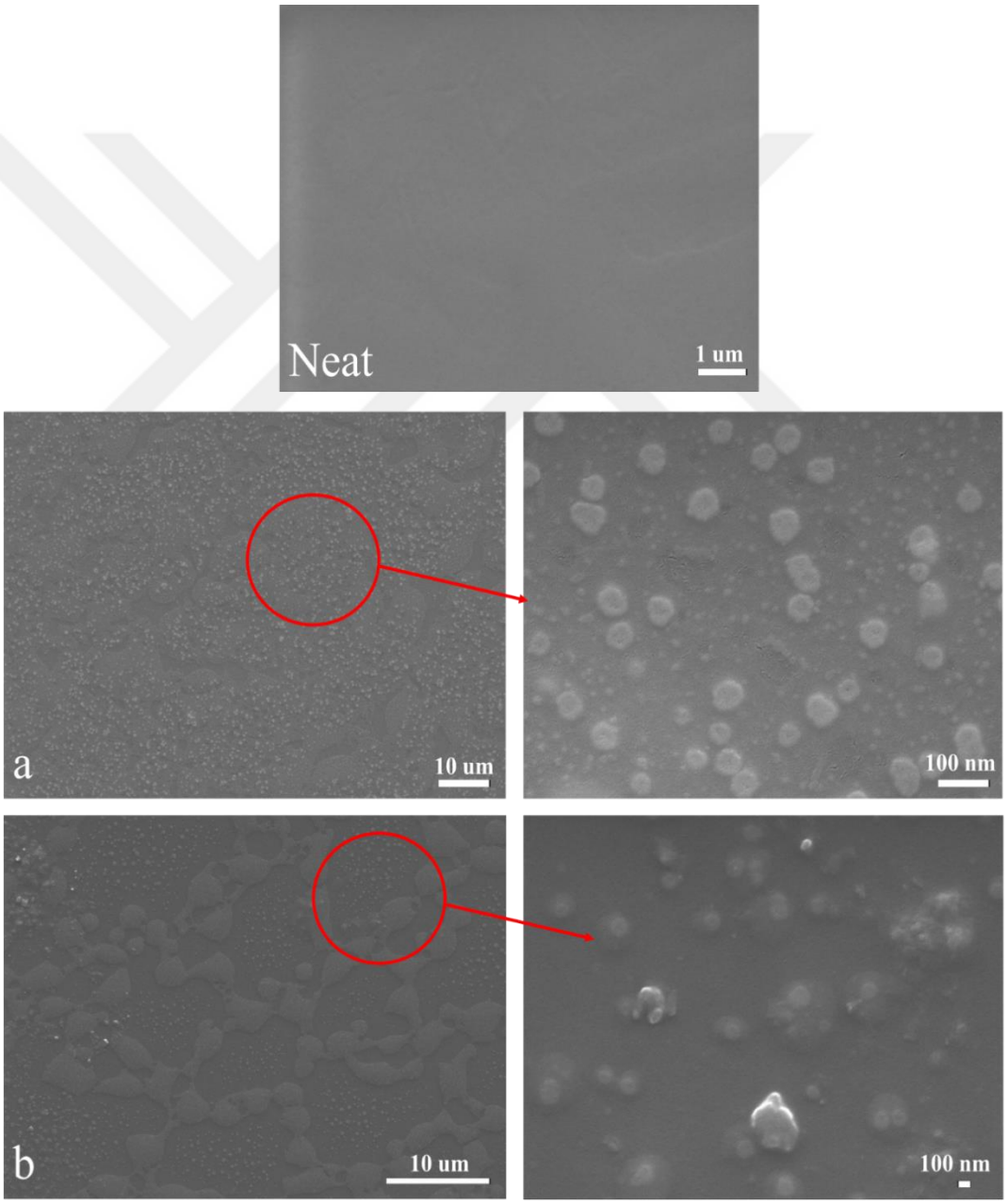

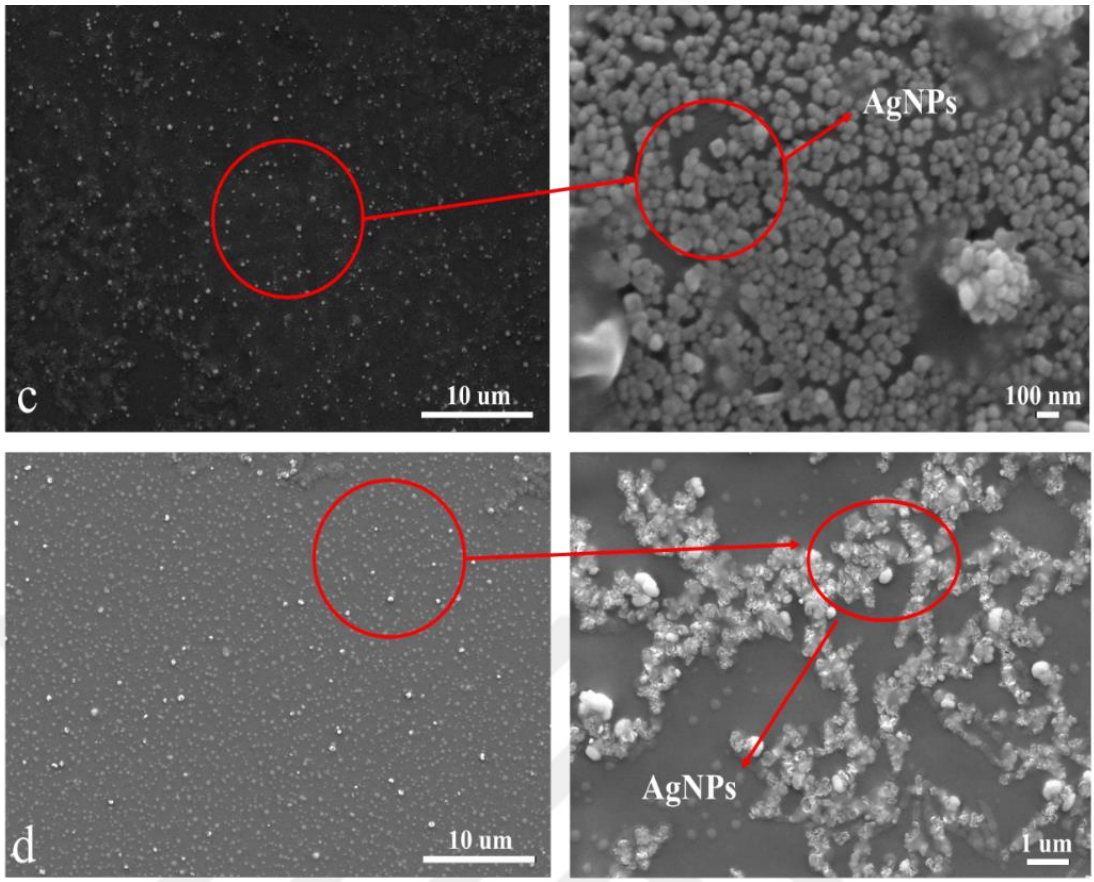

Figure 4.2 SEM images of a) Hemp/*St.John's Wort*-PVA. b) Rosemary/*Cherry Laurel*-PVA. c) AgNPs- Hemp/*St.John's Wort*-PVA and d) AgNPs- Rosemary/*Cherry Laurel*-PVA nanocomposite films and neat film.

When the EDS mapping was examined in Figure 4.3, it was seen that the silver nanoparticles were present and homogeneously distributed over the entire C sample surface. In some regions silver nanoparticles undergo agglomeration but the amount was at low level. EDS spectrum analysis was performed on the C sample and results are also shown in Figure 4.3(a). White dots in the sample surface are silver nano particles. In addition, in the results of the mapping and spectrum analyz, it was observed that there were also C and O main elements along the entire surface, apart from Ag. The amount of Ag on the sample surface is about 65.7% by volume. This ratio shows that the produced C sample is much more rich in AgNPs.

Similarly, in the Figure 4.3(b) EDS mapping and spectrum analyzes of the D sample, the presence of AgNPs can be distinguished. However, when the mapping analysis image in Figure 4.3(b) is examined, it can be seen that AgNPs agglomerated and were locally dispersed in the film. As in the C sample, the presence of C and O main elements is observed in this D sample as well. It is assumed that the basic C and

O elements seen in the EDS spectrum analysis come from the structure of PVA or from different factors. It is also given in the results of the EDS analysis found in similar studies (Li et al. 2022; Mokhtari-Hosseini et al. 2022a). Beside that, it was seen that the Ag element ratio in the D sample is 25% and this value is 40% less when compared to C sample. According to the SEM and EDS results, the rate of AgNPs synthesized green with Hemp seeds and St. John's Wort plant extracts was higher, and nanoparticle sizes could be synthesized in smaller sizes. Nevertheless Rosemary and Cherry Laurel leaves were also successful in the production of AgNPs by green synthesis.

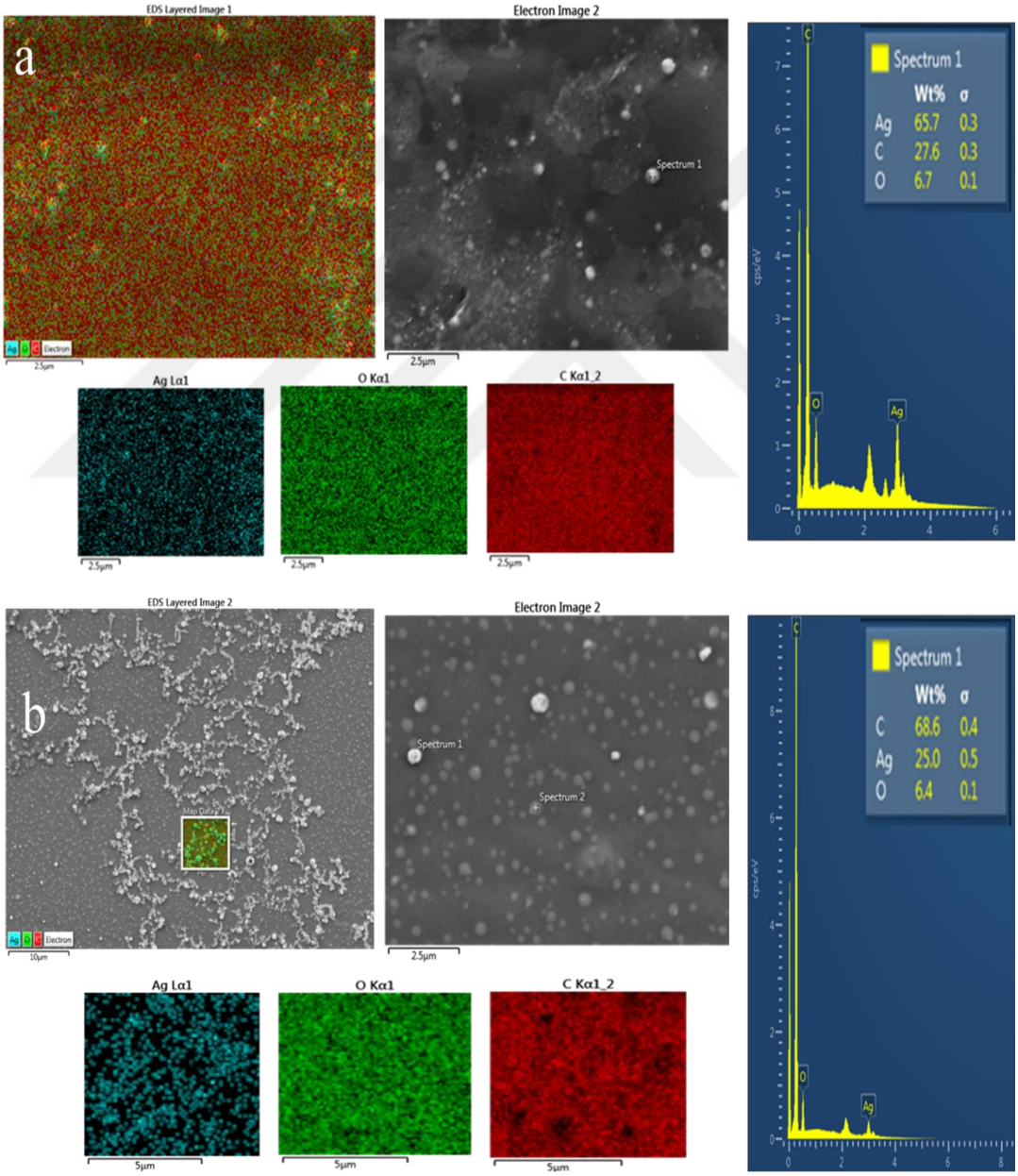

Figure 4.3 EDS mapping and spectrum analysis results of (a) AgNPs-Hemp-*St.John's Wort* nanocomposite and (b) AgNPs-Rosemary-*Cherry Laure* nanocomposite films.

4.1.2. X-Ray Diffraction Analysis

The film substrates were characterized using XRD with Rigaku Smart Lab CuKα radiation monochromatic filter in the range 20°–80°. XRD analyzes of silver and plant added films and only plant added films were carried out separately and the presence and crystallite sizes of silver nanoparticles were investigated. Debye-Scherer's equation 4.1 was used to calculate the crystallites size and microstrain of silver nanoparticles. Debye-Scherer's equation is;

$$D = \frac{K\lambda}{\beta cos\theta} \quad \textbf{(4.1)}$$

where D is the Crystallites size (nm), *K* the so-called shape or geometry factor which usually takes a value of about 0.9 (Scherer constant), λ the X-ray wavelength (k = 0.1541 nm), β the full width at half maximum (FWHM) of diffraction peak and ‘‘θ’’ the diffraction angle.

Williamson-Hall (W–H) equation 4.2 used for microstrain calculations. The microstrain values of AgNPs crystallites have been calculated by using W–H relation using the XRD peaks and the equation is;

$$Bcos\theta = \left(\frac{k\lambda}{D}\right) + 4\varepsilon sin\theta$$
$$Microstrain(\varepsilon) = \frac{\beta}{4tan\theta} \quad \textbf{(4.2)}$$

XRD analyses were performed on 1x1 mm-sized film samples. The XRD patterns of neat pure PVA film and the nanocomposite films prepared with Plant Extract/AgNPs are depicted in the range of $10° \leq 2\theta \geq 80°$ at room temperature with the rate of 2°/min. XRD analysis pattern results are shown in Figure 4.4. Neat sample which is pure PVA indicates a diffraction band at 2θ = 19.50°, which is attributed to the partially crystalline nature as a result of strong intermolecular hydrogen bonding between the PVA chains (Darwish et al. 2022). It was observed that the intensity of the main peak at 2θ = 19.50° decreased with AgNPs/Plant Extract modifications in the PVA matrix. All the prominent peaks (111), (200) and (220) and (311) at 2θ values of approximately 38˚, 44.2˚, 64.4˚, 77.6˚ reflects represent Bragg's reflections of the face-centred cubic (fcc) structure of silver and this results was found to similar in (Mudhafar

et al. 2022; Mokhtari-Hosseini et al. 2022b; Rajati et al. 2022) studies. The broadening of peaks in the X-ray diffraction pattern is generally related to smaller particle size. The XRD patterns clearly exhibit the presence of silver nanoparticles in nanocomposite forms. Since crystal structure formation did not occur in A and B samples, sharp peaks were not obtained in the XRD results.

FWHM and peak positions were determined from XRD and then calculated the crystallites sizes and microstrains of film samples and shown in Table 4.1. Crystallite size in monodisperse microstructures is usually approximated from X-ray diffraction patterns and grain size by other experimental techniques like transmission electron microscopy. A crystallite is a small or even microscopic crystal which forms, for example, during the cooling of many materials. The term is often used to refer to the size of individual crystalline domains in a material, such as nanoparticles, nanopowders, colloids, gels, and spray-dried agglomerates. In general, it corresponds to the coherent volume in the material for the corresponding diffraction peak. Sometimes it also corresponds to the size of nanoparticle grains (Abdul Halim et al. 2023; Al-Bermany et al. 2023; Donya et al. 2020; Morad et al. 2020; Sharif et al. 2022).

Average AgNPs crystallites size in C sample calculated to be 12 nm and in D sample calculated to be 21 nm. Also microstrain values were found $38x10^{-3}$ for C and $16x10^{-3}$ for D samples. The variation of lattice strain of the films shows that the microstrain is tensile ($\varepsilon>0$). Many factors can influence the structural properties of films like crystallinity state, preferential orientation, grain size, microstrain as well as the dislocation density, might be related, change of the film thickness, change of the concentrations of solution and nanoparticle sizes during production process (Dolabella et al. 2022; Shaaban et al. 2009). The calculated microstrain values for sample C is approximately 2.5 times higher than D sample. Due to the smaller size of AgNPs in sample C, the total surface area of the particles was higher. The factor that causes this situation is due to the fact that the microtension in a crystallite depends on the average crystallite size. In the literature, it has been mentioned that this behavior of nano-sized particles causes the spacing between planes to decrease as the particle sizes decrease (Darwish et al. 2022). The increase in the total surface area increases the effect of surface tension force and creates compression in the structure and thus a decrease in the distance between the planes occurs. This compressive force increases as the

crystallite size decreases and leads to an increase in micro-tension in the nanocrystalline. The fact that the microstrain of the C sample is 2 times higher than that of the D sample can also be explained by the high C=O and C=C bond ratios formed by the plant extracts and AgNPs in the C sample with PVA, which is shown in the FTIR spectra in Figure 4.5.

Table 4.1 Crystallites size and microstrain of AgNPs from Scherer's equation (D_{SCH}) and Williamson-Hall Plot.

Film Samples	**Crystallites Size**	**Microstrain(ε)**
AgNPs-Hemp-*St.John's Wort(C)*	12 nm	$38x10^{-3}$
AgNPs-Rosemary-*Cherry Laurel(D)*	21 nm	$16x10^{-3}$

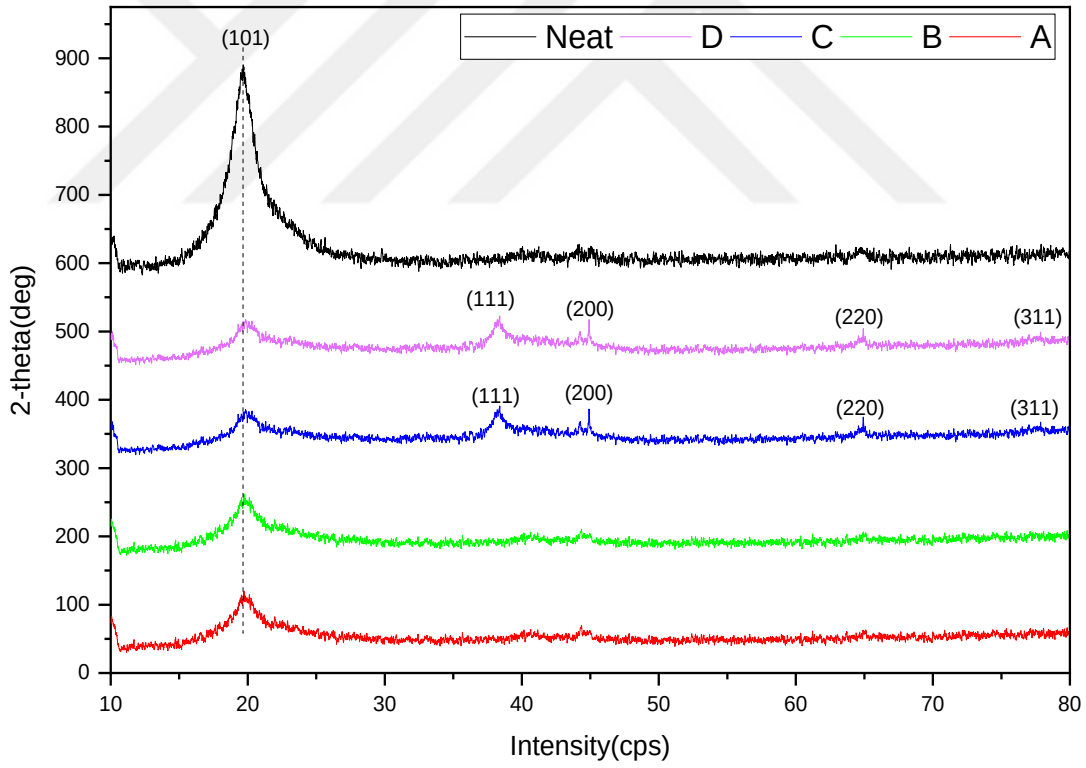

Figure 4.4 XRD results of neat film, plant extract and AgNPs modified nanocomposite polymer films.

4.1.3. Fouirer Transform Infrared Spektrofotometre (FTIR)

To characterize the influence of plant extracts and silver nanoparticles on the chemical structure PVA matrix, FT-IR analysis (Bruker Tensor 27) was performed in the wavenumber range of 650–4000 cm^{-1}. Nanocomposite films and neat film 1x1mm square samples were analyzed and interpreted by FTIR analysis. The FT-IR spectra of neat-PVA film and all other nanocomposite films are shown in Figure 4.5. The unique absorption peaks of PVA structure were seen in all spectra. 3267 cm^{-1} denoted the –O–H stretching vibrations, while the band at 2915 cm^{-1} ascribed to the asymmetric stretching vibrations of C–H (Mathew et al. 2019). At wavenumber regions consistent with the previously reported FT-IR spectra of PVA, CH_2 asymmetric stretching vibration (2910 cm^{-1}), C=C stretch (1648 cm^{-1}), C–H bending vibration of CH_2 (1410 cm^{-1}), C–H deformation vibration (1319 cm^{-1}), C–O stretching of acetyl groups (1084 cm^{-1}), CH_2 rocking (916 cm^{-1}), and C–C stretching vibration (825 cm^{-1}) were detected. The appearance of a new moderate band at 1648 cm^{-1} in the case of C and D film was due to the stretching vibrations of C=C bonds of heterocyclic compounds present in Hemp Seeds-St. John's Wort extracts.

FTIR analysis results given in Figure 4.5 indicate an increase. In the vibrations of the O–H, C–H and C=O groups in the PVA structure, after the AgNPs were added directly to the PVA matrix, some polymer chains were broken and other chains were formed instead. The increase of the FTIR spectrum in the range of 1300 to 1600 cm^{-1} corresponds to the C–H bond of CH_2 and indicates broken chains. AgNPs formed new bonds in this range. The band of C=O is weakened and shift from 1711 cm^{-1} to 1648 cm^{-1}, because oxygen atoms provide duplet filling in empty track on the surface of Ag atoms and also benzene rings in the plant extracts (Zhang et al. 2016; Abdelghany et al. 2019). The decrease of the FTIR spectrum in the range of 2500 to 3700 cm^{-1} indicates that the polymer chains produced correspond to the O–H stretch and C–H stretch bond (Ghanipour and Dorranian 2013). In addition, plant extracts caused a decrease in the stretching vibration bands of O–H and C–O bonds in the structure. This phenomenon indicates that plant extracts also alter the polymeric network of PVA. The new bonds formed between the hydroxylic bonds of the flavonoids in plant extracts and the PVA chain caused the formation of C=C bonds instead of C=O vibrations. C-H, C=C, C-O and C-C bond vibrations are stronger in the IR peaks of Hemp Seeds-St.John's Wort added films (A and C). These different intensities of

bonds formed in samples C and D better explain the AgNPs size differences in Figure 4.2 and 4.3 Hemp Seeds-St. John's Wort has the ability to break and form more bonds with the concentration of secondary metabolites in its content. All results show interaction between AgNPs/PVA and plant extracts. In addition, all these functional groups represent polyphenols, flavonoids and phenolic acids from secondary metabolites in plant extracts used in green synthesis, which may be responsible for metal salt reduction and stabilization of produced AgNPs (Batool et al. 2019).

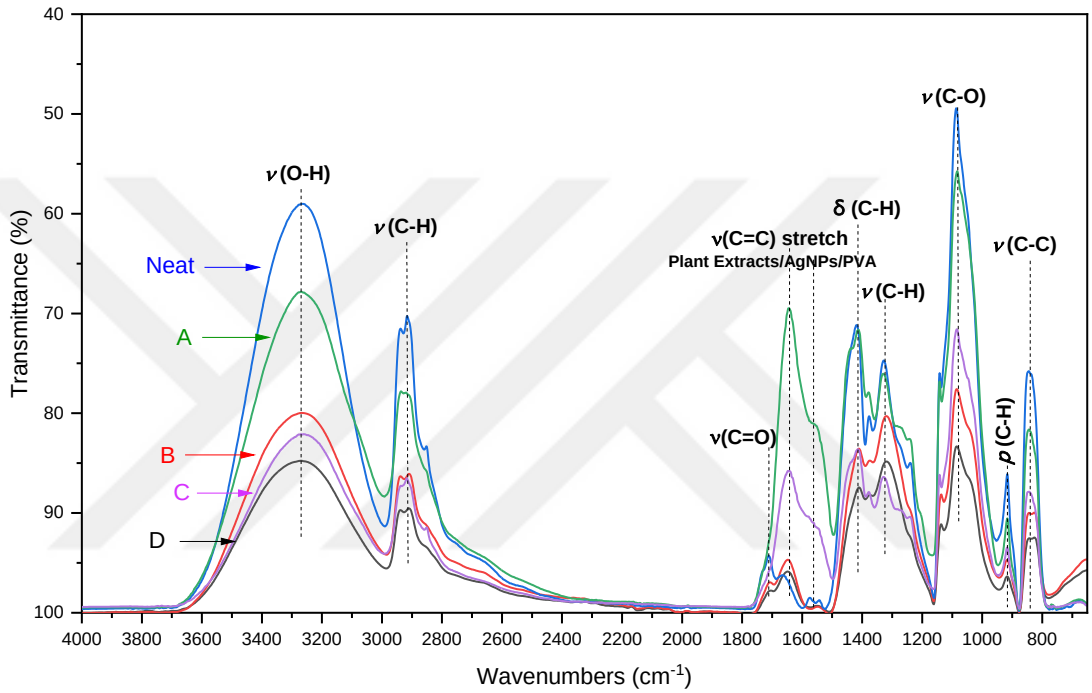

Figure 4.5 FT-IR spectra of fabricated film samples. (Neat) Non-modified PVA film, (A) Hemp Seeds-St. John's Wort extract containing PVA film, (B) Rosemary-Cherry Laurel extract containing PVA film, (C) Hemp Seeds-St. John's Wort-AgNPs containing PVA film, and (D) Rosemary-Cherry Laurel-AgNPs containing PVA film.

4.1.4. Differential Scanning Calorimetry (DSC)

Differential scanning calorimetry (DSC) was used to examine the crystallinity and stability of prepared nanocomposite films were studied. A small sample piece (~8 mg) was placed in an aluminum standard pan with a holed lid and analyzed with a DSC Q2000 (TA Instruments) DSC instrument. The melting temperature (T_m), decomposition (T_{Ds}) and glass transition temperature (T_g) are examined. Samples were scanned at a heating rate of 10 °C/min over the temperature range of − 25 to 200 °C in

a nitrogen atmosphere with an established flow rate of 10 mL min^{-1} .

Figure 4.6 shows DSC thermograms of Plant Extracts/AgNPs modifed and neat nanocomposite PVA samples. Three different endothermic phase transitions occurred for the neat sample, and these were at temperatures of 41.27 ˚C T_g, 134.13 ˚C T_m, 197.10 ˚C T_{Ds}. These thermal transformation temperatures obtained for PVA are suitable values according to the literature (Abd El-Kader et al. 2010). The thermal event occurring at 41.27 ˚C represents the crystal volume decompositions (glass transition temperature) in the PVA structure, the sharp endothermic peak at 134.13 ˚C represents the melting of the crystal structure, and the endothermic peak at 197.10 ˚C represents the thermal decomposition temperatures of PVA (Delgado-Rangel et al. 2019). The fact that the melting temperature of the neat sample is above 130 ˚C indicates that the crystallinity value of the PVA film is high (Bai et al. 2021). All samples clearly appear to have T_g temperature range of 41.27-43.10 ˚C. Addition of plant extract and nanosilver increased the glass transition temperatures of nanocomposite films by 2 ˚C. The weakness or shifts in T_g value seen in all polymer films are mainly due to the evaporation of water molecules as residual solvent. It is known that the decrease in the melting temperatures of the samples occurs due to the reduction of the crystallinity of the additives modified into PVA or the degradation of the polymer structure. Similarly, with the modification, an increase in the melting temperatures (T_m) occurred especially in the D sample, where plant extract and nano silver particles were found together. The melting temperatures of the films were increased from 134.14 ˚C to 150.54 ˚C. With the addition of plant extracts to the PVA structure, the decrease in the degree of crystallinity in the structure of polymer chains can also be seen from the XRD peaks in Figure 4.4. This decrease in the degree of crystallinity caused the melting curve of the D sample to be narrower and smaller in DSC thermograms. It can be said that the melting temperature of sample D is higher than that of the other samples due to the C=O and C=C bonds also seen in the Figure 4.5 FTIR spectras. Cross-linking between the secondary bonds in the structure of collagen and the hydroxyl -OH groups in the AgNPs and PVA structure increased the melting temperature. Although the addition of plant extracts and AgNPs caused the PVA films to exhibit thermal instability, it increased the melting temperature. There was no significant increase in the decomposition temperatures of the films. However, the sample with the highest Td temperature value was the D sample with 197.79 °C.

In other words, modification of plant extracts and AgNPs increased the degradation resistance of PVA nanocomposite films at high temperatures.

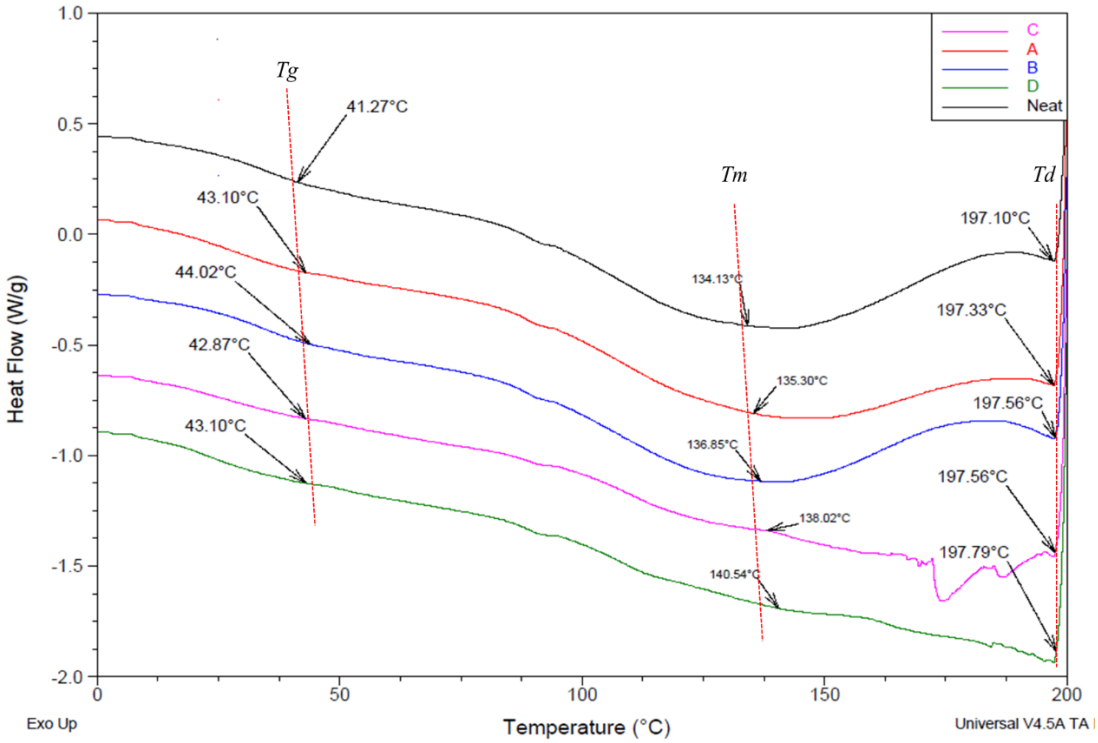

Figure 4.6 DSC curves of the neat sample and modified nanocomposite films.

4.1.5. Dynamic Mechanical Analysis (DMA)

Based on the results of microstructural, mechanical, antibacterial, and water absorption tests, the plant extracts used as the coating material were selected as hemp seeds St. John's Wort. The green-synthesized nanoparticle modifications to be applied to the coatings were chosen as 0.05, 0.1, 0.3, and 0.5% based on both the studies in the literature and the experimental studies. Dynamic mechanical analysis was performed on the nanocomposite films produced from the coating solutions prepared with the determined ratios, and their mechanical properties under thermal conditions were investigated. Thus, their resistance in the oral environment and high-temperature applications has been determined.

Dynamic mechanical analysis (DMA) was performed on a DMA, Q800 T.A Instruments in the tension mode. The experiments were performed at a heating rate of 3 °C/min, from 20 to 200 °C, at 1 Hz at a frequency to investigate the mechanical, dynamic mechanical properties of coating films. The sample sizes were 18 mm × 6

mm × 0.13 mm. The glass transition temperature T_g was determined by the peak of the tan δ curve. In addition, storage, and loss modulus have all been computed.

The storage (elastic) modulus (*E'*) is the ability of a material to store energy during a loading cycle. It also provides information on the crosslinking grade, material toughness, and fiber/matrix interfacial attachment. The loss (viscous) modulus (*E''*) is the viscous component of a material and its ability to dissipate mechanical energy through its internal molecular mobility. Tan Delta (tan δ) measures mechanical vibration damping. This indicates that the material loses energy owing to internal friction and molecular arrangement. This can reveal the material behavior in the rubbery region. The tan delta represents the ratio of the elastic (*E'*) to viscous (*E'*) properties. Glass transition temperature (T_g) is a crucial property of polymeric materials. This is the point at which a material changes from the glassy phase to the rubbery phase (Lee et al. 2022; Raja et al. 2022; Venkategowda et al. 2022).

Change of storage modulus of composite films with temperature is shown in Figure 4.7. The storage modulus decreases with increasing temperature but it increases with increasing amount of Ag nanoparticles in the films up to % 0.3 and 0.5. Furthermore, E′ increases more effectively at temperatures below 50 °C (the glass transition temperature of pure PVA) as the AgNPs concentration increases up to % 0.3 and 0.5. The dynamic mechanical analysis results given in Table 4.2 show that the storage modulus of A, D and E samples increased by 30%, 50% and 54%, respectively, compared to the neat sample with plant extracts and nanoparticle modifications. It was calculated that there was a decrease of 58% and 181% in samples B and C. (*E''*) is dependent on the fillers' shape, size and dimension that determine the elastic characteristics of composite materials. It is also depentdent on crosslink density, intermolecular adhesion and the type of interlink between filler and matrix (El-Deeb et al. 2022). It is estimated that these decreases are due to inhomogeneous distributions, low bonding rates with PVA chains and production conditions, which may have occurred due to the low ratio of nanoparticles modified to B and C samples compared to the matrix. Also the interaction between OH groups of PVA, plant extracts and moisture affects the crystalline regions. This OH groups moisture interaction is disturbed by AgNPs inclusion resulting in lower moisture content and lower mobility. The increase in the storage modulus of D and E nanocomposite films shows that Ag

nanoparticles (nanofillers) have a significant reinforcing effect. Nanofillers, which restrict the mobility of the polymer chain due to their large surface area and provide Van der Waals attraction to the polymer matrix, strengthened the mechanical properties of Ag-PVA nanocomposite films (Gautam and Ram 2010). In addition, 0.5% AgNPs modification allowed the highest strength temperature of the nanocomposite film to increase from 24 ˚C (Neat Sample) to 34 ˚C. E' tends to be wider in the glassy region, as the components are in a closed, tightly arranged, and frozen state and achieve high E' below T_g. As the temperature increases, E' experiences a sharp drop at about 30 to 60 °C, indicating a glassy/rubbery state transition. Micro-Brown movement of the polymeric chains near T_g reduces the value of the storage module. Thus, as the temperature increases, the molecular mobility increases; thus, the tightly packed structure loses its packed arrangement, which leads to a reduction of E (Mat Yazik et al. 2021).

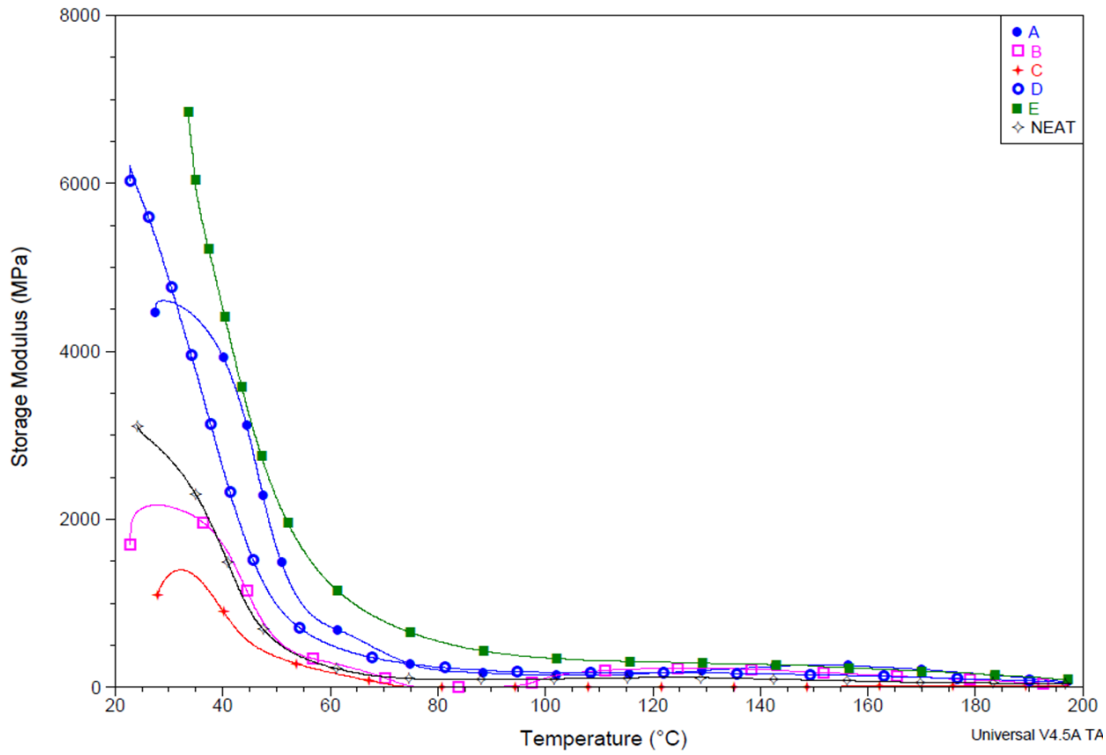

Figure 4.7 Storage modulus as a function of temperature of nanocomposite films for ESD coating.

The loss modulus (*E''*) of nanocomposite films are shown in Figure 4.8. Results show the viscous response and heat dissipation with peak values during the temperature increasing from 20 °C to 70 °C. The loss modulus exhibited similar

behavior with the storage modulus, increasing in samples D and E with AgNPs modifications of 0.3 and 0.5%, and similarly, samples B and C showed a dramatic decrease. This result indicates that the D and E samples have a high energy dissipation range compared to the neat sample. Addition of AgNPs caused the loss modulus peak to rise. This increase occurred as a result of strong bonding between nanoparticles, plant extracts and PVA and homogeneous distributions in the matrix. The decrease in peaks in samples A, B and C may be due to inhibition of the relaxation process in the composites or may be the result of insufficient crosslinking. This is possible when there is an increase in the number of chain segments and free volume with plant extract particles. This is largely due to the segmental immobilization of the matrix chain with inhomogeneous distribution on the fill surface (El-Deeb et al. 2022).

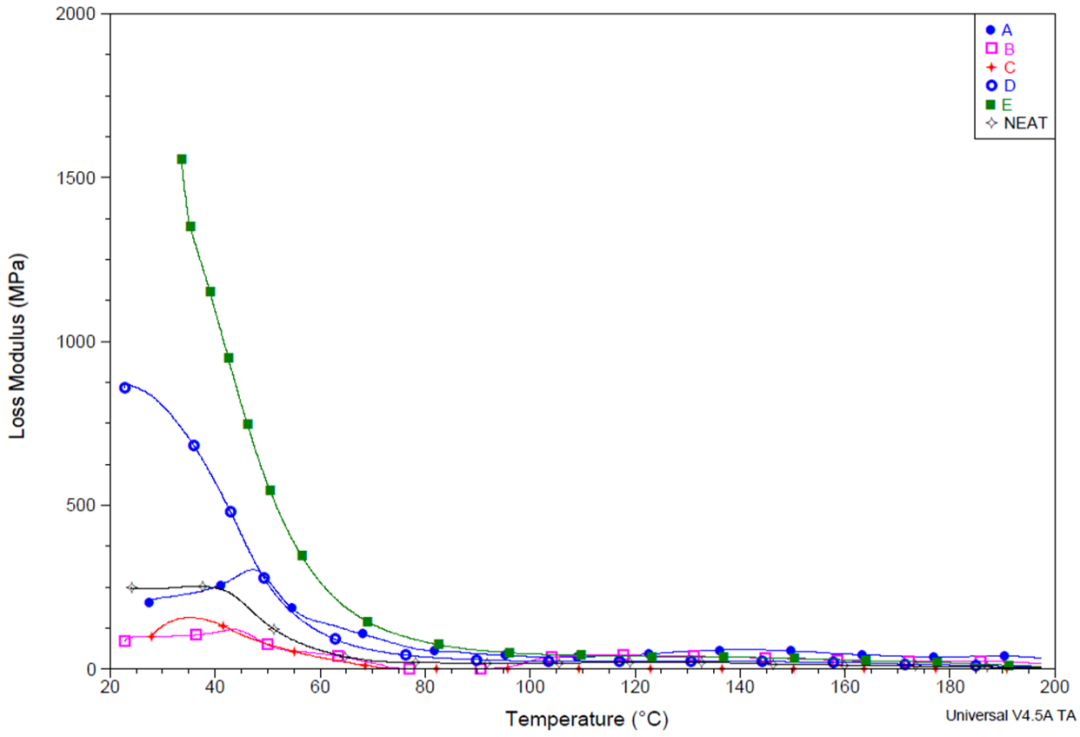

Figure 4.8 Loss modulus as a function of temperature of nanocomposite films for ESD coating.

Tan delta (peak value) usually decreases with the addition of a reinforcing filler or a filler that can interact with the polymer matrix. This is because the relaxation amplitude of polymer chain segments decreases due to the polymer-nano filler interaction. However the area under the tan delta peak incerases with incerase in filler content which is also an indication of damping characterstics of the filled polymer system. When increase the nano filler content the amount of free volume decreases.

This reduction in free volume reduces the mobility of atoms and increase the friction by large contact in polymer. So the storage modulus and tan delta get decreases. Broad tan delta is likely due to non-homogeneity of crosslink density, due to differing polymer chain lengths in the case of broad polydispersity. It can also see the broad response in both storage and loss modulus in Figure 4.7 and 4.8.

The tan delta results of nanocomposite films are shown in Figure 4.9. When the filler loading increases from 0.05 wt.% to 0.1 wt.% of AgNPs, the tan δ peak value decreases, however a further rise in filler loading to 0.3 and 0.5 wt.% of AgNPs leads to an increase in the tan δ peak value. The inclusion of a higher amount of fillers into the PVA matrix determines the formation of agglomeration and clusters of nanofiller, which gives rise to vacant spaces and enables polymer chains to move or rotate freely, thereby increasing the viscoelastic performance. It is also apparent that the incorporation of a hybrid nanoparticles and plant exctracs into PVA broadens the tan δ peak, compared to that of the neat sample. It is clearly seen that samples A, B and C show relaxations a (primary) and b (secondary) at 84, 63 and 75 ˚C, respectively. β relaxation is associated with rotational modes of dissociation and re-bonding of hydrogen bondings of amide groups in crystalline state with strong intermolecular bonds for the PVA/Plant Extracts/AgNPs bonds, while β relaxation indicates the motions of amorphous amide groups. Higher α relaxation temperature of PVA with increasing AgNPs contents indicates that the movement of main chains was restricted due to the increased number of stronger interfacial hydrogen bonds of AgNPs-PVA upon increasing AgNps contents. There is an irregularity in the rubber regions of the tan delta peaks of the B and C samples. It can be said that this behavior is caused by the irregular movements of the nano particles in the polymer after softening and the evaporation of water. After this transition, there is a sudden increase in the tan delta value of the B sample in the terminal region. The fact that it has a lower nano silver ratio than the C sample has enabled the structure of the composite film to become stable faster with the increase in temperature, with the polymer chains moving more easily. This behavior is observed similarly in sample B. On the other hand, D and E samples have tan delta values and peak behavior close to the neat sample (Burgaz et al. 2009). Additionally, the observed broad tan δ peaks showed that the glass transition temperature occurs over a temperature range instead of appearing as a sharp peak. The results showed that nano-silver modification with PVA over 0.3% increased the

rigidity of nanocomposites compared to the nat sample, and below 0.3%, it increased the viscoelasticity of the films. Similarly, the tan delta value of the A sample is 0.17, while the tan delta value of the neat sample is 0.25, indicating that plant extracts also provide elasticity to the nanocomposites.

The maximum peak point of the tan delta is called glass transition temperature (T_g). Also the primary relaxation (the α-peak) of tan delta corresponding to the T_g results from the initiation of micro-Brownian motion of the amorphous chain (Madian and Mohamed 2020; Rana et al. 2010). T_g values of nanocomposites are shown in Table 4.2. While the neat sample had a glass transition temperature of 50 ˚C, the sample with the highest T_g temperature was the C film with 52 ˚C. It was observed that the T_g temperature of the films decreased by 2 ˚C with nano silver modification of more than 0.3% formation of hydrogen bonds between PVA hydroxyl groups and water, and hydrogen bonds are the dominant interaction responsible for the structure as well as its molecular dynamics. It is possible that the interaction between OH^- groups and moisture is capable to destroy inter- and intrachain bonding in PVA affecting its crystalline regions; therefore, water acts as a plasticizer by an increase of the free volume in the amorphous phase (González-Campos et al. 2012).

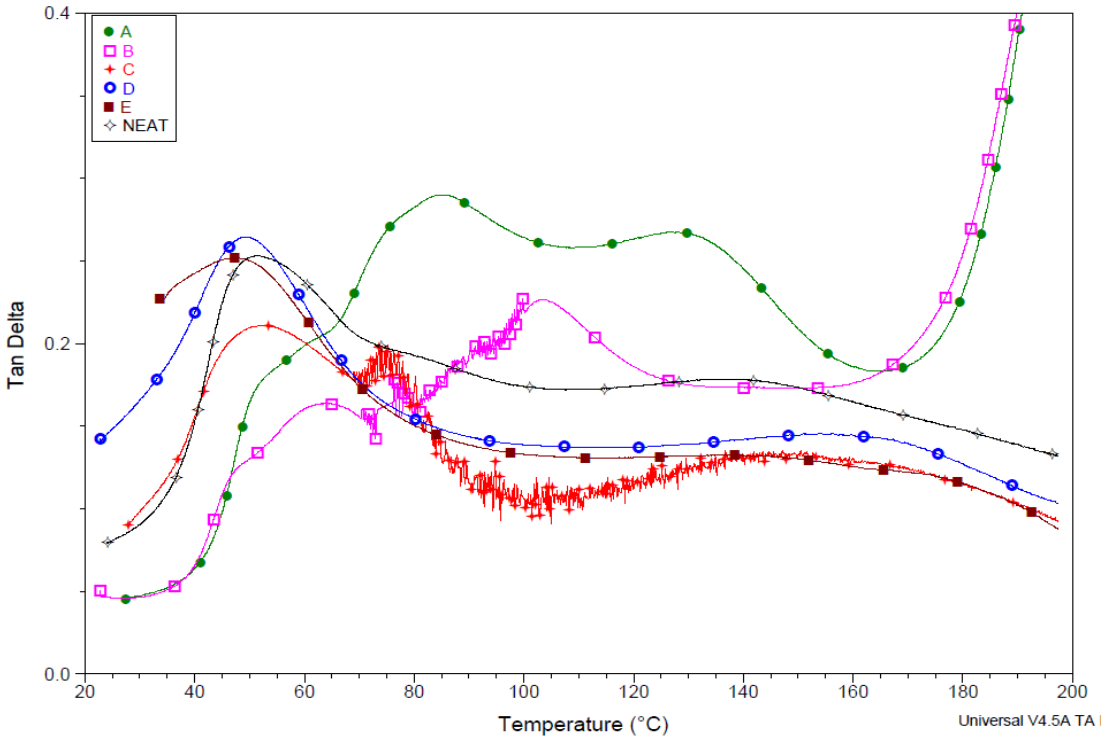

Figure 4.9 Tan δ as a function of temperature of nanocomposite films for ESD coating.

Table 4.2 Data of dynamic mechanical analysis.

Data Of Dynamic Mechanical Analysis				
	Loss modulus (E'') in MPa	**Storage modulus (E'') in MPa**	**Damping factor (tan δ)**	**T_g (°C)**
Neat	245	3115	0.25	50
A	202	4480	0.17	51
B	86	1968	0.12	47
C	99	1106	0.21	52
D	870	6211	0.26	49
E	1555	6851	0.24	48

4.2 Shore-D Hardness Tests

The Shore-D hardness for the samples were measured following an indentation technique by measuring the penetration depth of a durometer indenter with a Shore hardness meter. Test were conducted at room temperature and at least ten measurements were performed for each sample. Shore-D hardness tests were performed separately for nanocomposite films and neat film 2x2 mm square specimens. Hardness measurements were taken from 10 different regions on each sample and the averages of these values were calculated. The results of Shore-D hardness tests are presented in the Figure 4.10. Shore D hardness of all the polymer nanocomposites and reference sample were in the range of 27–50. As can be seen from the graph in Figure 4.7, the sample with the lowest hardness value is the reference sample with 27 and C sample has the highest hardness with a value of 49.6. It was obtained that the C sample has a hardness value of 85% higher than the reference sample. C sample also has a higher Shore hardness value than the D sample. The reason for this was AgNPs synthesized with Hemp seeds and *St. John's Wort* were smaller in size and that's mean this nano particles have larger surface area. With larger surface area nano particles filled the micropores in the polymer matrix and this made the C sample polymer structure much dense from the D samples. In addition, considering the microstrain values given in Table 4.1, the higher strain values between the crystal lattice structures of the C sample, indicate that the structure is more dense and rigid. It was observed that the hardness values of A and B composite films containing only plant extracts were quite close to the hardness values of AgNPs modified films. The

hardness value of the B sample was 48% higher than the reference sample. Factors such as high homogeneity, the difference in the bonds of the functional groups in plant extracts with the polymer and micro porosity may have caused the B sample to have a higher hardness value. Despite this, sample A also has a higher hardness value of 57% compared to the reference sample, and these results show that even polymer composite films with only plant extract have much higher hardness values compared to the reference samples.

The FTIR results given in Figure 4.5 showed that the C=C stress (1648 cm^{-1}) peaks formed as a result of the reaction of the plant extract containing nanocomposite films with PVA were higher than the neat sample. In addition, C–H bending vibration of CH_2 (1415 cm^{-1}), C–H deformation vibration (1327 cm^{-1}), C–O stretching of acetyl groups (1086 cm^{-1}) peaks of A and C samples were observed higher from samples B and D. It is known that the presence of C=C bonds increases the mechanical strength (Zhang et al. 2019) and therefore, as seen from the FTIR results, the C sample has the highest strength due to the high number of C=C, C-H and C-O bonds.

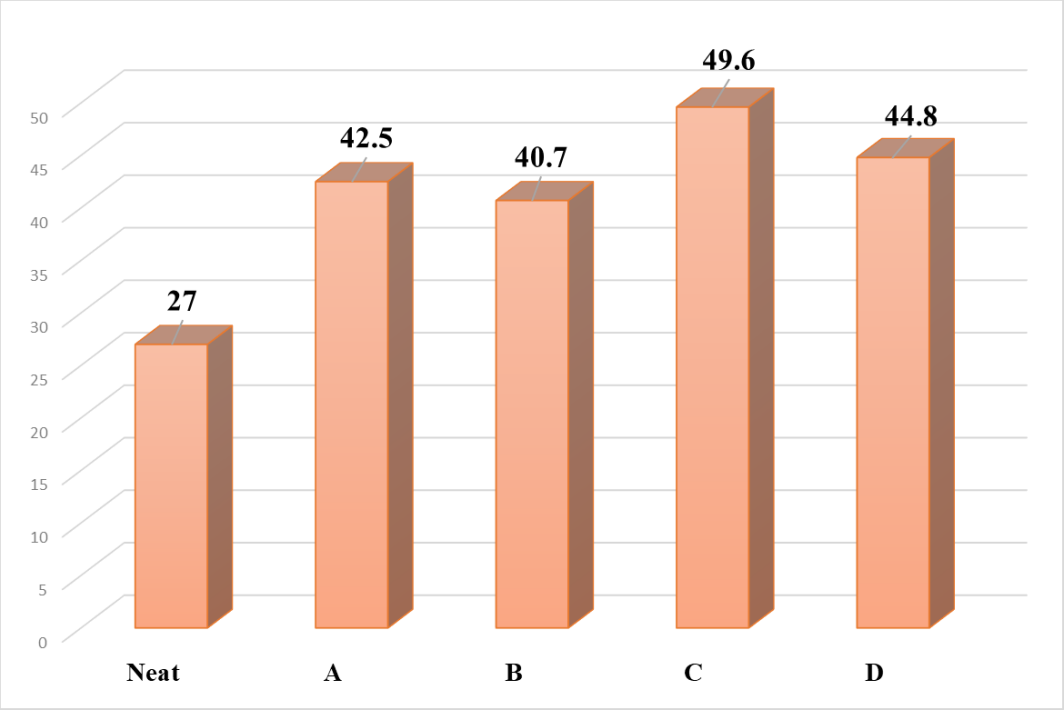

Figure 4.10 Shore-D hardness of polymer nanocomposite films.

4.3. Swelling Properties

Water swelling ability of all produced nanocomposite films and PVA (reference) films were investigated. First, the initial weights of the samples were measured before swelling test. Afterwards all samples were placed in 100 mL distilled water in separate petri dishes and kept at room temperature for 9 h. After that, the final weights of the samples taken out of the water were measured after the excess water was filtered. Swelling ratio of membrane *S* was found according to Equation (3);

$$S = (Ws - Wd)/Wd * 100\% \quad \textbf{(4.2)}$$

where W_s and W_d is the weight of wet film at equilibrium of absorption and the weight of dry film respectively.

The film samples volume changes before and after swelling test are shown in Figure 4.11. For the swelling test, 5 g pieces were cut from all nanocomposite films and they were kept in water for 9 hours at room temperature (27 ˚C). The swelling ratio results of the reference and polymer nanocomposite samples are shown in Figure 4.12. The swelling behavior of the films kept in water was visibly evident. It was calculated that the reference sample absorbed approximately 25% more water than samples C and D, and 19% less water than samples A and B, respectively. Since the swelling ratio of the polymer films depends on the polymer concentraions, crosslinks and hydroxyl groups formed between plants and PVA, the samples A and B might have a higher swelling ratio (Safaee-Ardakani et al. 2019; Qin et al. 2020). Apart from that, the higher water absorption rate of samples A and B containing only plant extracts can be attributed to the hydrophilic properties of Hemp seeds (Momeni et al. 2021), Rosemary (Darie-Niţă et al. 2018), St. John's Wort (Jarzębski et al. 2020) and Cherry Laurel (Vega et al. 2021) extracts. The reason why the water absorption rates of the samples C and D are much lower than the reference, samples C and D may be that AgNPs added to the films reduce the crosslink density, crystallinity and hydrophilic properties in the polymer matrix structure (Ounkaew et al. 2020). With the smaller size and larger surface area of AgNPs in the C and D samples, microporosity in the polymer matrix might was reduced compared to reference, A and B samples and this leads the reduce the swelling ratio.

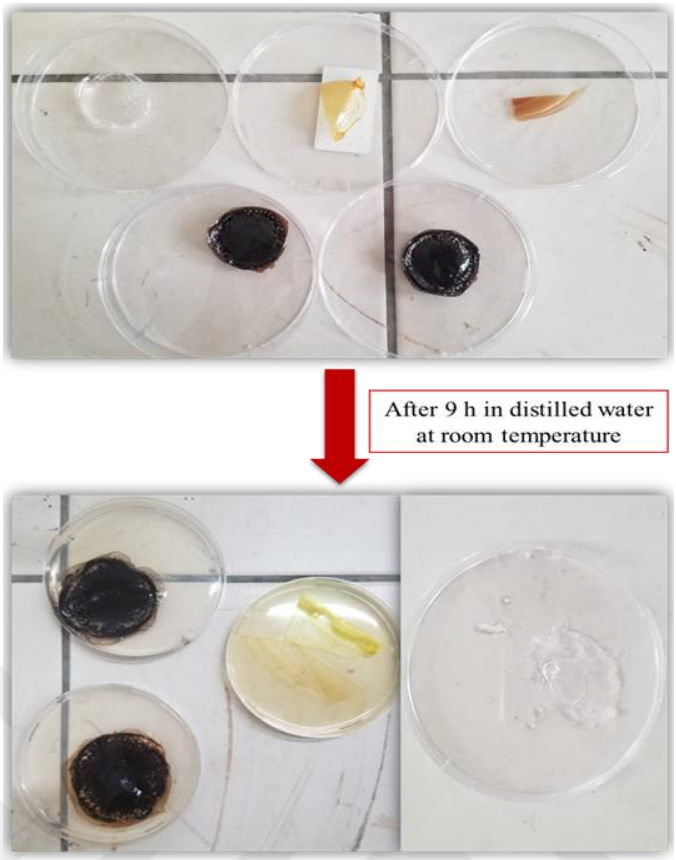

Figure 4.11 The nanocomposite film samples before and after swelling test.

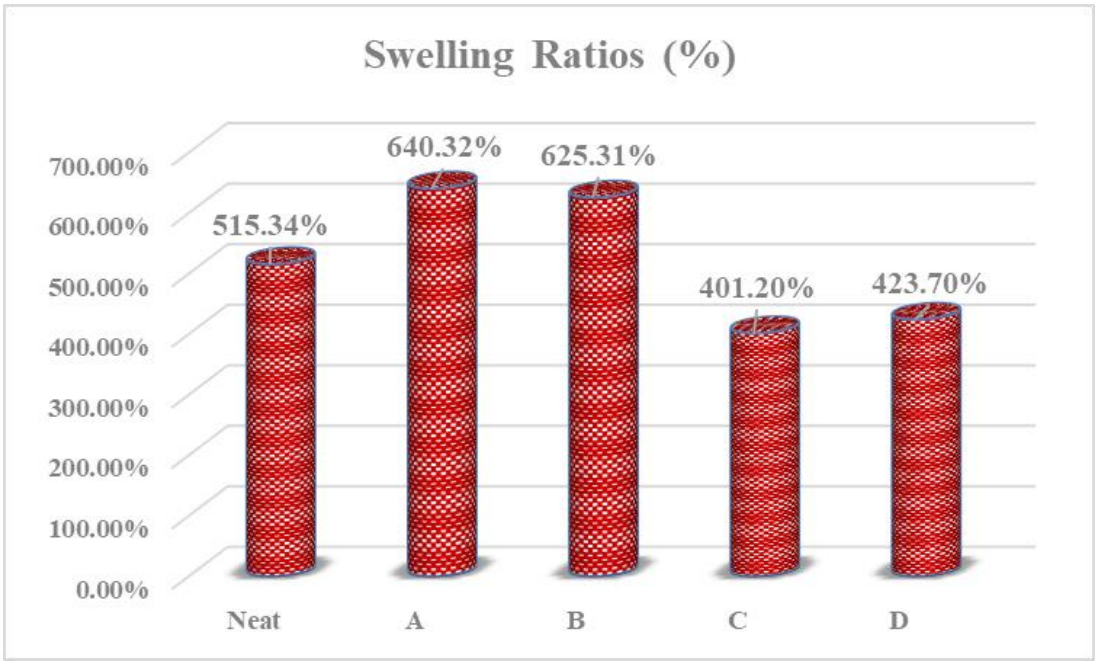

Figure 4.12 The swelling ratio (%) of all nanocomposite composite film samples.

4.4. Antibacterial Tests

The antibacterial activity both of AgNPs modified and non-modified PVA nanocomposite films were investigated. Antibacterial activities of the films were determined against gram-negative bacteria (*E. Coli*) and gram-positive bacteria (*S. Aureus*) by contact killing method. The 1x1mm sized polymer films sterilized with 70% ethanol and dried, was placed on the surface to spread the suspension and to reduce evaporation. The prepared bacterial suspension was applied to the polymer nanocomposite surfaces. After waited for 1m, *E. Coli* or *S. Aureus* suspensions were took from the surfaces and placed into the nutrient agar (NA) agar medium. Each agar plate was kept for incubation at 37 °C for 24 h. In addition, control groups were formed on the agars by placing bacterial solutions that did not contact the polymer nanocomposite films surface. All tests were carried out under the same conditions for each sample.

Antimicrobial tests were carried out on 1 mm x 1 mm nanocomposite films by contact technique. Bacterial growth in petri dishes after antibacterial tests are given in Figure 4.13 (a) and (b) show the bacterial groups and in petri dishes the top row was Staphylococcus aureus, the bottom group was E. Coli. The first row bacterial groups examined in two groups were placed in the petri dishes without contacting the produced PVA films which they were the control groups. The other two rows of bacteria groups were placed in the petri dish by contacting with all polymer nanocomposite films to see the bacterial growths.

Figure 4.13 (a) and (b) show activity of nanocomposite films against S. Aureus and E. Coli for C and D film samples. Since the control group bacteria suspensions were not contacted with the films, bacterial growth occurred in this regions. Bacterias contacted with C and D films before placed in bottom rows, did not grow on the petri dishes. In other words, the green synthsized AgNPs modified nanocomposite films killed the bacterias with contact and growth did not occur since AgNPs has antibacterial effect. In addition, when the unit colony (CFU/mL) numbers in 1 mL in Figure 4.14 are examined, it was seen that the bacterial growth in C and D samples was 0, control group were able to grow to a maximum of about 10^7 CFU/mL for both bacteria under the stated conditions. This graph shows that polymer nanocomposite films were very successful in killing bacteria and showed %100 antibacterial

efficiency with modification of green synthesized AgNPs. These results show that the Hemp seeds, St. John's Wort, Rosemary and Cherry Laurel leaf extracts had been very successful and effective in the synthesis of nano silver and have given antibacterial properties to the films. In Figure 4.13 (c) and (d), antibacterial activity of nanocomposite films against S. Aureus, and E.Coli for the plant extract added A and B film samples are given. Bacterial growth took place in two different plant extract-added films. That result shows the samples A and B were not effiecient against S. Aureus and E. Coli bacterias. The plant extracts used in the study did not show antibacterial efficiency against E. Coli and S. Aureus bacteria, but many studies have shown that hemp seed, rosemary, St. John's Wort and Cherry Laurel leaf extracts can be effective against many gram positive, gram negative and fungi other than these two bacteria (Vega et al. 2021; Jarzębski et al. 2020; Darie-Niţă et al. 2018; Momeni et al. 2021).

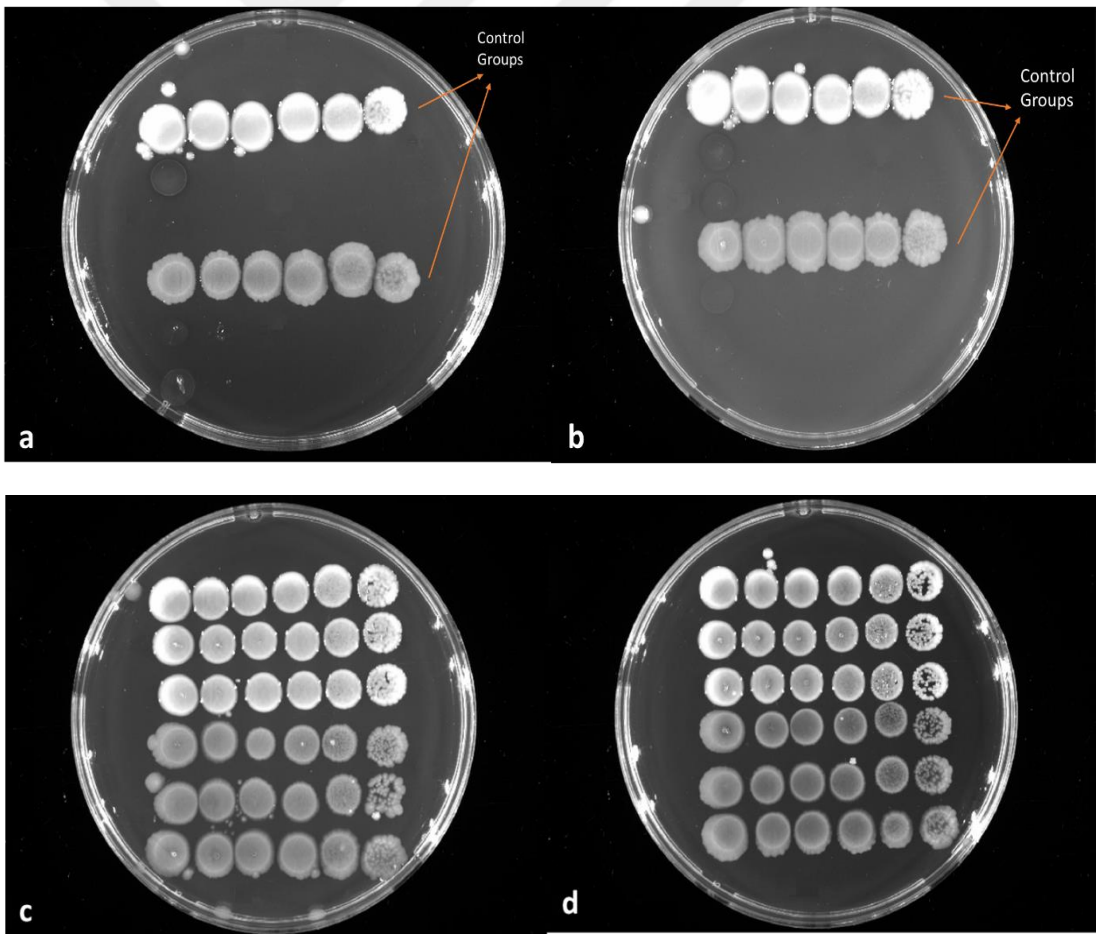

Figure 4.13 Antibacterial activity of nanocomposite films against S. Aureus. And E.Coli, a) Hemp-*St. John's Wort*/AgNPs/PVA, b) Rosemary-*Cherry Laurel*/AgNPs/PVA, c) Hemp-*St. John's Wort*/PVA and d) Rosemary-*Cherry Laurel*/PVA.

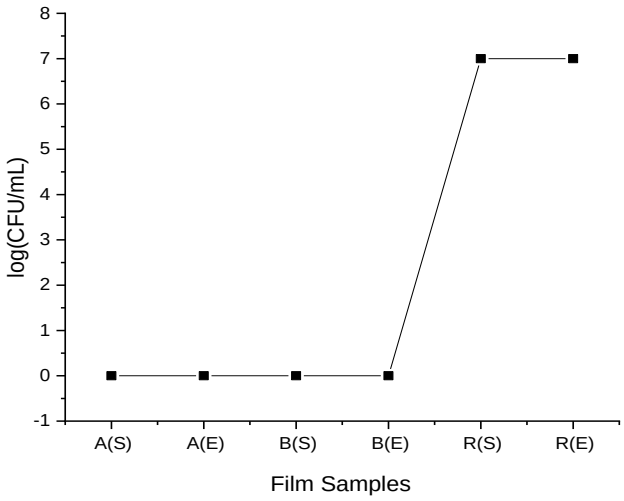

Figure 4.14 Log CFU/mL of AGNPs added nanocomposite blend films against S. Aureus(S) and E.Coli(E).(A sample is Hemp-*St. John's Wort*/AgNPs/PVA, B sample is Rosemary-*Cherry Laurel*/AgNPs/PVA and R sample is reference).

4.5. Characterizations of Electrospray Deposited Ti-6Al-4V Surfaces

4.5.1. Microstructural Analysis

SEM images of the coating surfaces show that the thin films formed on the surfaces are composed of fiber structures made of PVA. During the coating applied by electrospray deposition, the polymer coating material sprayed from the needle tip with electrostatic forces accumulates on the surface as nano-sized fibers. It is clearly seen in Figure 4.15 that the unmodified neat coating surface consists entirely of these fibers. It was determined that the fiber structures were homogeneously distributed on all coating surfaces and the nanoparticles in the AgNP-containing films were deposited on these fibers and embedded in the fibers and covered on the substrate surface. When the EDS spectrum and mapping results of all coating surfaces are examined, it is seen that the C and O elements come from the structure of PVA at a high rate. The element Ti, which is the main material of the coating substrates, is seen in the EDS results of all coating surfaces. Other alloying elements, Al and V, were clearly detected in the EDS results, especially of the neat sample surface. The K, Na, Mg and P elements seen in the EDS results come from plant extracts. The presence of these elements in plant extracts has been demonstrated in previous EDS analyzes and is also shown in Figures 4.1 and 4.16.

The presence of silver nanoparticles is seen in both SEM images and EDS analyzes given in Figures. Although the particles cannot be detected clearly in the SEM

images of sample B, which has the lowest nano silver content in the coating, it is clear that nano silver particles are present on the coating surface in Figure 4.17 EDS mapping results. The surfaces where the presence of silver nanoparticles were most clearly observed were the coatings of samples C, D and E. The white round-shaped particles embedded in the fibers or on their surface are nano silvers. EDS mapping and spectrum analyzes prove that these white spherical particles are nano silvers. Nano silver sizes were calculated from SEM images and Image J application as an average of 34 nm and the results are shown in Figure 4.21. As seen in Figures 4.18, 4.19 and 4.20, the nanoparticles are homogeneous in the coatings in terms of size and distribution. From this point of view, it has been proven that nano silver particles synthesized green from Hemp Seeds and St. John's Wort can be produced in very low nano sizes, spherical and homogeneous. A homogeneously dispersed coating surface could be successfully produced with nano silver particles modified into 0.3% and 0.5% PVA. Measurements of the thickness of the coatings and side section views are shown in the SEM images in Figures 4.19 and 4.20. The coating thickness (98 μm) of sample E with higher nanoparticle density was also found to be higher. In sample D, the coating thickness was calculated as 27 μm on average during imaging from the SEM device. While the substrate samples were removed from the panel of the electrospray device after coating, minor separations occurred in the edge regions of the coatings. Therefore, the gaps and redundancies seen in the SEM images of the pavement section were formed. However, when the cross-sections of the coatings were examined, it was seen that the coating surfaces and thicknesses were produced homogeneously. The result of the EDS line analysis on the section in Figure 4.19 clearly shows the contents of the coating material and the substrate material. While the presence of Ti disappears in the area where the substrate ends, the presence of silver and the amount of C from PVA increase at a high rate. When the cross-section EDS line analysis of the E sample is examined in Figure 4.20, similarly, when it comes to the section where the coating material is located, there is a high amount of silver, but titanium is not visible.

The factors such as the homogeneity of the coating surfaces, the presence, distribution and morphological properties of nano silvers, coating contents and distributions were examined by SEM and EDS analyzes. According to these results, coatings made by electrospray deposition were successfully produced as a thin film on the surface of Ti6Al4V substrates.

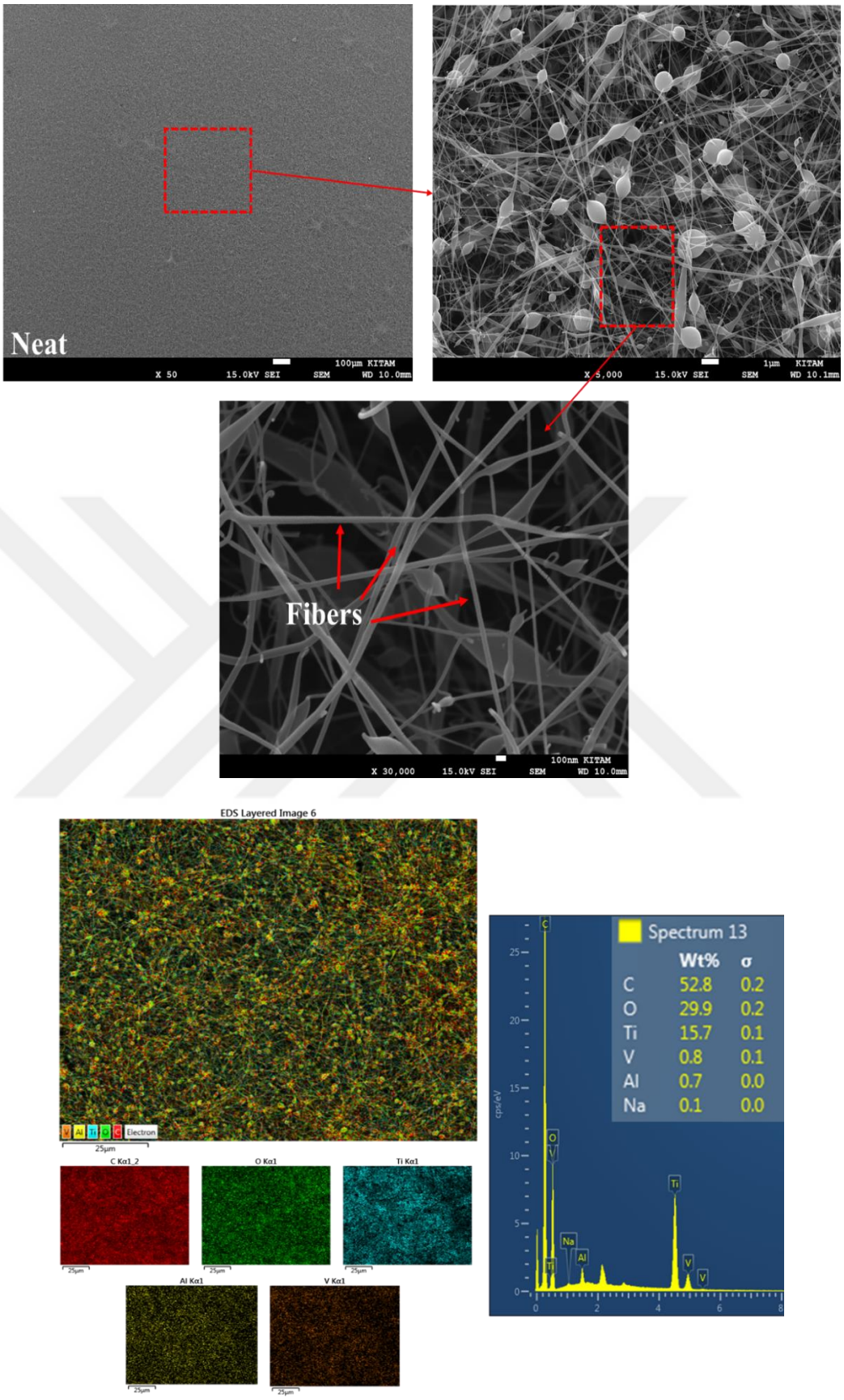

Figure 4.15 SEM images and EDS spectrum and mapping analysis results of neat sample coated surface.

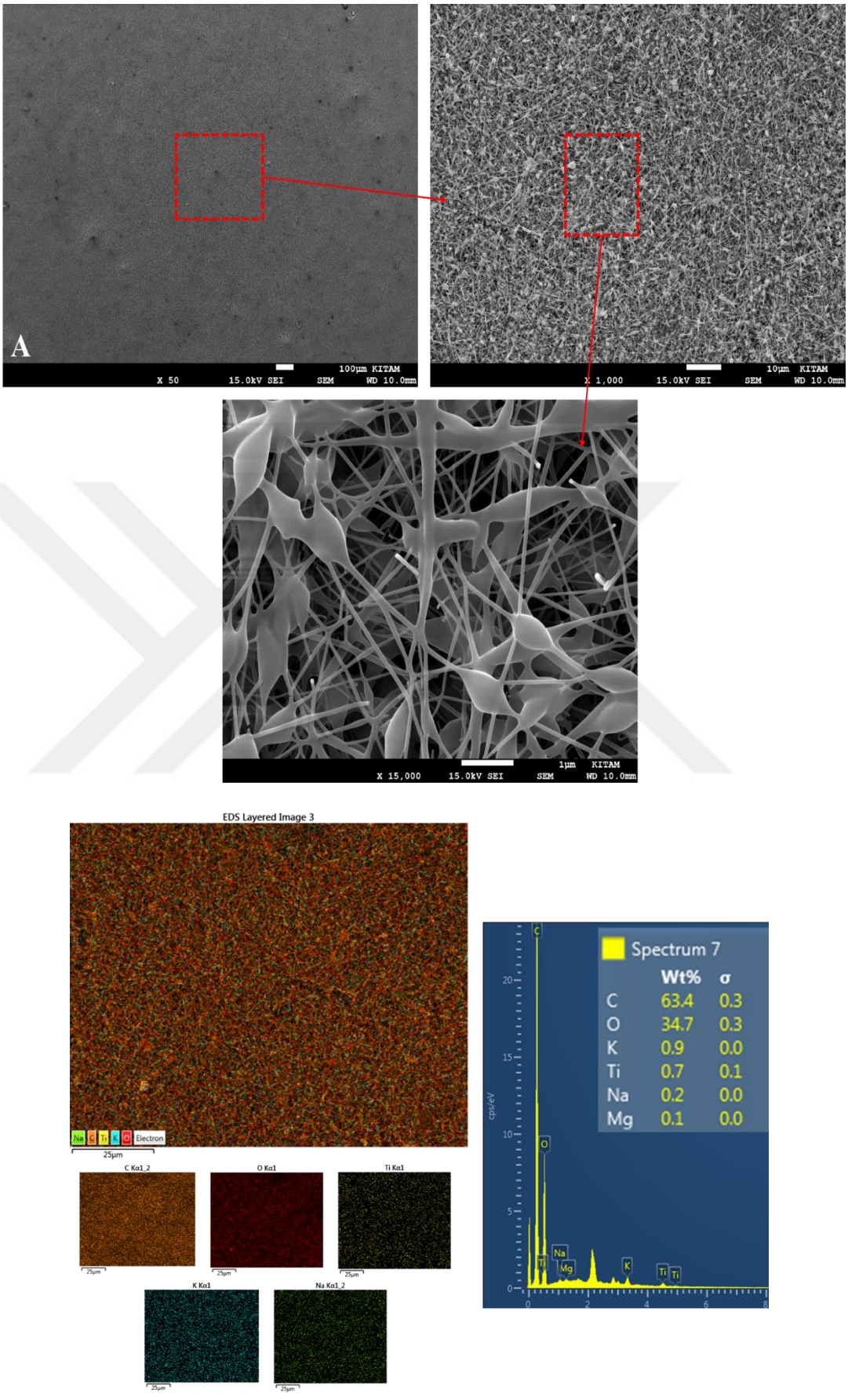

Figure 4.16 SEM images and EDS spectrum and mapping analysis results of A sample.

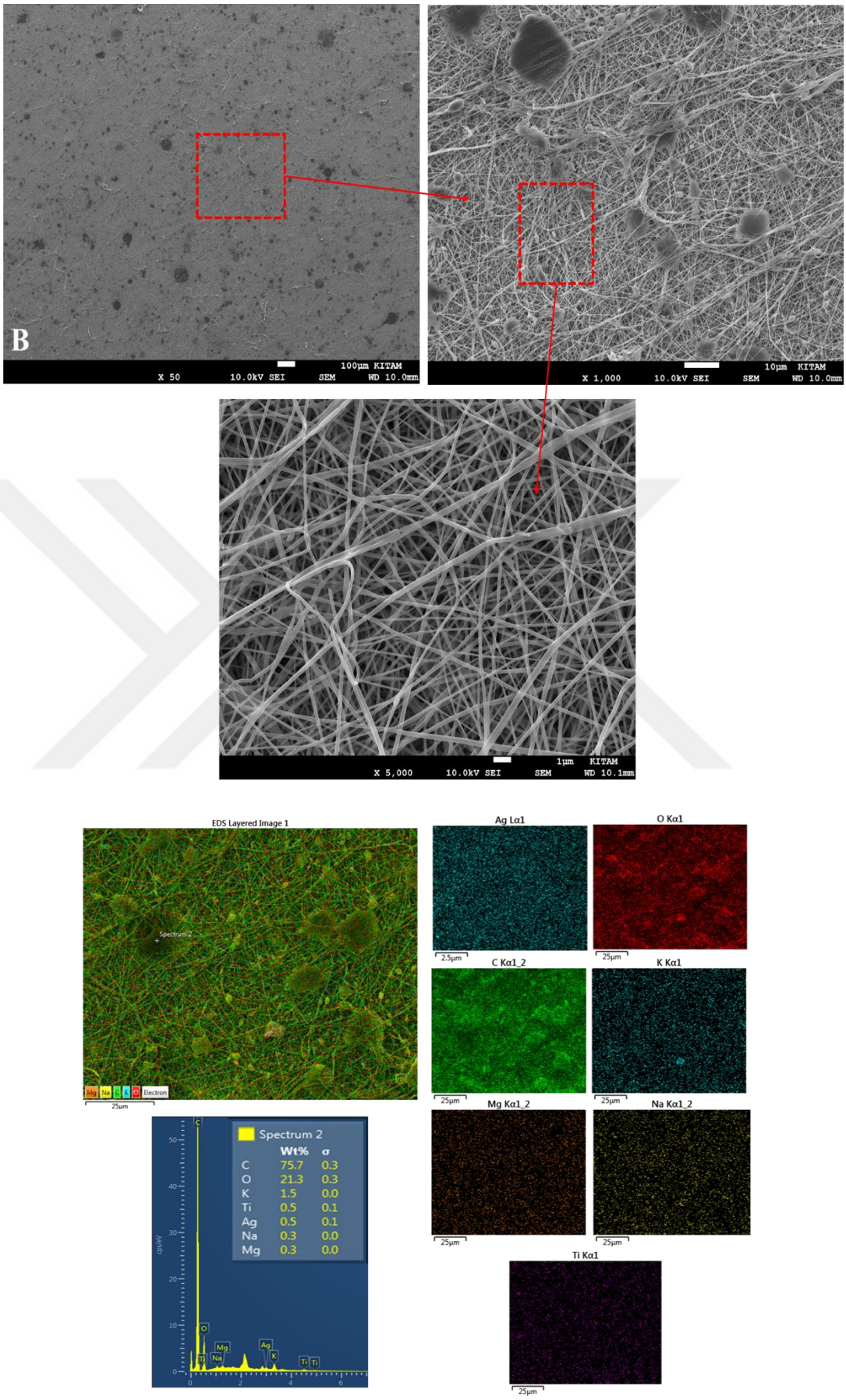

Figure 4.17 SEM images and EDS spectrum and mapping analysis results of B sample.

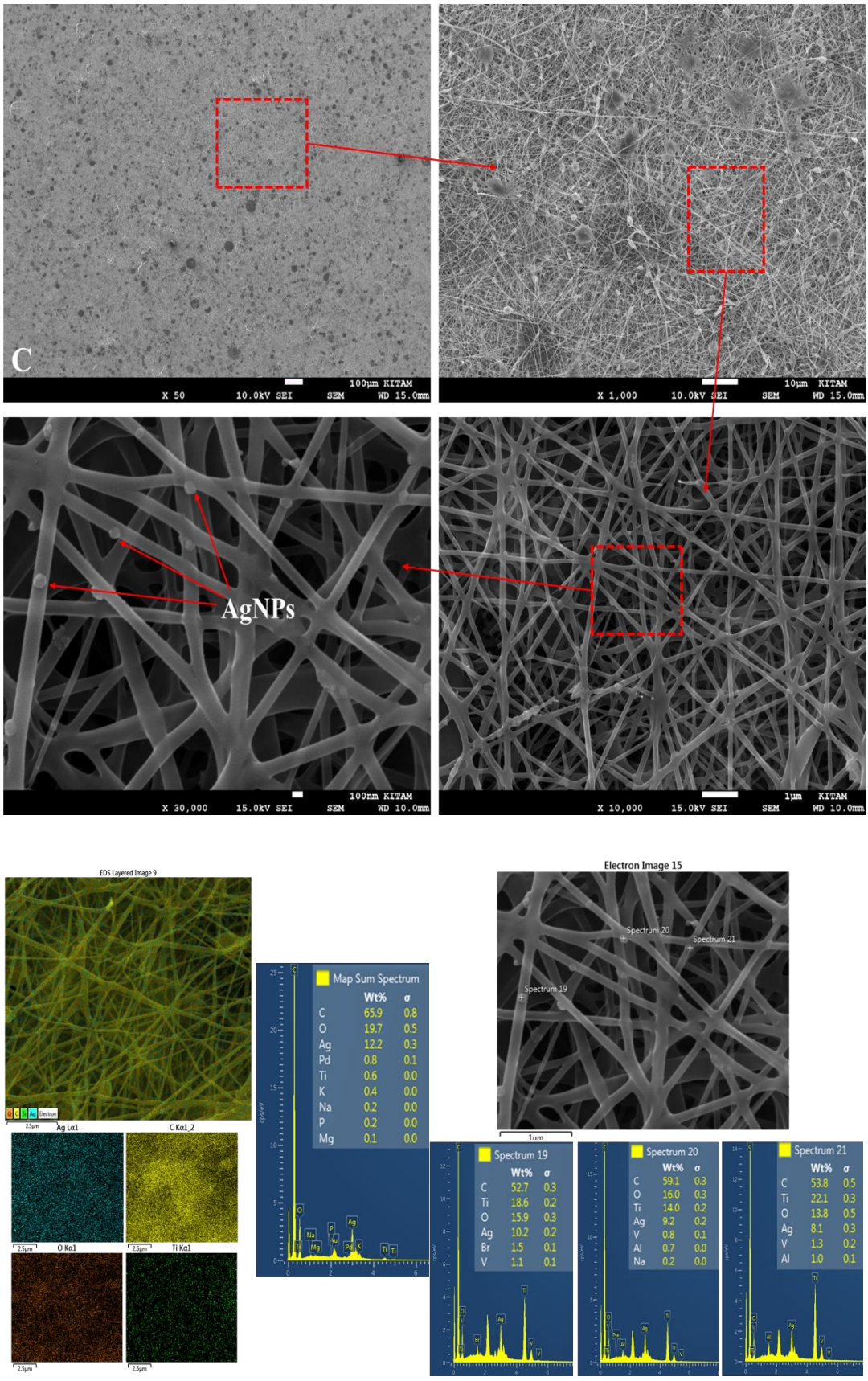

Figure 4.18 SEM images and EDS spectrum and mapping analysis results of C sample.

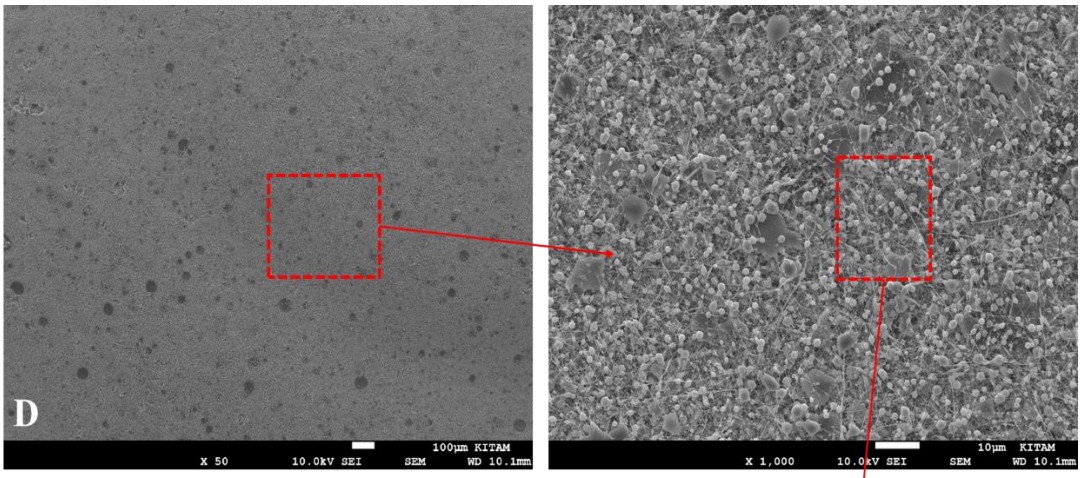
D
X 50 10.0kV SEI SEM WD 10.1mm
100µm KITAM
X 1,000 10.0kV SEI SEM WD 10.1mm
10µm KITAM

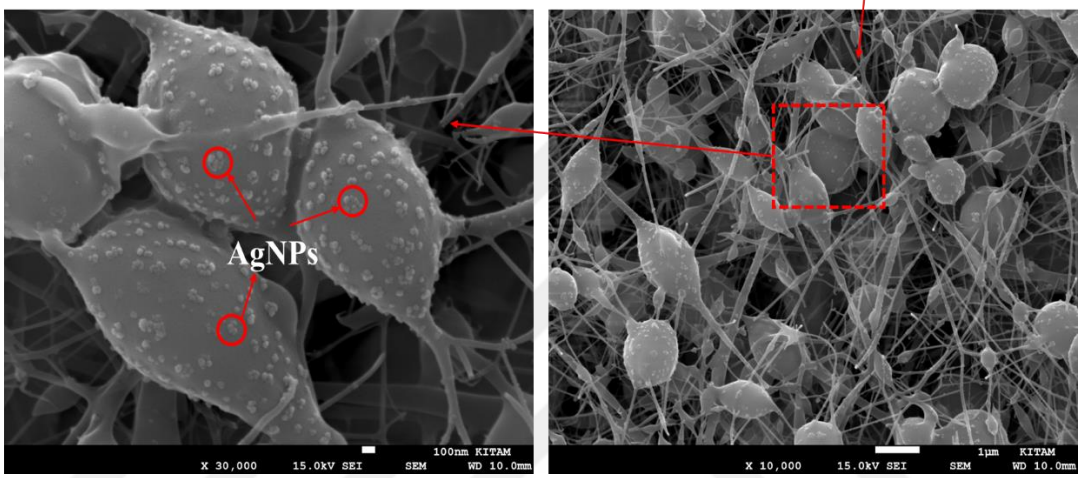
AgNPs
X 30,000 15.0kV SEI SEM WD 10.0mm
100nm KITAM
X 10,000 15.0kV SEI SEM WD 10.0mm
1µm KITAM

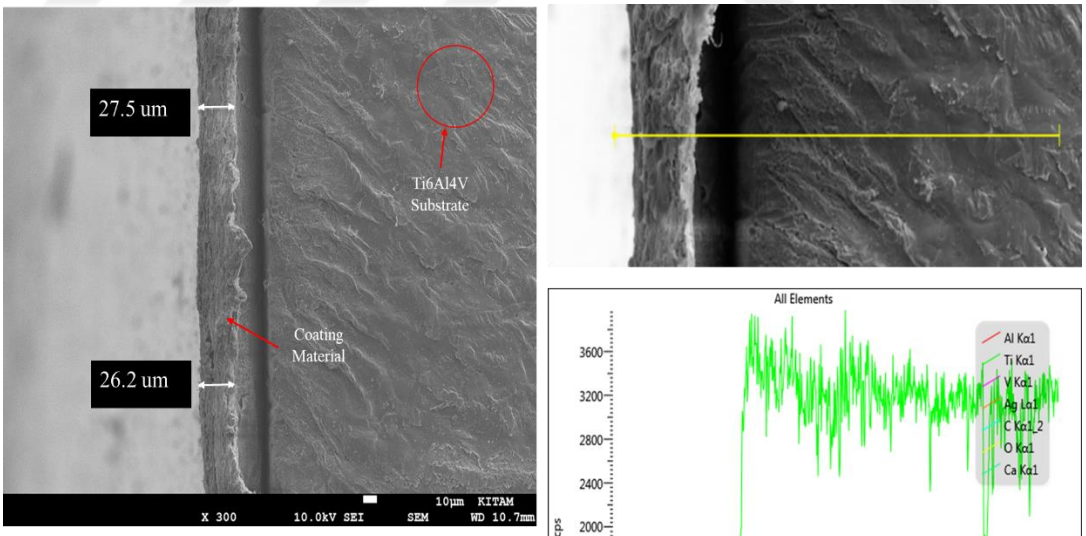
27.5 um
Ti6Al4V
Substrate
Coating
Material
26.2 um
X 300 10.0kV SEI SEM WD 10.7mm
10µm KITAM

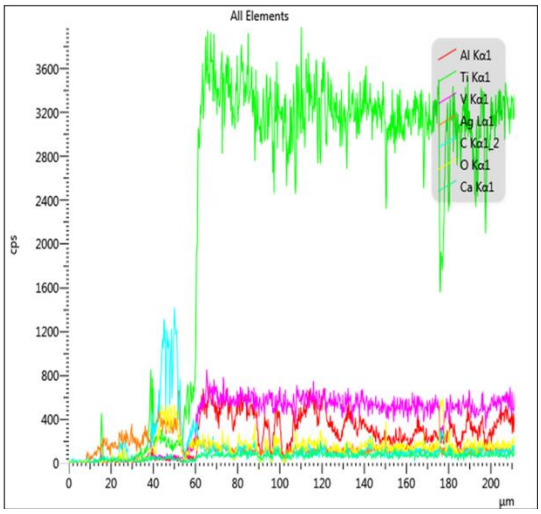
All Elements
Al Kα1
Ti Kα1
V Kα1
Ag Lα1
C Kα1_2
O Kα1
Ca Kα1
cps
µm

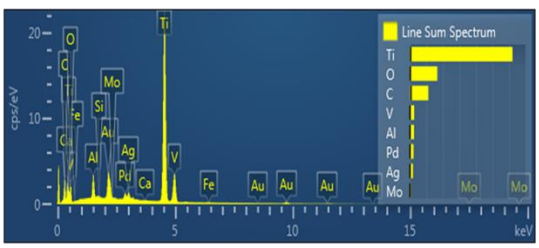
Line Sum Spectrum
Ti
O
C
V
Al
Pd
Ag
Mo
cps/eV
keV

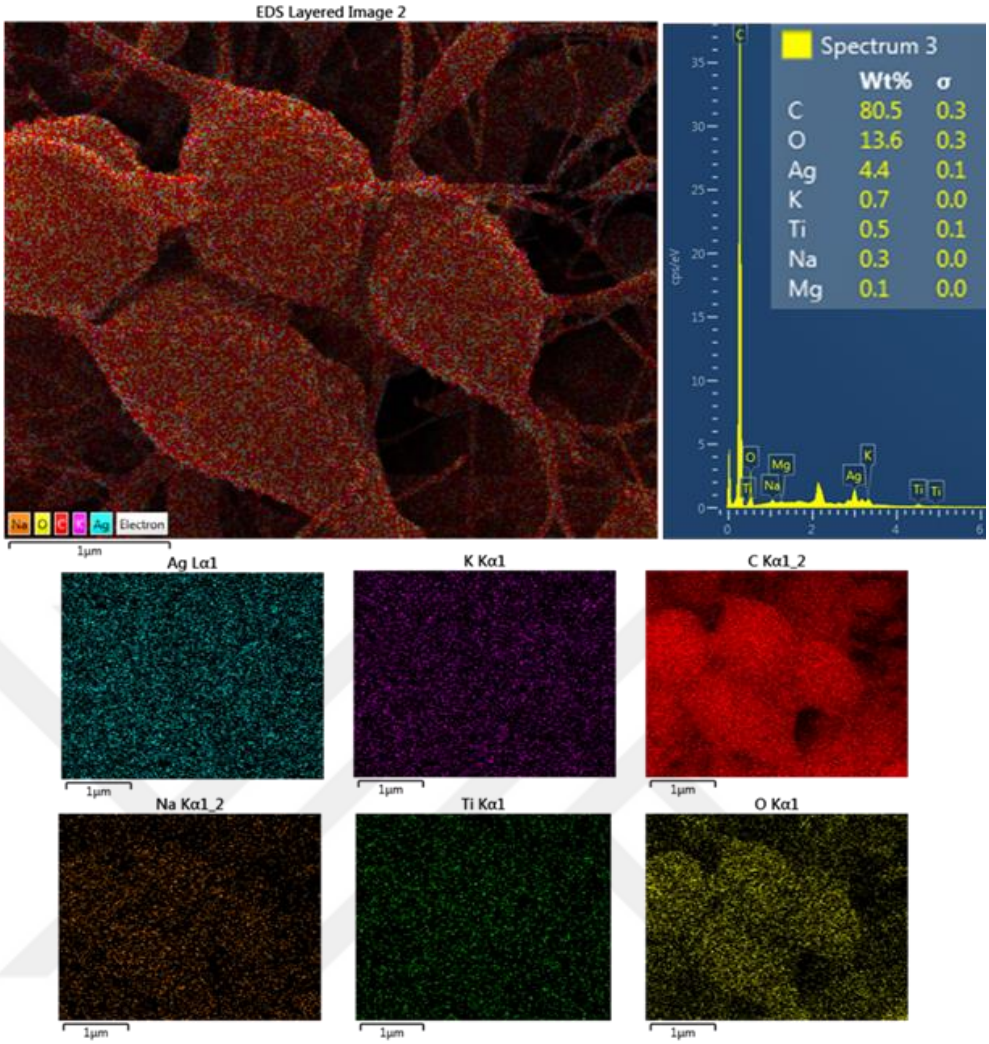

Figure 4.19 SEM images and EDS spectrum and mapping analysis results of D sample.

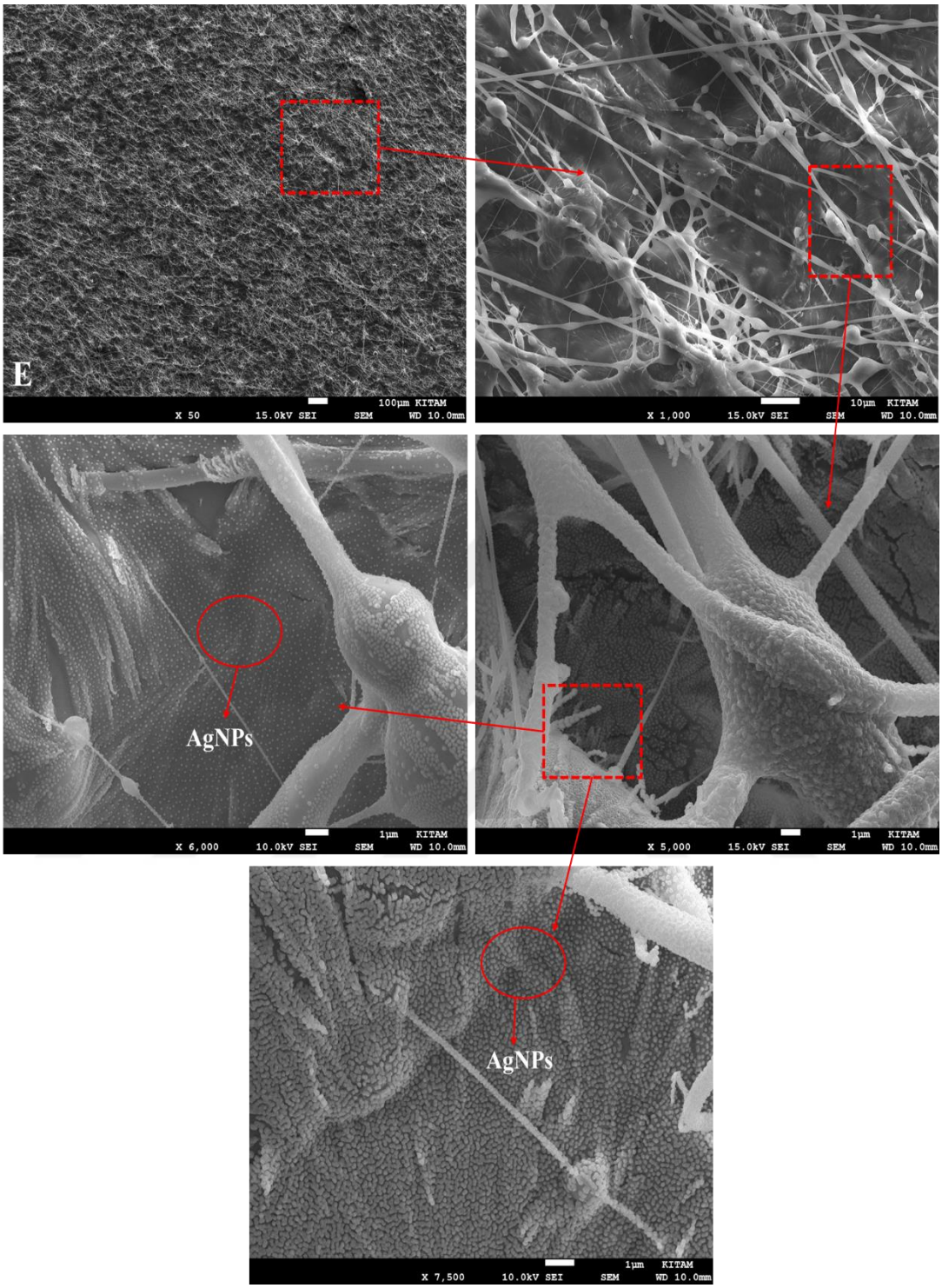
E
X 50 15.0kV SEI SEM WD 10.0mm
100µm KITAM
X 1,000 15.0kV SEI SEM WD 10.0mm
10µm KITAM
AgNPs
X 6,000 10.0kV SEI SEM WD 10.0mm
1µm KITAM
X 5,000 15.0kV SEI SEM WD 10.0mm
1µm KITAM
AgNPs
X 7,500 10.0kV SEI SEM WD 10.0mm
1µm KITAM

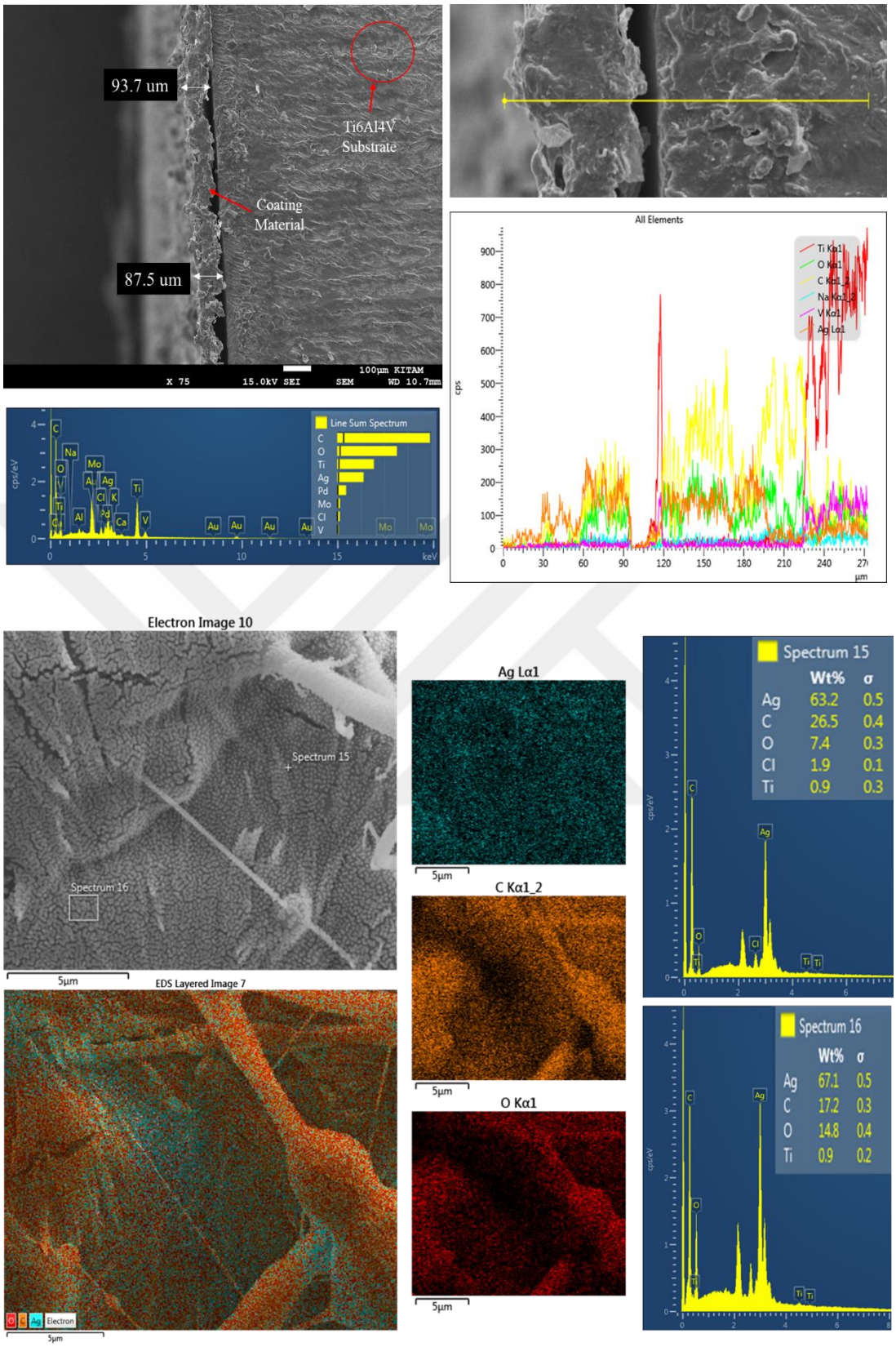

Figure 4.20 SEM images and EDS spectrum and mapping analysis results of E sample.

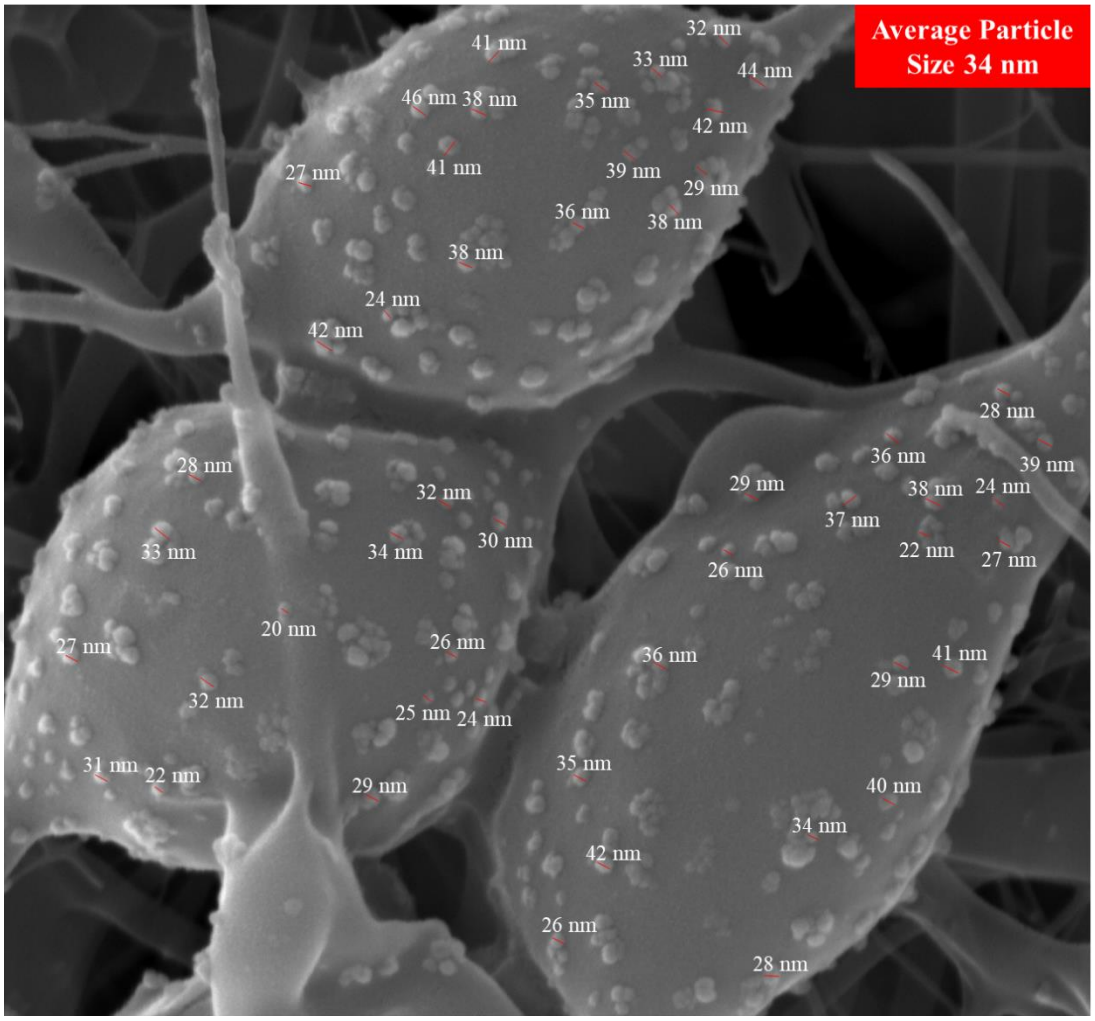

Results

File Edit Font Results

	Area	Mean	Min	Max	Angle	Length
1	68.005	108.202	98	116.963	-85.764	42.193
2	58.290	104.283	90	110.556	-46.736	36.382
3	75.291	106.221	90.400	117.000	-53.130	46.753
4	63.147	111.310	92.000	124.509	-49.899	38.711
5	53.432	115.231	106.000	123.469	-50.906	32.128
6	68.005	117.972	105.000	132.222	-63.435	41.817
7	60.719	143.227	131.833	167.542	-67.751	37.044
8	58.290	124.316	102.000	147.155	-61.189	35.572
9	55.861	108.688	100.331	116.107	-33.690	33.714
10	65.576	140.066	125.456	159.497	-51.340	39.916
11	58.290	119.228	112.244	136.488	-43.264	36.382
12	68.005	132.690	106.754	161.023	-58.671	41.962
13	58.290	122.619	100.000	142.004	-46.736	36.382
14	72.862	154.706	140.901	179.649	-33.690	44.952
15	58.290	146.081	128.450	177.295	-50.194	36.515
16	53.432	101.175	80.000	113.429	-46.975	31.977
17	43.717	96.370	83.000	103.727	-45.000	26.448
18	58.290	109.697	98.000	119.966	-30.964	36.349
19	48.575	109.506	86.000	124.867	-51.582	28.842
20	53.432	119.474	108.357	132.143	-124.439	33.069
21	51.004	119.285	96.500	133.900	-27.216	30.668
22	58.290	134.767	126.000	141.292	-40.601	35.920
23	68.005	157.681	147.000	164.500	-33.690	42.143
24	68.005	165.341	134.170	213.936	-61.991	41.482
25	53.432	146.535	123.327	182.551	-35.218	32.429

Nanoparticle Sizes

Results

File Edit Font Results

	Area	Mean	Min	Max	Angle	Length
26	38.860	163.792	133.500	184.667	-30.964	22.718
27	43.717	158.629	126.500	180.960	-55.840	26.367
28	46.146	151.878	126.000	170.042	-42.797	28.673
29	60.719	136.977	111.615	160.938	-34.019	37.605
30	60.719	133.019	111.000	157.083	-51.710	37.726
31	48.575	123.227	108.906	140.274	-42.879	29.774
32	53.432	128.022	104.837	161.000	-67.166	32.128
33	48.575	122.023	103.000	134.961	-42.879	29.774
34	41.289	116.635	100.867	134.777	-71.565	24.641
35	63.147	111.646	97.194	139.000	-45.000	39.671
36	55.861	117.810	95.207	142.000	-71.565	34.498
37	68.005	106.590	94.000	118.926	-51.009	42.107
38	51.004	119.005	100.025	135.695	-69.775	31.556
39	60.719	103.749	93.000	111.500	-34.992	38.046
40	68.005	114.721	86.000	138.502	-124.287	41.497
41	65.576	94.664	86.000	104.041	-46.548	40.788
42	60.719	102.192	86.000	112.667	-75.379	37.044
43	43.717	111.864	90.000	126.000	-45.000	26.448
44	53.432	113.129	101.444	121.500	-123.311	32.634
45	48.575	106.294	100.000	113.704	-42.879	29.774
46	46.146	100.612	90.000	106.764	-34.992	28.535
47	46.146	100.985	88.250	107.840	-45.000	27.550
48	51.004	96.444	83.000	104.000	-45.000	30.856
49	51.004	115.359	88.000	138.260	23.962	30.698
50	63.147	109.408	84.000	119.170	-40.101	38.711

Nanoparticle Sizes

Figure 4.21 Nanoparticle size and distributions from SEM image and Image J application size measurements.

4.5.2. Atomic Force Microscopy (AFM) Analyses

AFM is an analysis that can be performed under atmospheric conditions, in a vacuum, or in liquids. It forms the AFM instrument as a cantilever (usually made of silicon nitride, silicon, or tungsten) with a sharp tip with a radius of curvature of several nm (i.e., a very sharp tip). When the tip approaches a specific surface (for example, in AFM contact mode), atomic forces build up between it and the surface, causing the console to bend reflecting the laser beam, allowing measurements to be collected. Various forces occur during AFM measurement: van der Waals, electrostatic, magnetic, capillary, ionic, and repulsive forces. The AFM technique is often used in biomedical and coating applications. AFM offers the possibility to characterize the surface topography and roughness parameters that have a significant impact on the osseointegration and interfacial stability of biocompatible coatings and implants applied to metal substrates (Del Olmo et al. 2021; Kravanja and Finšgar 2021; Stojkovska et al. 2020).

AFM analyses were conducted to evaluate the surface topography of the selected coated subtrates and analysize the surface roughness by atomic force microscopy (AFM, NanoSurf Flex Amf C3000). Coated surfaces were imaged in a scan sizes of 10 μm × 10 μm, 25 μm × 25 μm and 50 μm × 50 μm. The surface line and area roughness values was listed in Table 2 in terms of the main AFM parameters as average roughness (Ra-Sa), root-mean-square (RMS) roughness (Rq and Sq), maximum profile peak height (Rp and Sp) and maximum pit height (Rv and Sv). Surface topography was obtained with a speed-scan of 1 Hz.

The AFM 2D and 3D images of all coated samples are shown in Figure 22, 23, 24, 25, 26 and 27. The structures of the fibers coated on Ti-6Al-4V surfaces by electrospray deposition are also clearly seen in the AFM images. With the silver nanoparticle modification, it was understood that the fiber thicknesses were thicker, homogeneous in size and distribution compared to the neat sample and sample A. AgNPs are clearly present in 2D and 50 x 50 μm images of B, C, D and E samples. The nanoparticles on the surfaces of the fibers are easily visible, but they are not evident in all images due to the magnification restriction and the embedding of the fibers in PVA. As given in Table 4.3, the surface roughness values increased as the amount of nanoparticle modification applied to the coatings increased, and this was expected as stated in previous studies (Hermani et al. 2022; Samide et al. 2022; Wang

et al. 2022). However, the roughness values of the coatings modified with nano silver and plant extracts were lower than the neat and A sample. This is due to the homogeneous distribution of nanoparticles in PVA and the coating solution can be prepared as a stable solution. As confirmed by the FTIR results given in Figure 4.5, it was proven that plant extracts and AgNPs changed the chemical structure of PVA, resulting in the formation of new bonds and thus homogeneous and stable dispersion of these additives in the solution. This can be explained by the more uniform deposition of nanoparticle modified coatings on the surface by electrospray compared to the neat sample in the AFM results. The sample with the lowest roughness value (Ra) is sample B with 184 nm, followed by sample C with 201 nm. When the area roughness (Sp-v) values were examined, it was seen that there were coating surfaces as high as 5200 nm. It is known that nanoparticle agglomeration in some regions is caused by incorrect spraying of the electrospray device, environmental conditions or a homogeneously immiscible solution. In addition, it is estimated that the roughness values on the surface may vary as a result of more wear of some surfaces during the etching process applied to the alloy surface before coating. Although it seems like a negative situation, the rough surfaces of biomaterials such as implants is an important factor that increases osseintegration.

Wound healing and osseintegration performances of metallic dental implants depend on surface modifications. The bonding of pro-osteogenic cells with the implant surface depends on the amount of roughness on the surface. Because rough surface increases hydrophilicity and surface area. For this reason, the chemical bonding and cell regeneration between living tissue and implant surface can be strengthened by optionally providing nano-microroughening on the implant surfaces (Albrektsson and Wennerberg 2019; Cappellini et al. 2023; Walter et al. 2022; Xu et al. 2022; Zhu et al. 2021). In addition, living tissue compatibility, cell regeneration, infection prevention and wound healing can be achieved with bioactive materials on the implant surface (Ding et al. 2022; Ranjit et al. 2023; Wan et al. 2022; Yahya Rahnamaee et al. 2022). AFM analysis reveals that the surfaces of Ti-6Al-4V alloys can be produced both as rough and bioactive. In comparison to coatings with pure PVA, rougher surfaces can be obtained with nano silver modification. In this way, it is predicted that implants can be produced with more biocompatible, anti-infective and wound-preventing and antibacterial effects. As a result, Atomic Force Microscopy (AFM) images revealed

that the surface roughness of nano silver modified coatings was lower than that of plant extracts added and neat samples.

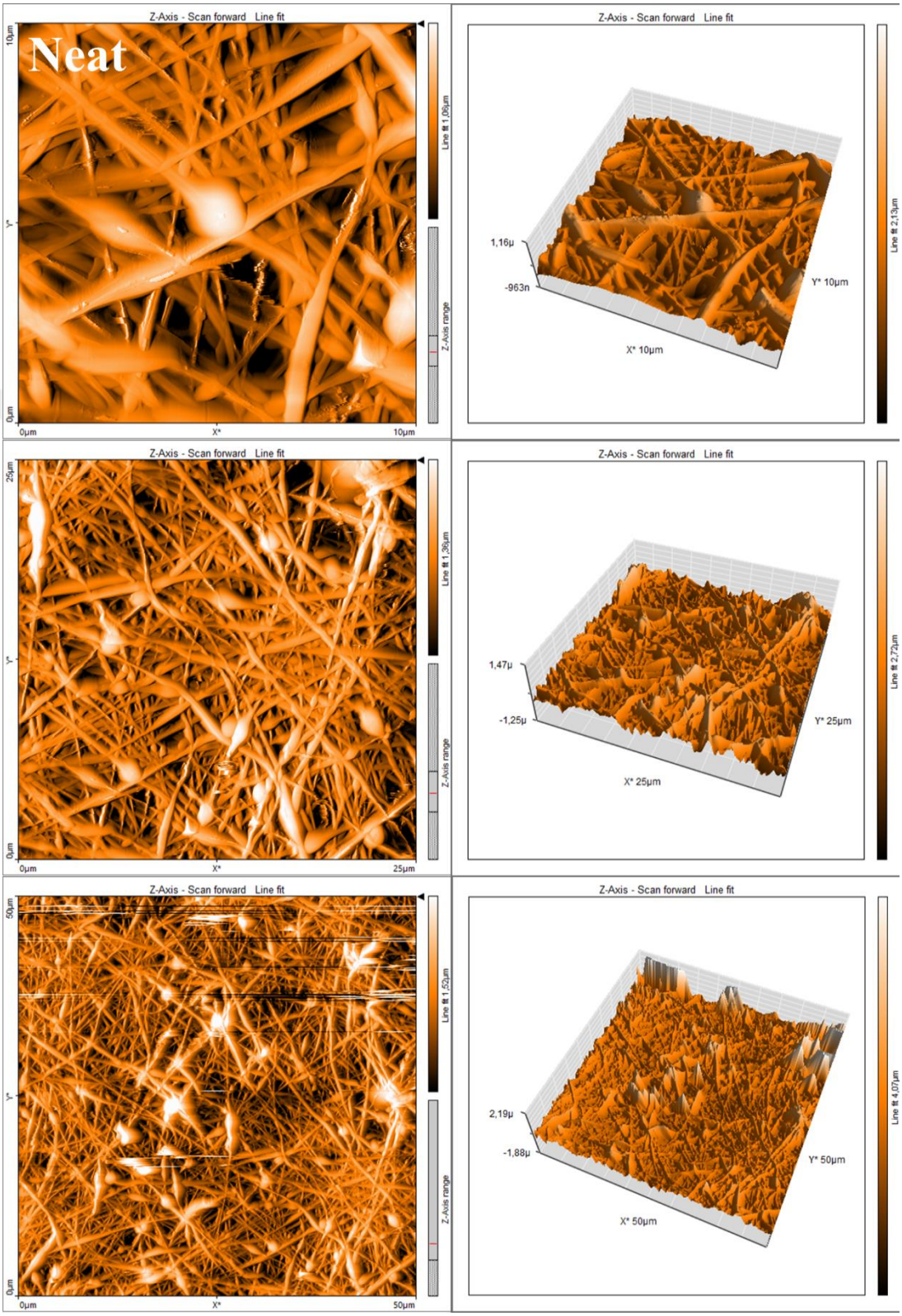

Figure 4.22 2D and 3D AFM images of the neat coated sample at scan sizes of 10 µm × 10 µm and 50 µm × 50 µm.

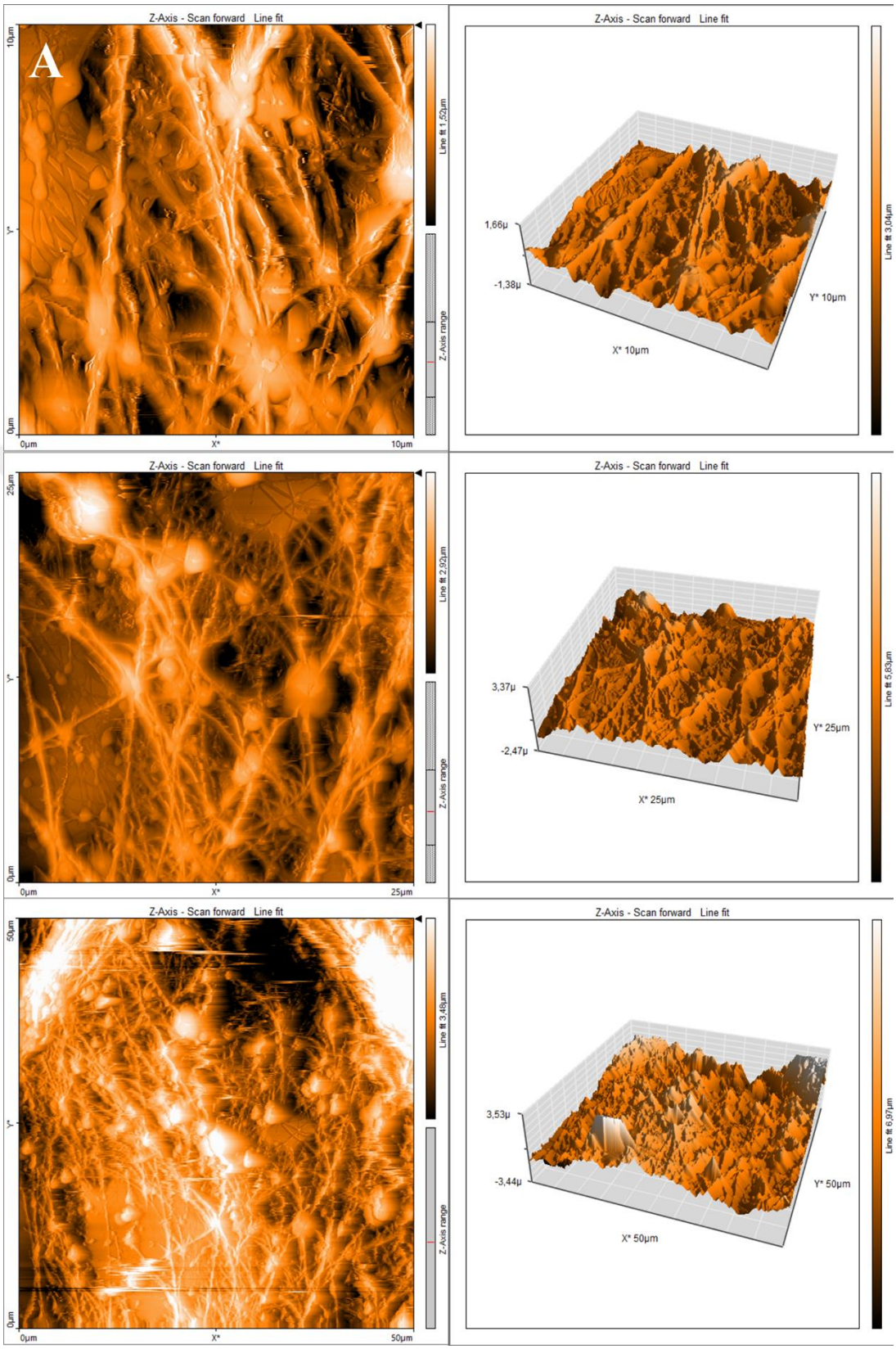

Figure 4.23 2D and 3D AFM images of the coated sample A at scan sizes of 10 µm × 10 µm and 50 µm × 50 µm.

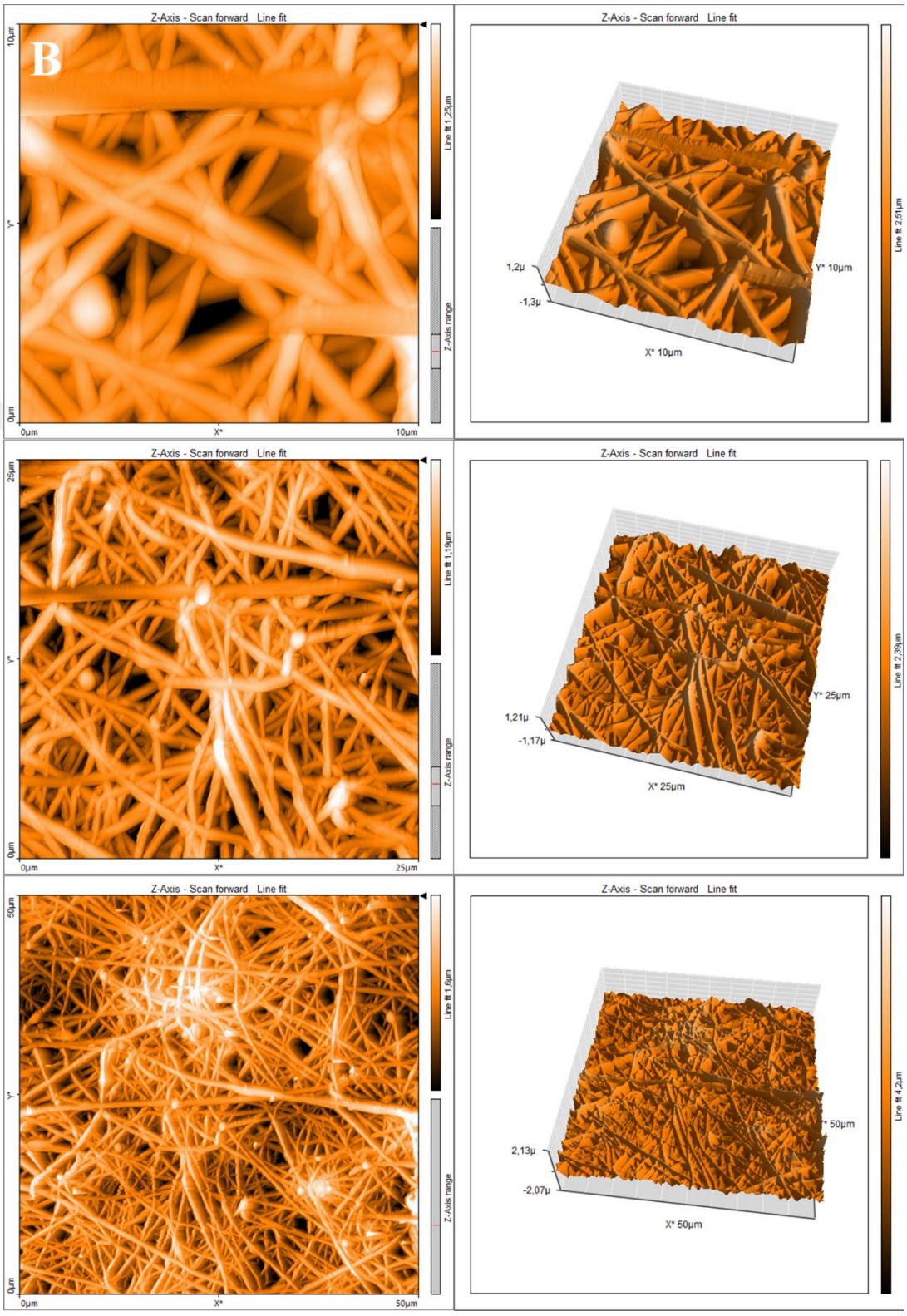

Figure 4.24 2D and 3D AFM images of the coated sample B at scan sizes of 10 µm × 10 µm and 50 µm × 50 µm.

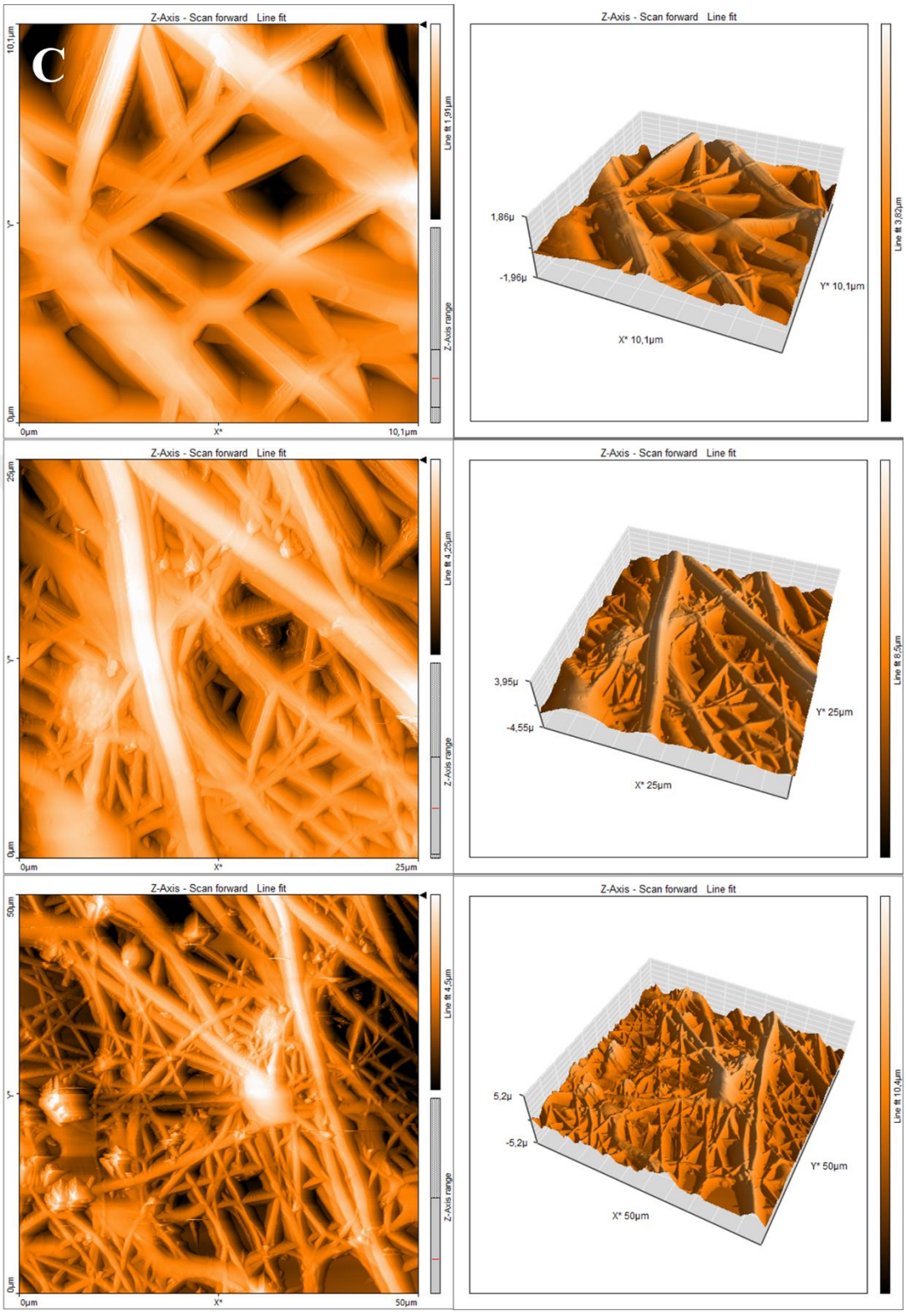

Figure 4.25 2D and 3D AFM images of the coated sample C at scan sizes of 10 µm × 10 µm and 50 µm × 50 µm.

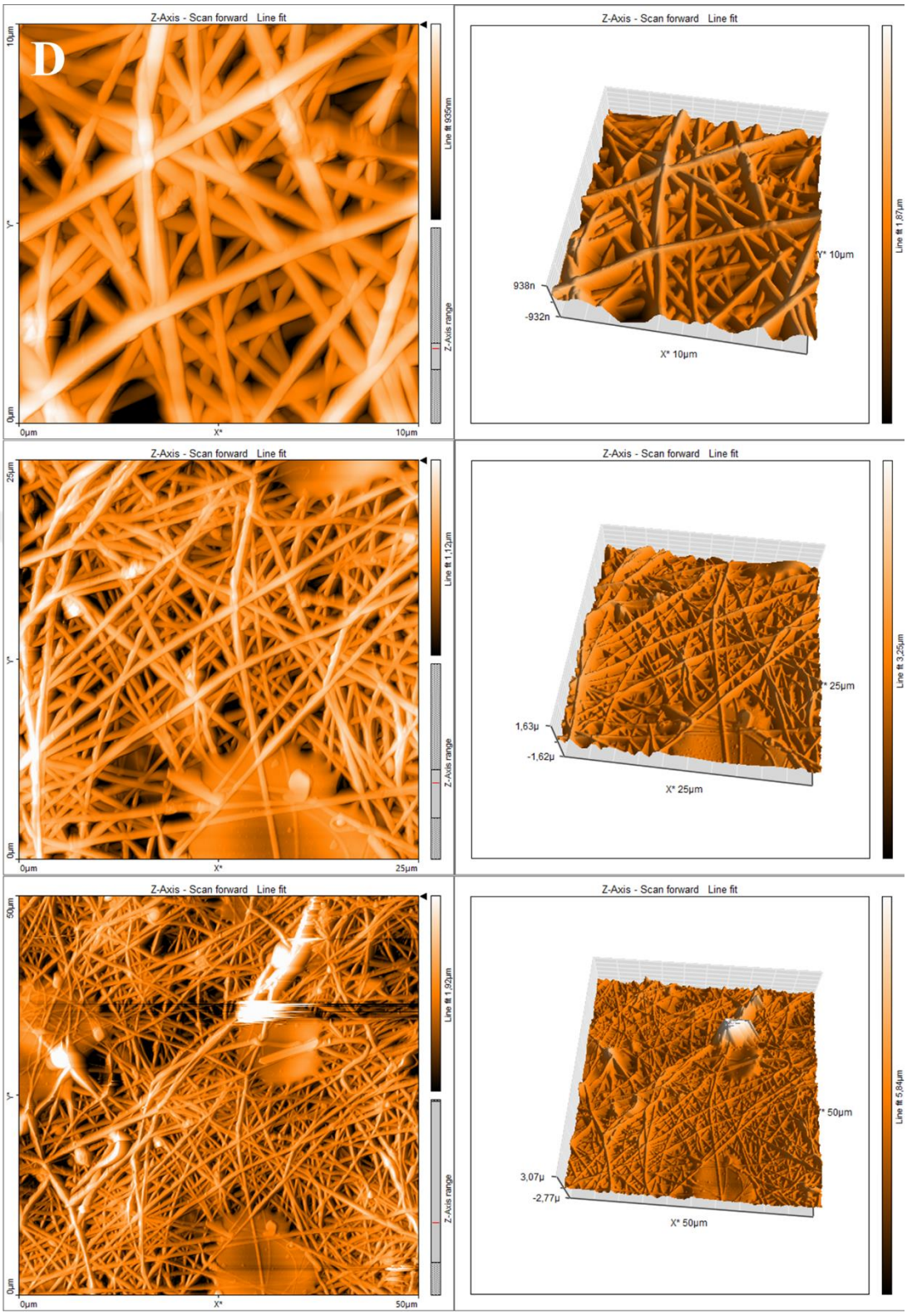

Figure 4.26 2D and 3D AFM images of the coated sample D at scan sizes of 10 µm × 10 µm and 50 µm × 50 µm.

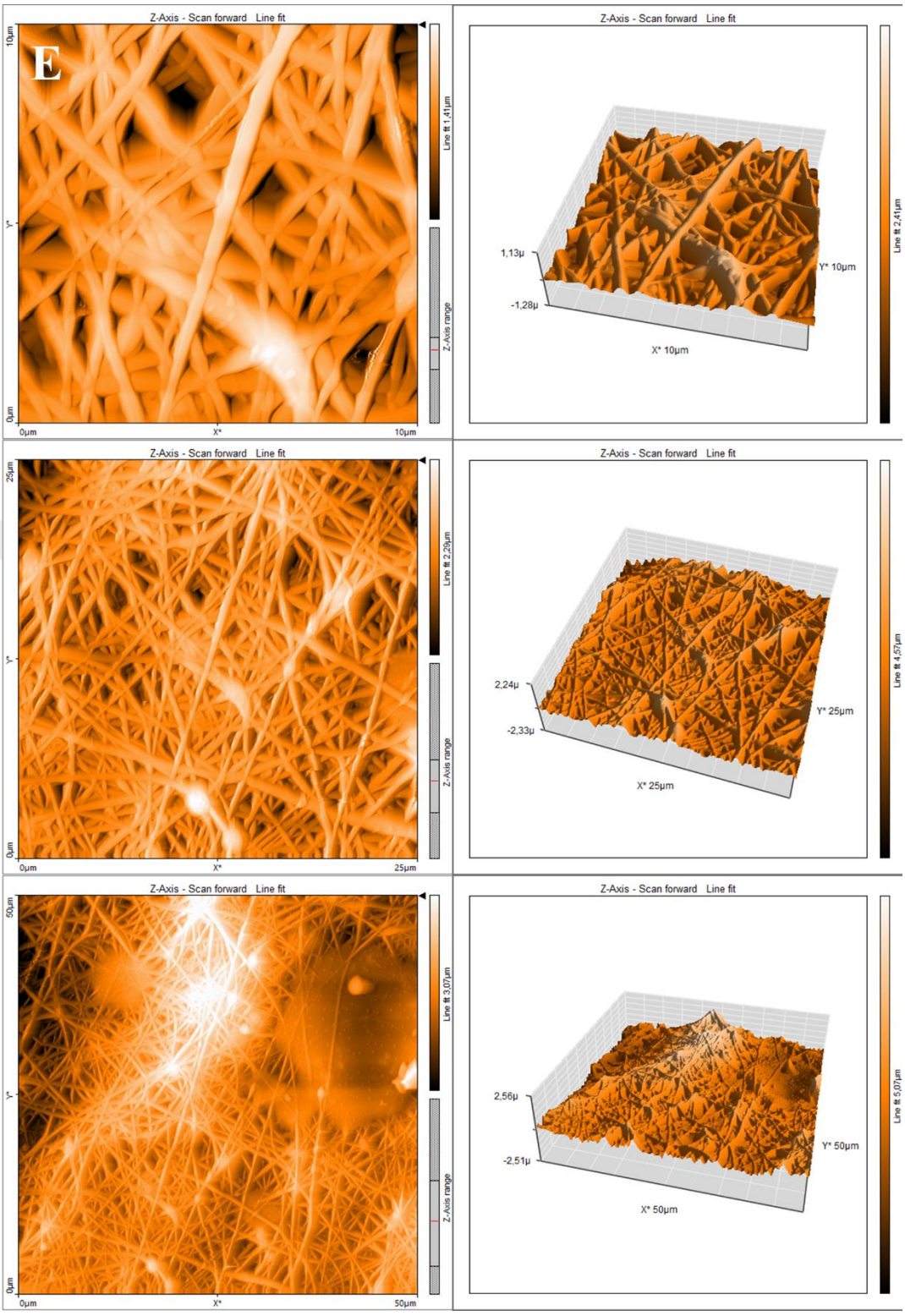

Figure 4.27 2D and 3D AFM images of the coated sample E at scan sizes of 10 µm × 10 µm and 50 µm × 50 µm.

Table 4.3 Line and area surface roughness values from AFM analysis of samples coated with electrospray deposition.

	Line Roughness				Area Roughness (2.51 nm^2)			
	Ra(nm)	**Rq(nm)**	**Rp(nm)**	**Rv(nm)**	**Sa(nm)**	**Sq(nm)**	**Sp(nm)**	**Sv(nm)**
Neat	310	365	911	666	208	307	5000	3000
A	514	633	1561	1488	662	887	5100	3080
B	184	237	686	734	225	347	5200	1796
C	201	252	579	536	204	260	1645	984
D	250	322	1036	850	313	407	2584	1501
E	295	348	716	710	274	365	5200	2275

4.6. Antibacterial Effects of Electrospray Deposited Surfaces

A modification of the Japanese Industrial Standard JIS Z 2801 was used as the method to test the antibacterial activity of AgNPs modified nanocomposite coated samples with %0.05-0.1-0.3 and 0.5 mass ratios. Escherichia coli (ATCC 25922) and Staphyloccus aureus (NCTC-13552) bacteria were prepared at 5 x 10^5 CFU/mL, 1 cm x 1 cm test samples were placed inside. A culture of 5 x 10^5 CFU/mL prepared without sample was used as a control. Eppendorf tubes containing samples were shaken at 100 rpm for 4 hours. The sample was kept in an ultrasonic water bath for 30 seconds to separate the microorganisms adhering to the surface, then vortexed. Dilution was carried out by transferring 100 µL of suspension into 900 µL of physiological saline (FTS). Petri dishes containing Plate Count Agar (PCA) were divided into eight and 25 µL of each dilution was seeded. The experiments were carried out in triplicate. As a result of incubation for 24 hours at 37 °C, the antimicrobial activity value of colonies forming units (CFU) was counted. The difference in growth between the positive control and the culture treated with polymer nanocomposite-coated samples was evaluated logarithmically and recorded.

Figure 4.28 shows the bacterial colonies growth areas of bacteria placed on agars. The medium named K shows the bacterial growth of the control culture. Insemination was performed on the medium for each sample with 6 different bacterial counts. These bacteria amount and names from 1 to 6 are used as x10^6, 10^5,10^4, 10^3, 10^2 and 10^1, respectively. Table 4.4 shows the sample concentrations and the logarithmically reduced amounts of bacteria in the media after the antibacterial test. In

addition, these reduction rates are given comparatively in Figure 4.29 graphically. It was determined that the E coating sample containing the highest amount of AgNPs was the sample with the highest $\log_{10}$ reduction. Bacteria growth was decreased with ratios of 1.6 (10-fold) against E.Coli and 2.5 (100-fold) against S.Aures. As the amount of AgNPs decreased, there was a decrease in the effect against bacteria, but this decrease was almost negligible. Even the sample B with the lowest AgNPs content inhibited S.Aures bacterial growth up to 100 times. As a result of antibacterial investigations, AgNPs and plant extracts modified electrospray coatings have shown that they are 100 times more effective against gram positive bacteria and 10 times effective against gram negative bacteria.

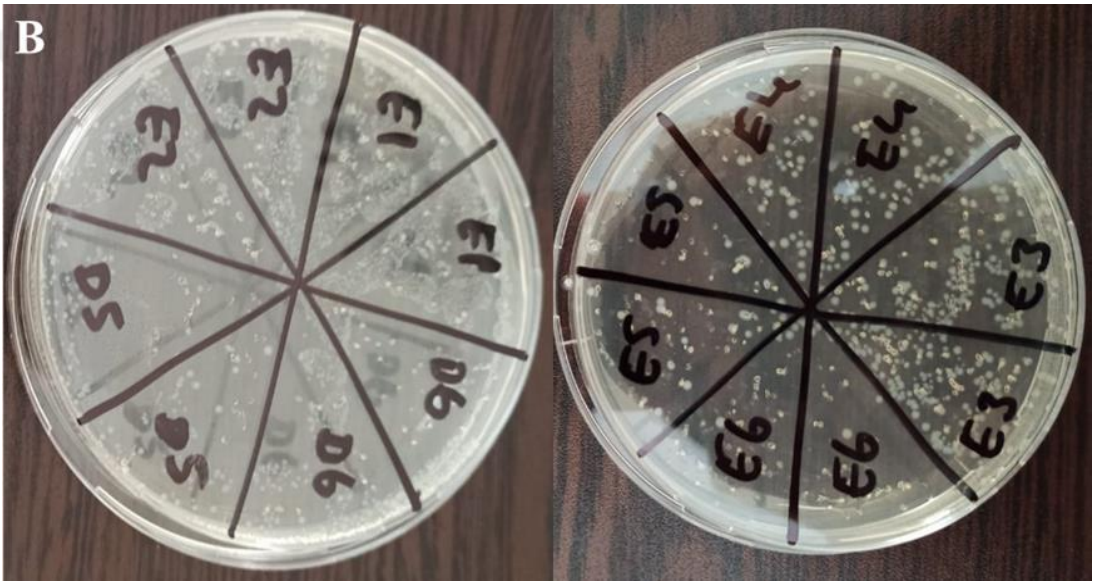

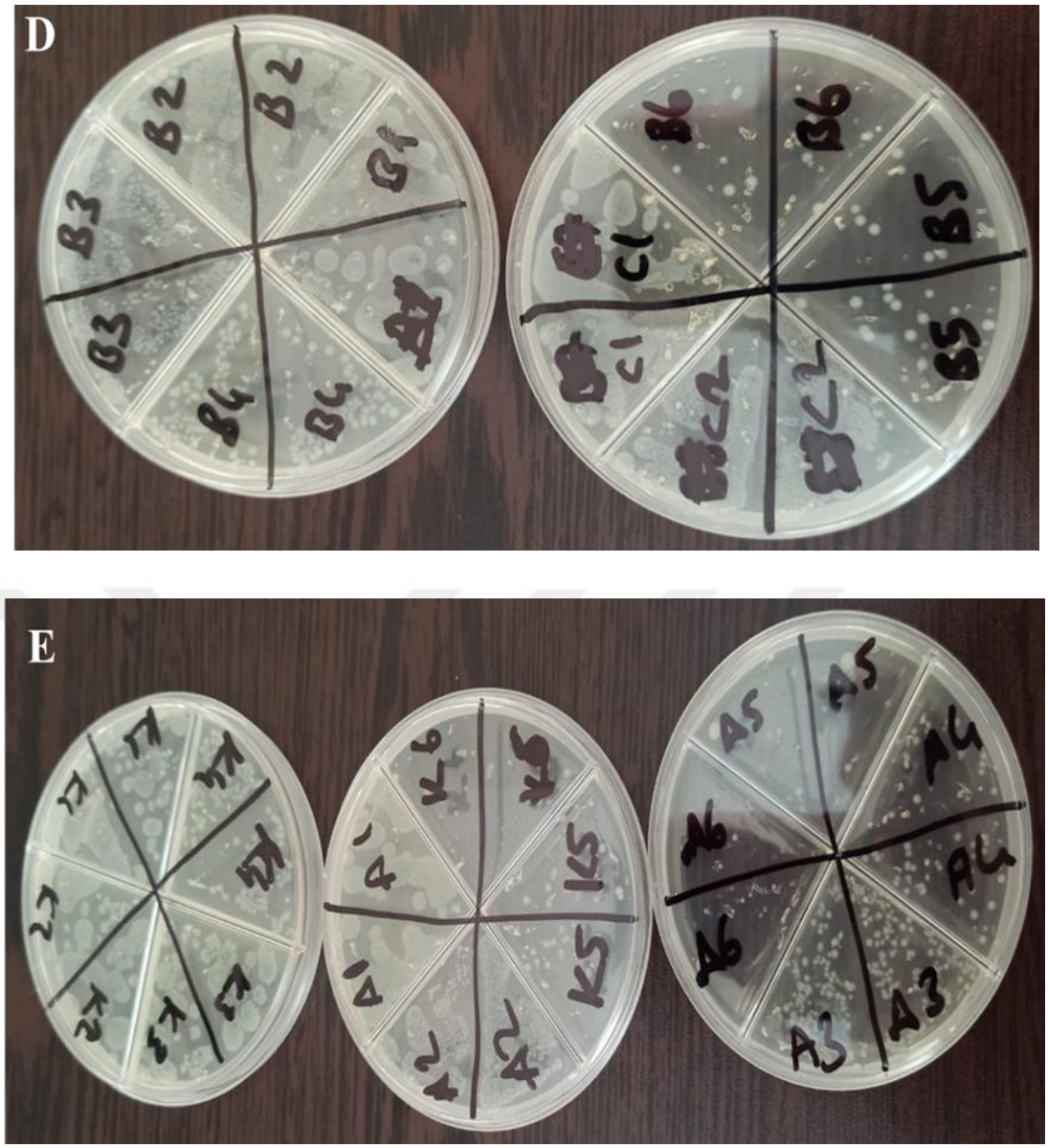

Figure 4.28 Bacterial colonies growth of S. Aureus. And E. Coli, E) Hemp-St. John's Wort/0.5% AgNPs/PVA, D) Hemp-St. John's Wort/0.3% AgNPs/PVA, C) Hemp-St. John's Wort/0.1% AgNPs/PVA and B) Hemp-St. John's Wort/0.05% AgNPs/PVA coated samples surfaces.

Table 4.4 Antibacterial effect comparisons with logarithmic growth difference (CFU. mL^{-1}).

	log_{10} reduction		**Concentration after incubation (CFU. mL^{-1})**	
Samples	**E. coli**	**S. aureus**	**E. coli**	**S. aureus**
Control			$1.5\pm0,5x10^5$	$1.4\pm0,2x10^5$
Sample E	1.6	2.5	$1.7\pm0,2x10^5$	$8.2\pm0,4x10^3$
Sample D	1	2,4	$2.2\pm0,3\ x10^5$	$6.2\pm0,4x10^3$
Sample C	1.1	2.2	$2.5\pm0,4x10^4$	$3.2\pm,0,2x10^3$
Sample B	1.2	2.1	$5.0\pm0,6x10^4$	$3.0\pm0,4x10^3$

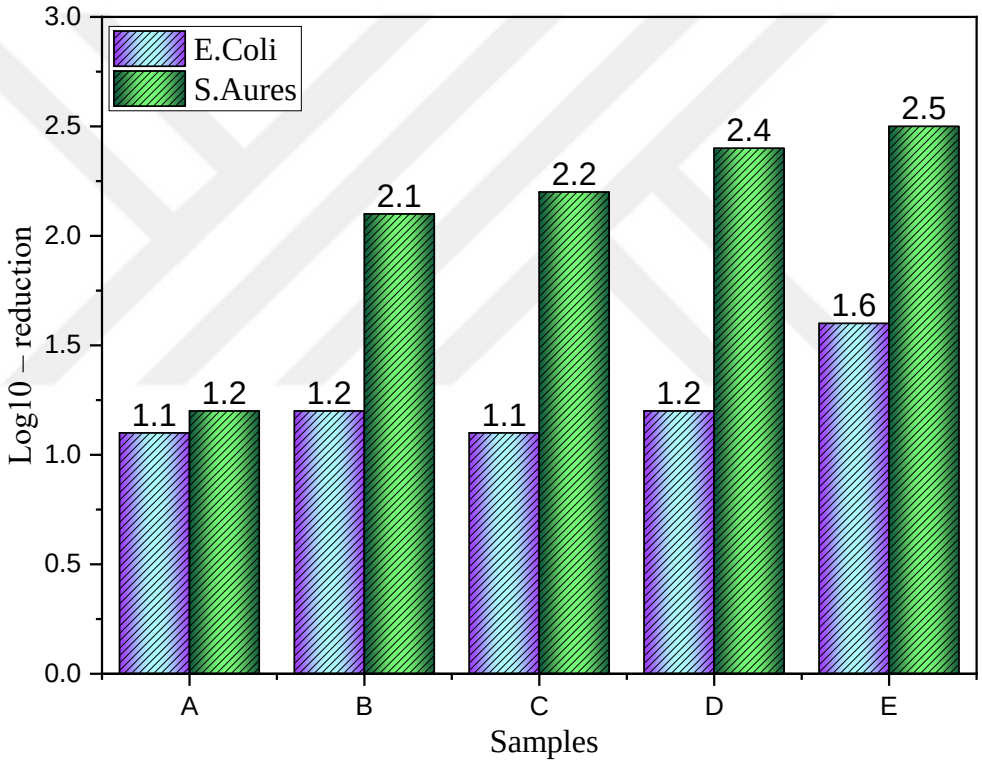

Figure 4.29 log10 growth reductions for AgNPs modified coated samples against E.Coli and S.Aures bacteries.

4.7. Scratch Tests

The scratch test was applied to determine the coating mechanical properties of Ti6Al4V substrates coated with AgNPs/Plant Extract modified PVA by electrospray method. The test was carried out with Mohs 6 hardness pencil produced from Orthoclase stone under 20 mm/sec speed, 5 and 10 kN forces. The strengths of the

coatings were compared from the scratch depths and images on the surfaces. Figure 4.30 shows the scratch test setup, mohs hardness pencil and coating sample. The surface of the coating was scratched by moving the hardness pen with the device in the horizontal direction.

Comparative images of scratches on pavement surfaces under 5 and 10 kN loads are shown in Figure 4.31. According to the width and depth of the lines formed on the surfaces, it was determined that the hardest and most durable coating samples were D and E with 0.3-0.5% AgNPs modified. D and E were the samples in which the coatings were eroded the least with the applied force. In addition, the other nano-silver particle modified coatings B and C also suffered much less wear than the neat and A sample. The scratches on the surface of sample B modified only with plant extracts clearly show that it is harder than the neat coating sample under 10 kN. According to the scratch test results, the hardness ranking of the coating samples is as follows; E>D>C>B>A>Neat. From the scratch test results, it was revealed that the samples with the best mechanical properties were AgNPs modified coatings. It was observed that the scratch resistance increased with the increase of nano silver additive ratio. In addition, it has been understood from sample B that more durable surfaces can be obtained than neat PVA coatings by modifying only the plant extracts.

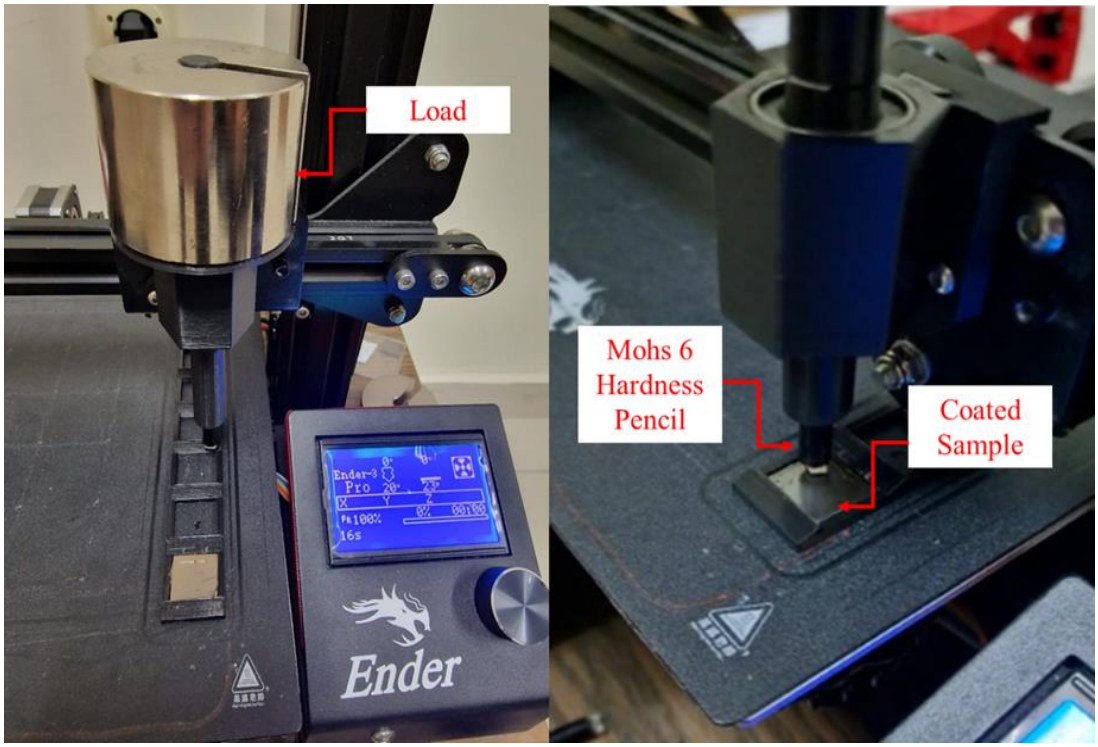

Figure 4.30 Scratch test setup and scratch test stage.

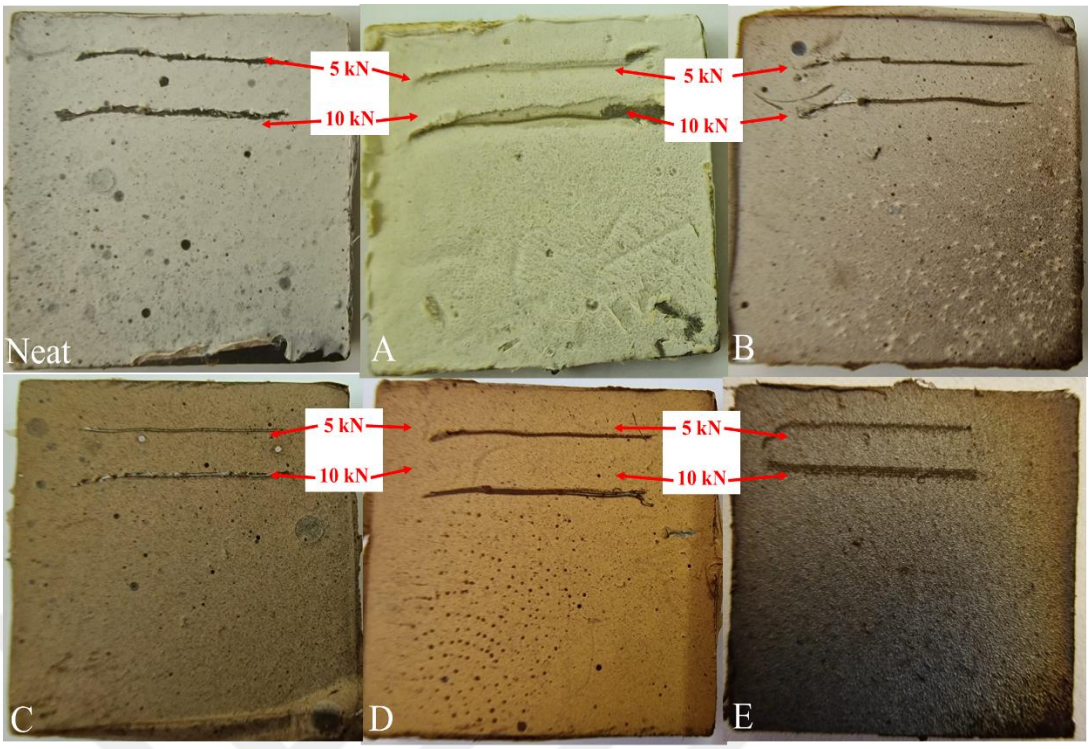

Figure 4.31 Sample coating surfaces after scratch test; Scratch line images after 5 and 10 kN loads.

4.8. Chemical Stability, Durability and Weight Change in Aqueous Environments of Coatings

In order to determine the durability of the coatings in aqueous media and in different temperature conditions, the mass changes in the aqueous media and the changes in the pH of the environment were measured. Durability tests were carried out in the incubator by moving it circularly at 40 rpm and keeping it at 25 and 37 °C for 2 weeks. As shown in Figure 4.32, neat, A, B, C, D and E coating samples were placed in separate beakers with the coating surface facing up. 30 mL of distilled water was added to the beakers and the mouths of the beakers were covered with parafilm to prevent the water from evaporating at the temperature. Before starting the test and after tests, the pH levels of the water in each sample were measured using the OHAUS Starter 3000 device. The weights of the coating samples were measured before and after 2 weeks samples were removed and dried to constant weight to determine mass changes.

Due to the high degree of hydroxylation of its molecular chain, PVA-based materials are highly permeable to water vapor and have a high degree of water

sensitivity and solubility. However, since this solubility starts at temperatures of 90 ˚C and above, its durability can be high in in-body use. In addition, Polyvinyl alcohol (PVA) is a semi-crystalline, chemically and thermally stable polymer with high mechanical strength and the ability to form excellent polymeric films (Hamid et al. 2022; Sarkhel et al. 2023; Zeng et al. 2023). In order to simulate the durability and stability of the coatings for in-body use, the test temperature was determined as 37 °C, as applied in similar literature studies (Hajinaebi et al. 2022; Januariyasa et al. 2020; Lin et al. 2021; Mahanty and Shikha 2022; Wu et al. 2021; Wu et al. 2023) . In order to analyze the condition of the coatings in room temperature environments, another test was carried out at 25 °C. Physical images of post-test coatings are shown in Figures 4.33 and 4.34. Color changes in coatings are caused by plant extracts, nano silvers and drying after coating. As can be seen, the coating B samples were the most damaged. This may be due to the poor bonding of the coating to the substrate surfaces. This weakness may also have occurred as a result of insufficient surface roughening and coating environmental conditions.

Figure 4.32 Incubator assembly for degradation testing and coating samples placed in the assembly in beakers.

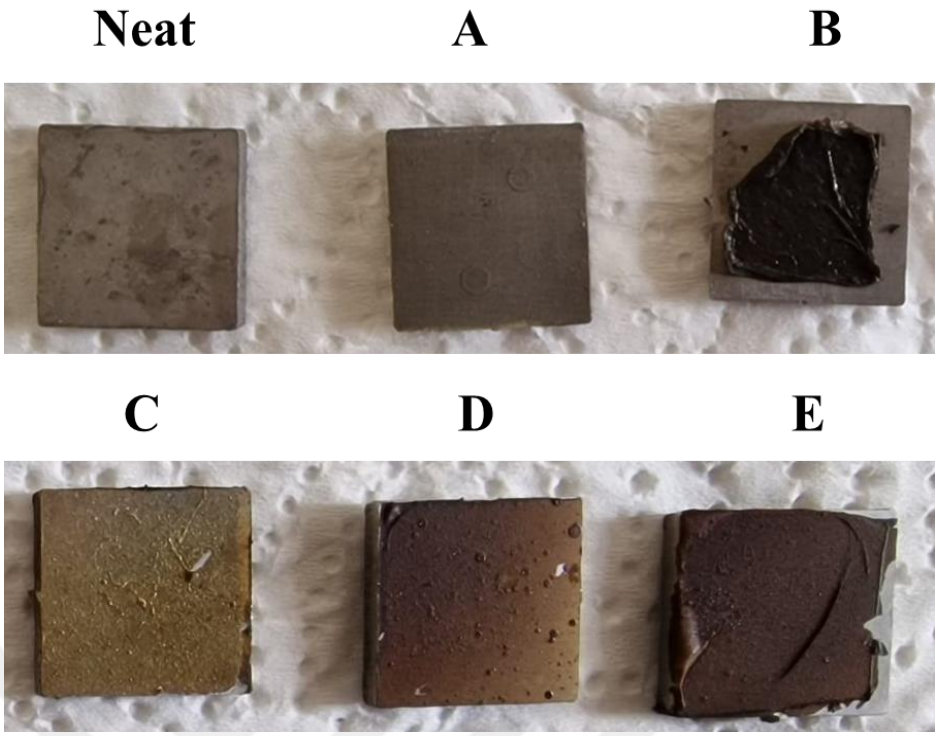

Figure 4.33 Coating Surfaces After Waited in Distilled Water at 27 ˚C for 2 Weeks.

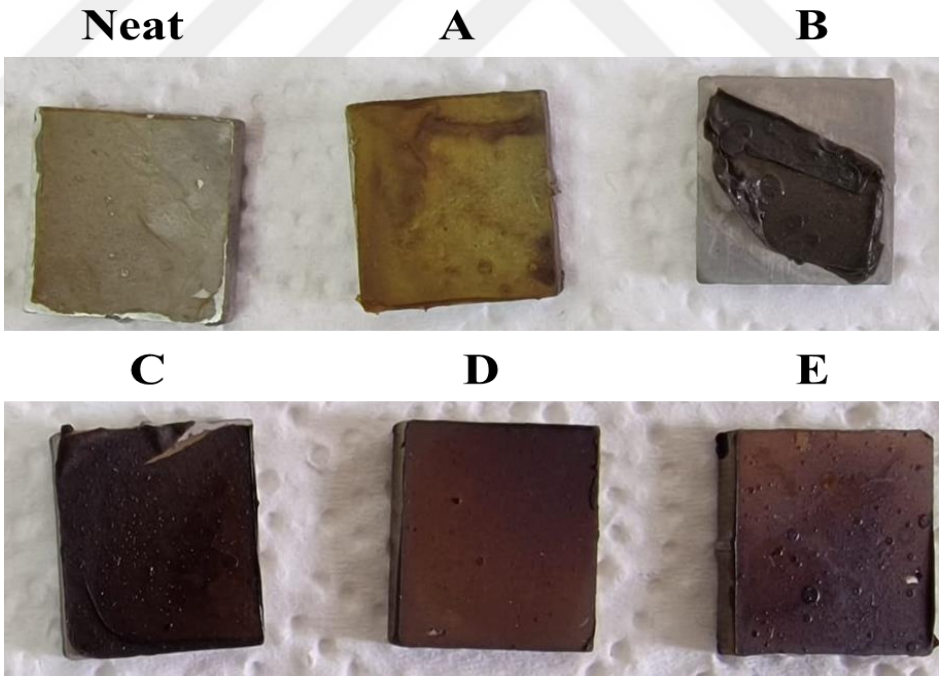

Figure 4.34 Coating Surfaces After Waited in Distilled Water at 37 ˚C for 2 Weeks.

The weight changes of the coatings given in Figures 4.35 and 4.36 revealed that there is increase in weights of the coatings. As known, this increase is due to the hydrophilic properties of PVA. In addition, Figure 4.12 swelling ratios results prove this property. While the swelling ratio of the films with plant extracts increases compared to the neat sample, the swelling ratios decrease with the addition of nano silver. These similar behaviors of the films are also seen in the durability tests of the coatings. In the tests performed at 37 ˚C, it was determined that the mass gains increased in A, B and C samples compared to the mass gains occurring at 27 ˚C, but remained at similar rates in D and E samples. The "polymer backbone" in PVA is hydrophilic because it contains water-loving carboxylic acid groups (–COOH). When water is added to superabsorbent polymers, a polymer/solvent interaction occurs; hydration and the formation of hydrogen bonds are two of these interactions. When the neutral polymer comes into contact with water or aqueous solutions, these positive and negative charges in its structure interact with water molecules. Because the water molecule (H_2O) is a polar molecule because positive charges are concentrated on the hydrogen atoms and negative charges are concentrated on the oxygen atoms. While this increases the strength of the bonds between water molecules, it also allows water to interact with electrically charged particles. Ag^+ ions interacting with the oxygen atom of the water dissolve in the water and leave the chain. Since the COO^- ions remaining on the polymer chains have the same charge, they start to repel each other with electrostatic force. Thus, the polymer chains expand. However, thanks to the cross-links that provide network formation between the chains, the polymer is insoluble in water and the expanding polymer ball can take more water into it. As the COO^- ions on the chain interact with the water molecules, the water that enters between the polymer chains is retained by the polymer. Ag^+ ions leaving the polymer chain move freely in the polymer network, but they do not leave the polymer network because they are attracted, albeit weakly, by the COO^- in the polymer chains. Therefore, the ion density in the polymer network is higher than in the polymer environment. Due to this density difference, water moves from a less dense medium to a more dense medium and enters between the polymer chains and the polymer swells.The increase in temperature caused the PVA chains to move, increasing their bonding with water molecules and causing an increase in weight gain. Nano silvers modified in coatings prevented water from entering the coating structure by bonding with polymer chains and filling the micro pores in the matrix. The low weight gains of

D and E samples at high temperatures mean that the strength of these coatings is increased compared to other samples. Apart from that, it was determined that the weight gains in the A, B and C samples were higher than the neat sample. This increase is due to the amount of fiber deposited on the substrate surface and homogeneous coating distribution, as can be seen from the microstructure images in Section 4.5.1.

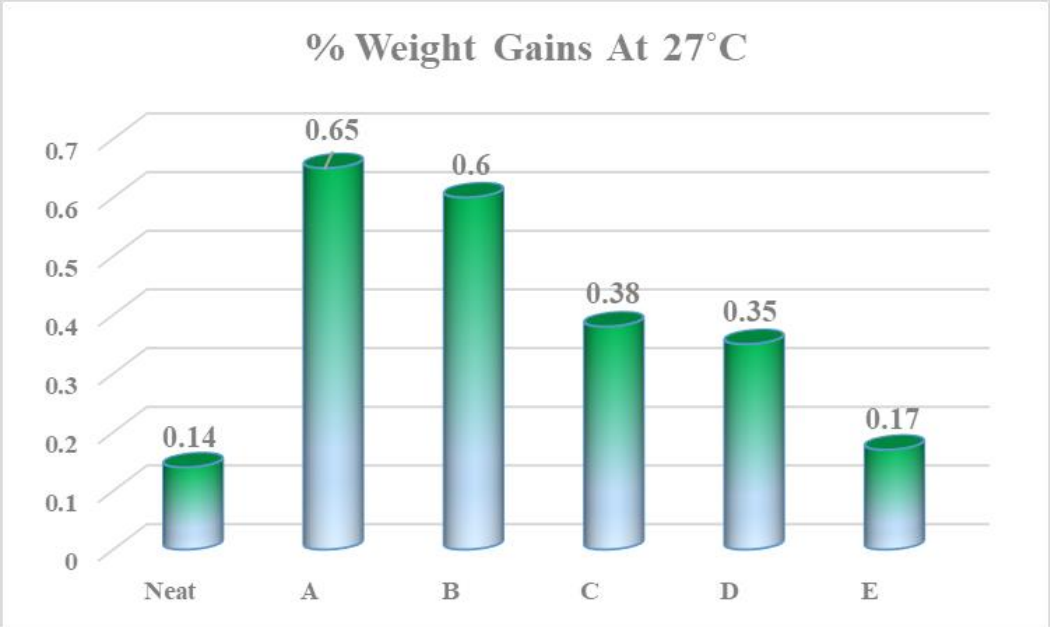

Figure 4.35 % Weight gains of the coated samples kept in water at 27 °C for 2 weeks.

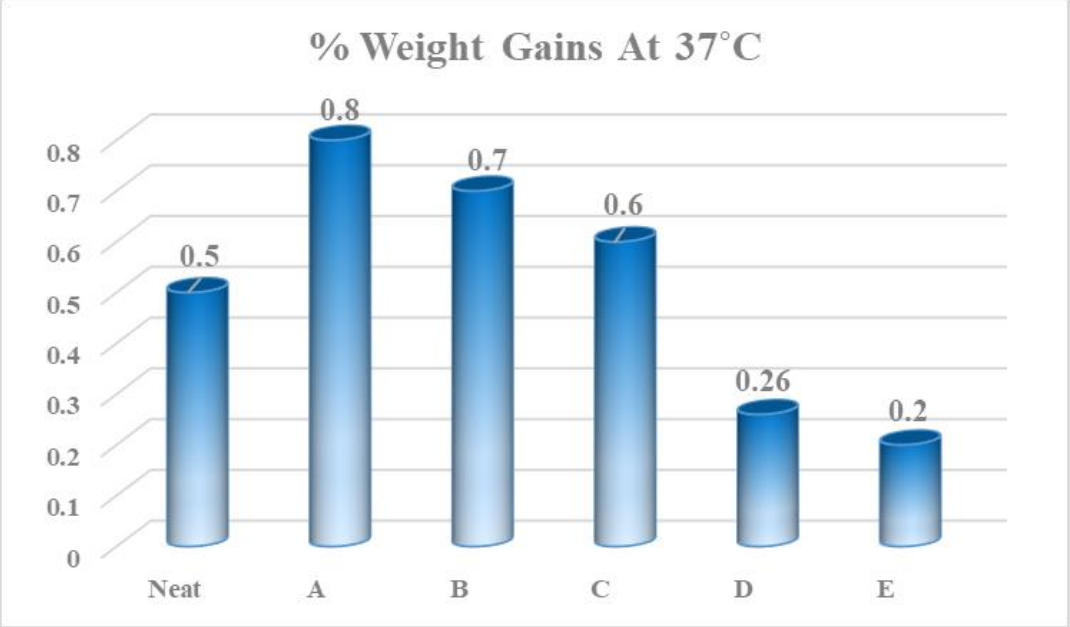

Figure 4.36 % Weight gains of the coated samples kept in water at 37 °C for 2 weeks.

The migration of AgNPs occurred in high temperatures and acidic conditions. Therefore, hot and acidic foods have the highest rate of migration of AgNPs. The migration mechanisms of AgNPs into the liquid medium depend on the release of separated AgNPs from the matrix and the dissolution of silver ions after oxidation. The AgNPs dissolution rate is dependent on the environmental status, their physicochemical properties, particle size, shape, crystallinity and surface functionalization (Azizi-Lalabadi et al. 2021). High pH environment resulting from the rapid ion exchange between the alkaline ions from the coating surface and the hydrogen ions from the solution (Hadzhieva and Boccaccini 2022).

The pH changes of the water environment of the samples whose durability tests were carried out are given in Tables 4.5 and 4.6. It was determined that the pH change rates decreased with the increase in the amount of nano silver in the coating in direct proportion to the mass gains. In fact, pH changes in samples C, D, and E containing nano silver particles in high temperature tests showed only 0.1 fluctuations. In the tests performed at both temperatures, the most chemically stable sample was C. These results proved that plant extracts and green synthesized nano-silver modified ESD coatings have chemical stability, high physical strength and do not critically change the pH of the aquatic environment for in-body use.

Table 4.5 pH changes of the coated samples kept in water at 27 °C after 2 weeks.

pH Changes at 27 ˚C		
	Initial Value	**2 Week**
Neat	7.14	7.23
A	7.23	7.18
B	7.18	7.13
C	7.15	7.14
D	7.04	7.08
E	7.03	7.13

Table 4.6 pH changes of the coated samples kept in water at 37 °C after 2 weeks.

	pH Changes at 37 ˚C	
	Initial Value	**2 Week**
Neat	7.8	6.85
A	7.13	7.06
B	7.14	7.03
C	7.08	7.08
D	7.11	7.12
E	7.06	7.07

4.9. HaCat And A549 Cells Viability Determination By MTT Assay

The biological properties of AgNPs, mainly their size, shape and surface chemical structure, affect many of their properties, including their antimicrobial activity and cytotoxicity. Nanoparticles are cytotoxic for several different cell lines, mostly by inducing an increase of reactive oxygen species (ROS) production, a decrease in mitochondrial function, DNA damage, and apoptosis. These toxic effects of nonaparticles occur after certain concentrations. For this reason, it is critically important to determine the maximum nano silver concentration that can be used in polymeric coating materials in dentistry in this study. Because the release of nano silver ions from the coating material to living tissues may be delayed and this toxic effect may occur after certain rates.

The cytotoxic effect of green synthesized silver nanoparticles on A549 lung carcinoma epithelial cells and HaCaT immortalized human keratinocyte cells was determined by the Methylthiazoledphenyl-tetrazolium bromide (MTT) test. The methylthiazoledphenyl-tetrazolium bromide (MTT) test is based on the measurement of mitochondrial metabolic activity, an indicator of cell viability. The colorimetric assay was performed by reducing a yellow tetrazolium salt (3-(4,5-dimethylthiazol-2-yl)-2,5-diphenyltetrazolium bromide (MTT) to purple formazan crystals by metabolically active cells. Living cells contain NAD(P)H-dependent oxidoreductase enzymes that reduce MTT to formazan. The water-insoluble formazan crystals were dissolved in a solution, and the absorbance values of the obtained colored solution were measured at 540-570 nanometers by means of a spectrophotometer. Viable

HaCaT cells were seeded into 96-well plates in DMEM containing high glucose supplemented with 10% FBS, 100 U/mL Penicillin - 0.1 mg/mL Streptomycin and 0.05 µg/mL Amphotericin B. Three replicates were seeded at a density of 1×10^4 cells per well. The plates were incubated for 24 h in a humidified incubator with 5% CO_2 at 37 °C to allow the cells to adhere to the surface. At the end of the incubation period, the culture medium was removed from the wells, and nanoparticles prepared in different concentrations of DMEM-H were distributed to the wells. The medium in the control group wells, prepared in three replicates, was renewed with fresh culture medium pre-warmed to 37 °C. The culture medium containing sterile deionized water, which was used as a solvent for nanoparticles, was placed in the wells in 3 repetitions as a solvent control. To measure the background absorbance values of the media prepared for the experimental groups, the media were distributed to the wells where there were no cells. After application, the plates were incubated for 24 h in an incubator containing 5% CO_2 at 37 °C. After incubation, 5 mg/mL MTT (Sigma-Aldrich®, M2128) reagent dissolved in 1x PBS (Phosphate Buffer Saline) was added to each well in an amount equal to 10% of the volume of culture medium. The plates were incubated again for 4 h in an incubator containing 5% CO_2. Following incubation, a 0.01 N solution of HCL (Supelco®, 109973) containing 10% SDS (Sigma-Aldrich®, 75746) was added to the wells as a solvent. After the plates were incubated for less than 16 h at 37 °C in a CO_2 incubator, the absorbance values in the wells were determined using a BioTek® 800™ TS microplate reader spectrophotometer at 570 nm.

The significance levels of the differences between the absorbance values of the experimental groups from which the background absorbance values were removed were determined by one-way analysis of variance (one-way ANOVA) in Prism 7.00 (GraphPad Software, Inc.), followed by Tukey's post-hoc test. In addition, p values were graded as significant (*) between 0.01 and 0.05, very significant (**) between 0.001 and 0.01, highly significant (****) between 0.0001 and 0.001 (***), and less than 0.0001.

Figure 4.37 shows the results of toxicity tests performed on living cell HaCaT. The viability rates of the cells were determined for the silver nanoparticles used at certain concentrations after the test. The toxic effects of AgNPs produced by green synthesis on HaCaT cells were seen at values higher than 110 µg/mL. This value was determined as 50% viability concentration (lowest half-maximal inhibitory concentration (IC50) levels) of viable cells. Viability of 90% and above was observed

at concentrations lower than 62 µg/mL. Ali et al., 2022, synthesized nanoparticles using *T. apollinea* plant and performed toxicity tests on HaCaT cells and found the toxicity value of 4.65 µg/mL. Wunnoo et al. 2021, showed that nano silver particles synthesized using Eucalyptus camaldulensis leaf extract did not exhibit toxic effects up to 8 µg/mL in their test on HaCaT cells. Khatoon et al. 2019, revealed that the silver nanoparticles synthesized using ampicillin were above 80% of HaCaT cell viability at concentrations of 100 µg /mL and below. S.R. et al. 2022, reported that silver nanoparticles synthesized using Dictyota ciliolata extract had a toxic effect in large amounts at a concentration of 40 µg/mL. When the toxicity rates of nano silvers produced by green synthesis in the literature were compared with the nanoparticles synthesized in this study, it was calculated that nano silvers synthesized with Hemp seed and St. John's Wort had an average of 65% less toxic effects (Montano et al. 2019; Rolim et al. 2019; Skóra et al. 2021; Zepon et al. 2023). The use of hemp seeds and St.John's Wort Extracts polyphenols to synthesize AgNPs is responsible for the capping of the obtained nanomaterial with phytochemicals that act as potent antioxidant and anti-inflammatory agents, reducing the potential toxicity of the nanoparticles.

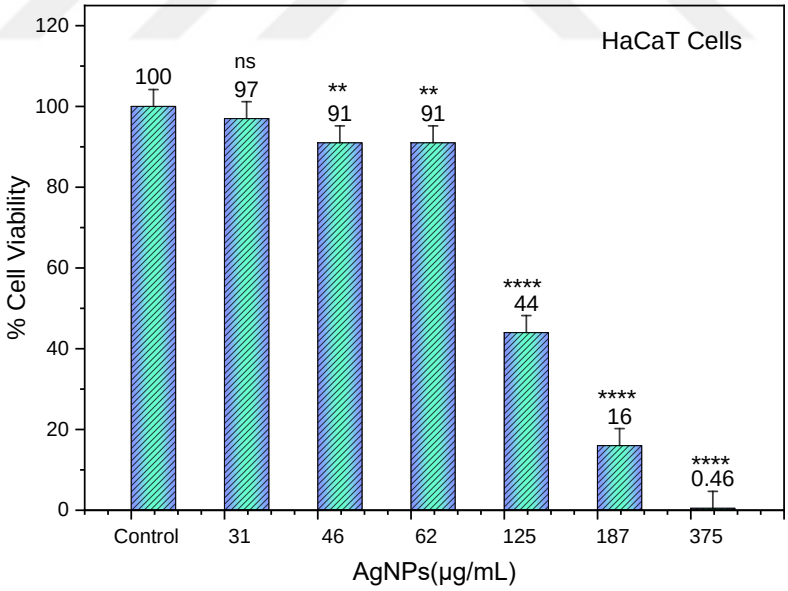

Figure 4.37 Cytotoxic effects exhibited by biosynthesized silver nanoparticles normal live HaCaT cells, as determined using MTT assay after 24 h of treatment. Data represent mean ± standard deviations of five replications. The statistical signifcance is indicated as follows: ** p<0.0041 and **** p<0.0001. ("ns" means not significant).

Figure 4.38 shows the results of toxicity tests performed on lung cancer A549 cells. This test was carried out to demonstrate the lethal effect of silver nanoparticles

produced by green synthesis on cancer cells. The use of nanoparticles in cancer treatment has become widespread in recent years. Increasing the lethal effect of nanoparticles, especially on cancer cells, has become important issues. The viability rates of the cells were determined for the silver nanoparticles used at certain concentrations after the test. It was determined that the use of nano silver particles synthesized using Hemp seeds and St. John's Wort extracts at concentrations higher than 137 µg/mL caused up to 50% death of A549 lung cancer cells. At concentrations lower than 62 µg/mL, 95% and higher viability was achieved. Comparing half-life concentrations, it was calculated that A549 cancer cells showed 20% higher resistance to green synthesized silver nanoparticles than HaCaT live cells. Prathipkumar et al. 2023, revealed that nano silvers synthesized with heneicosane extract had a lethal effect on A549 cancer cells at concentrations higher than 82 µg/mL. Karan et al. 2022, have been reported that nano silver particles synthesized with curcumin have a lethal effect at concentrations of 250 µg/mL and higher. Viswanathan et al. 2023, reported that nano silver produced with Champia parvula could kill A549 cancer cells at concentrations of 12.5 mg/mL and above. On the other hand, Pandey et al. 2023 and S R et al. 2022 reported that they found the concentrations required for the survival of A549 cancer cells at 50% and below, as 6% and 15% µg/mL, respectively, of nano silver produced with Blumea lacera and Dictyota ciliolata extracts. In fact, these studies in the litterature showed that nano silver synthesized with Hemp Seeds and St. St. John's Wort has a lower toxic effect on living and cancer cells, while on the other hand, they killed cancer cells and revealed their usability in the treatment of cancer diseases. The biological compounds in the plant extracts have been effectively utilized as capping and reducing agents in the formation of nanoparticles that can block the activity of A549 lung cancer cell proliferation.

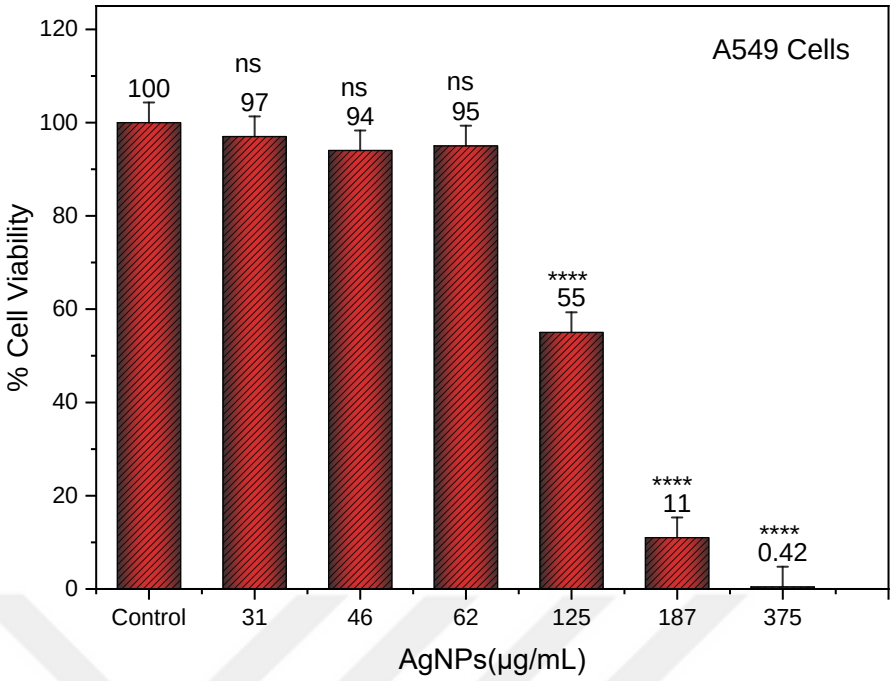

Figure 4.38 Cytotoxic effects exhibited by biosynthesized silver nanoparticles on lung adenocarcinoma A549 cells, as determined using MTT assay after 24 h of treatment. The values are the means (n=5) with standard deviation (error bars). Bars labeled with **** represent statistically significant results ($p < 0.001$). ("ns" means not significant).

5. CONCLUSIONS AND SUGGESTIONS

The present study aimed to increase the antibacterial effects, mechanical, chemical and thermal resistance of the biomaterials by coating the metallic biomaterials used in the dental field with plant extracts and bio-synthesized nano silver using a natural polymer, and to provide all these with the lowest toxic effects. In order to ensure that the polymer material to be used in coatings has the most suitable properties, first of all, nanocomposites were produced by solvent casting method and the characterization of these films was carried out. These films were produced with Hemp Seeds, St. St. John's Wort, Rosemary and Cherry Laurel, the plant species intended to be used in the coating. In addition, nano silvers used in coatings to provide antibacterial properties were synthesized green using these plants and modified into nanocomposite films. SEM and EDS analysis showed that nano green synthesed silver nano particles were spherical in shape and homogeneously dispersed in the films. The sizes of nanoparticles produced with Hemp seeds and St. John's Wort were much smaller than those produced with Rosemary and Cherry Laurel leaves. However, all plant extracts used in the study were very successful in AgNPs synthesis with a greener and cleaner way. The results of the XRD tests also showed the presence of nano silver particles in the films. Samples C and D have Shore-D hardness values 2 times higher than the neat sample. It has been observed that as the green synthesized AgNPs decrease in size, they cause an increase in the hardness values of the films they are modified. The hardness values of the samples A and B were also found to be considerably higher than the reference samples. Even the plant extract modification alone was effective in increasing the mechanical strength of polymer composite films. The swelling test results also showed that the samples C and D would have the highest mechanical strength. AgNPs in the films have decreased the water absorption rate and increased the hardness strength by filling the micropores in the PVA structure and increasing the cross-links. FTIR results also revealed that green synthesized nano silvers and plant extracts modified nano composite films formed C=C bonds with PVA, resulting in higher mechanical properties. It has been shown that nano-silver modification gives antibacterial properties to polymer nanocomposite films, as expected. After these characterizations, it was decided to use Hemp Seeds and St. John's Wort in the preparation of coating solutions, and the nano silver ratios to be 0.05, 0.1, 0.3 and 0.5.

In the study, Ti-6Al-4V alloy, which is widely used in dentistry, was used as veneer bases. Electrospray Deposition method was used as the coating method. After the coatings prepared in the determined compositions, a series of tests were performed to determine the properties and strengths of the samples. According to the SEM/EDS analyzes performed after coating, the green synthesis of AgNPs was achieved by using plant extracts and nanoparticles with an average size of 34 nm were produced. In addition, different minerals from plant extracts were also detected in the coating content. Dynamic and mechanical analyzes showed that D and E were the samples with the highest thermal and mechanical strengths from the coating films. Antibacterial tests have revealed that all coatings with nano silver additives reduce bacterial growth up to 100 times. The sample with the highest antibacterial effect was 0.5% AgNPs modified sample E. The scratch test performed to determine the mechanical properties showed that the sample with the hardest coating surfaces were the samples C, D and E. Also plant extracts modification to PVA increased the mechanical strength of the coatings. The chemical and mechanical stability of nano silver modified samples C, D and E in water at 37°C were found to be higher than the other samples. It was determined that nano silvers synthesized green with a mixture of Hemp Seeds and St. John's Wort extracts did not show any toxic effect in the toxicity tests performed on HaCaT live cells and A549 lung cancer cells, from nano silver concentrations to be used at 62 μg/mL and below.

This study provided a framework for investigating plant extracts and nano-silver-modified polymer nanocomposite coating applications in the healthcare field. In light of the empirical findings obtained, this study offers a new understanding of the antibacterial and biocompatible production of metallic biomaterials using plant extracts. In addition, it is thought that these biocomposite materials will have a wide range of uses for scientific and biomedical environments, thanks to their low raw material and production cost, easy production, human health and environmentally friendly production method, high thermomechanical strength and low toxic effect compared to their equivalents.

1. Publication bibliography

3RD INTERNATIONAL POSTGRADUATE CONFERENCE ON MATERIALS, MINERALS & POLYMER (MAMIP) 2019. Penang, Malaysia, 31 October–1 November 2019: AIP Publishing (AIP Conference Proceedings).

Abd El-Kader, F. H.; Gafer, S. A.; Basha, A. F.; Bannan, S. I.; Basha, M. A. F. (2010): Thermal and optical properties of gelatin/poly(vinyl alcohol) blends. In *J of Applied Polymer Sci* 118 (1), pp. 413–420. DOI: 10.1002/app.30841.

Abdelghany, A. M.; Menazea, A. A.; Ismail, A. M. (2019): Synthesis, characterization and antimicrobial activity of Chitosan/Polyvinyl Alcohol blend doped with Hibiscus Sabdariffa L. extract. In *Journal of Molecular Structure* 1197 (7), pp. 603–609. DOI: 10.1016/j.molstruc.2019.07.089.

Abdul Halim, Md; Karmakar, Subrata; Sourav Das, Sree; Geerts, Wilhelmus J.; Haque, Ariful; Beall, Gary W. (2023): Crystallite size-dependent magnetic moment in hydrogen bridged manganese tetracyanonickelate based two-dimensional metal-organic frameworks. In *Journal of Magnetism and Magnetic Materials* 571, p. 170573. DOI: 10.1016/j.jmmm.2023.170573.

Ahmad, Rais; Mirza, Anam (2017): Green synthesis of Xanthan gum/Methionine-bentonite nanocomposite for sequestering toxic anionic dye. In *Surfaces and Interfaces* 8 (8), pp. 65–72. DOI: 10.1016/j.surfin.2017.05.001.

Ahmadi, Shideh; Asim, Nilofar; Alghoul, M. A.; Hammadi, F. Y.; Saeedfar, Kasra; Ludin, N. A. et al. (2014): The Role of Physical Techniques on the Preparation of Photoanodes for Dye Sensitized Solar Cells. In *International Journal of Photoenergy* 2014 (12), pp. 1–19. DOI: 10.1155/2014/198734.

Ahmed, Omnia; Sibuyi, Nicole Remaliah Samantha; Fadaka, Adewale Oluwaseun; Madiehe, Madimabe Abram; Maboza, Ernest; Meyer, Mervin; Geerts, Greta (2022a): Plant Extract-Synthesized Silver Nanoparticles for Application in Dental Therapy. In *Pharmaceutics* 14 (2). DOI: 10.3390/pharmaceutics14020380.

Ahmed, Reem Hassan; Mustafa, Damra Elhaj (2020): Green synthesis of silver nanoparticles mediated by traditionally used medicinal plants in Sudan. In *Int Nano Lett* 10 (1), pp. 1–14. DOI: 10.1007/s40089-019-00291-9.

Ahmed, Shams Forruque; Mofijur, M.; Rafa, Nazifa; Chowdhury, Anika Tasnim; Chowdhury, Sidratun; Nahrin, Muntasha et al. (2022b): Green approaches in synthesising nanomaterials for environmental nanobioremediation. Technological advancements, applications, benefits and challenges. In *Environmental research* 204 (Pt A), p. 111967. DOI: 10.1016/j.envres.2021.111967.

Akiyode, Olufunke; Boateng, Joshua (2018): Composite Biopolymer-Based Wafer Dressings Loaded with Microbial Biosurfactants for Potential Application in Chronic Wounds. In *Polymers* 10 (8). DOI: 10.3390/polym10080918.

Alahmad, Abdalrahim; Feldhoff, Armin; Bigall, Nadja C.; Rusch, Pascal; Scheper, Thomas; Walter, Johanna-Gabriela (2021a): Hypericum perforatum L.-Mediated Green Synthesis of Silver Nanoparticles Exhibiting Antioxidant and Anticancer Activities. In *Nanomaterials (Basel, Switzerland)* 11 (2). DOI: 10.3390/nano11020487.

Alahmad, Abdalrahim; Feldhoff, Armin; Bigall, Nadja C.; Rusch, Pascal; Scheper, Thomas; Walter, Johanna-Gabriela (2021b): Hypericum perforatum L.-Mediated Green Synthesis of Silver Nanoparticles Exhibiting Antioxidant and Anticancer Activities. In *Nanomaterials (Basel, Switzerland)* 11 (2). DOI: 10.3390/nano11020487.

Al-Bermany, Ehssan; Mekhalif, Ali Tao'mah; Banimuslem, Hikmat A.; Abdali, Karar; Sabri, Mohammed M. (2023): Effect of green synthesis bimetallic Ag@SiO2 core–shell

nanoparticles on absorption behavior and electrical properties of PVA-PEO nanocomposites for optoelectronic applications. In *Silicon* 15, p. 187. DOI: 10.1007/s12633-023-02332-7.

Albrektsson, Tomas; Wennerberg, Ann (2019): On osseointegration in relation to implant surfaces. In *Clinical implant dentistry and related research* 21 Suppl 1, pp. 4–7. DOI: 10.1111/cid.12742.

Alcudia, Ana; Begines, Belén; Rodriguez-Lejarraga, Paula; Greyer, Valeria; Godinho, Vanda Cristina Fortio; Pajuelo, Eloísa; Torres, Yadir (2022): Development of porous silver nanoparticle/polycaprolactone/polyvinyl alcohol coatings for prophylaxis in titanium interconnected samples for dental implants. In *Colloid and Interface Science Communications* 48 (5), p. 100621. DOI: 10.1016/j.colcom.2022.100621.

Aldeen, Thana Shuga; Ahmed Mohamed, Hamza Elsayed; Maaza, Malik (2022): ZnO nanoparticles prepared via a green synthesis approach. Physical properties, photocatalytic and antibacterial activity. In *Journal of Physics and Chemistry of Solids* 160 (8), p. 110313. DOI: 10.1016/j.jpcs.2021.110313.

Alharbi, Njud S.; Alsubhi, Nehad S.; Felimban, Afnan I. (2022a): Green synthesis of silver nanoparticles using medicinal plants. Characterization and application. In *Journal of Radiation Research and Applied Sciences* 15 (3), pp. 109–124. DOI: 10.1016/j.jrras.2022.06.012.

Alharbi, Njud S.; Alsubhi, Nehad S.; Felimban, Afnan I. (2022b): Green synthesis of silver nanoparticles using medicinal plants. Characterization and application. In *Journal of Radiation Research and Applied Sciences* 15 (3), pp. 109–124. DOI: 10.1016/j.jrras.2022.06.012.

Ali, Muna A.; Soliman, Sameh S.M.; Bajou, Khalid; El-Keblawy, Ali; Mosa, Kareem A. (2022): Identification of phytochemicals capping the exogenously biosynthesized silver nanoparticles by T. apollinea (Delile) DC. living plants and evaluation of their cytotoxic activity. In *Biocatalysis and Agricultural Biotechnology* 42 (1), p. 102336. DOI: 10.1016/j.bcab.2022.102336.

Aljohny, Bassam Oud; Almaliki, Abdullah Abdulaziz Ali; Anwar, Yasir; Ul-Islam, Mazhar; Kamal, Tahseen (2021): Antibacterial and Catalytic Performance of Green Synthesized Silver Nanoparticles Embedded in Crosslinked PVA Sheet. In *J Polym Environ* 29 (10), pp. 3252–3262. DOI: 10.1007/s10924-021-02110-9.

Anchan, Sanjana; Pai, Shraddha; Sridevi, H.; Varadavenkatesan, Thivaharan; Vinayagam, Ramesh; Selvaraj, Raja (2019): Biogenic synthesis of ferric oxide nanoparticles using the leaf extract of Peltophorum pterocarpum and their catalytic dye degradation potential. In *Biocatalysis and Agricultural Biotechnology* 20 (1), p. 101251. DOI: 10.1016/j.bcab.2019.101251.

Angel Ezhilarasi, A.; Judith Vijaya, J.; Kaviyarasu, K.; John Kennedy, L.; Ramalingam, R. Jothi; Al-Lohedan, Hamad A. (2018): Green synthesis of NiO nanoparticles using Aegle marmelos leaf extract for the evaluation of in-vitro cytotoxicity, antibacterial and photocatalytic properties. In *Journal of photochemistry and photobiology. B, Biology* 180, pp. 39–50. DOI: 10.1016/j.jphotobiol.2018.01.023.

Arularasu, M. V.; Devakumar, J.; Rajendran, T. V. (2018): An innovative approach for green synthesis of iron oxide nanoparticles. Characterization and its photocatalytic activity. In *Polyhedron* 156 (5), pp. 279–290. DOI: 10.1016/j.poly.2018.09.036.

Azizi-Lalabadi, Maryam; Garavand, Farhad; Jafari, Seid Mahdi (2021): Incorporation of silver nanoparticles into active antimicrobial nanocomposites. Release behavior, analyzing techniques, applications and safety issues. In *Advances in colloid and interface science* 293, p. 102440. DOI: 10.1016/j.cis.2021.102440.

Bai, Zhongxiang; Wang, Tianyou; Zheng, Xin; Huang, Yanping; Chen, Yining; Dan, Weihua (2021): High strength and bioactivity polyvinyl alcohol/collagen composite hydrogel with tannic acid as cross-linker. In *Polym Eng Sci* 61 (1), pp. 278–287. DOI: 10.1002/pen.25574.

Balachandar, Ramalingam; Navaneethan, Rajendran; Biruntha, Muniyandi; Ashok Kumar, Krishna Kumar; Govarthanan, Muthusamy; Karmegam, Natchimuthu (2022): Antibacterial activity of silver nanoparticles phytosynthesized from Glochidion candolleanum leaves. In *Materials Letters* 311 (6), p. 131572. DOI: 10.1016/j.matlet.2021.131572.

Bapat, Malini S.; Singh, Hema; Shukla, Sudheesh K.; Singh, Prabal Pratap; Vo, Dai-Viet N.; Yadav, Alpa et al. (2022): Evaluating green silver nanoparticles as prospective biopesticides. An environmental standpoint. In *Chemosphere* 286 (Pt 2), p. 131761. DOI: 10.1016/j.chemosphere.2021.131761.

Bari, Sarang S.; Chatterjee, Aniruddha; Mishra, Satyendra (2016): Biodegradable polymer nanocomposites. An overview. In *Polymer Reviews* 56 (2), pp. 287–328. DOI: 10.1080/15583724.2015.1118123.

Baskovich, Brett; Sampson, Edith M.; Schultz, Gregory S.; Parnell, Laura K. S. (2008): Wound dressing components degrade proteins detrimental to wound healing. In *International wound journal* 5 (4), pp. 543–551. DOI: 10.1111/j.1742-481X.2007.00422.x.

Batool, Sadaf; Hussain, Zakir; Niazi, Muhammad Bilal Khan; Liaqat, Usman; Afzal, Muhammad (2019): Biogenic synthesis of silver nanoparticles and evaluation of physical and antimicrobial properties of Ag/PVA/starch nanocomposites hydrogel membranes for wound dressing application. In *Journal of Drug Delivery Science and Technology* 52 (3), pp. 403–414. DOI: 10.1016/j.jddst.2019.05.016.

Bernstein, Michael J.; Franssen, Thomas; Smith, Robert D. J.; Wilde, Mandy de (2022): The European Commission's Green Deal is an opportunity to rethink harmful practices of research and innovation policy. In *Ambio. DOI:* 10.1007/s13280-022-01802-3.

Bibi, Ismat; Nazar, Nosheen; Ata, Sadia; Sultan, Misbah; Ali, Abid; Abbas, Ansar et al. (2019): Green synthesis of iron oxide nanoparticles using pomegranate seeds extract and photocatalytic activity evaluation for the degradation of textile dye. In *Journal of Materials Research and Technology* 8 (6), pp. 6115–6124. DOI: 10.1016/j.jmrt.2019.10.006.

Brånemark, P. I. (1983): Osseointegration and its experimental background. In *The Journal of prosthetic dentistry* 50 (3), pp. 399–410. DOI: 10.1016/s0022-3913(83)80101-2.

Brayner, Roberta; Fiévet, Fernand; Coradin, Thibaud (2013): Nanomaterials. A danger or a promise? ; a chemical and biological perspective / Roberta Brayner, Fernand Fiévet, Thibaud Coradin, editors. London: Springer.

Buga, Csaba; Chen, Chun-Cheng; Hunyadi, Mátyás; Csík, Attila; Hegedűs, Csaba; Ding, Shinn-Jyh (2021): Electrosprayed calcium silicate nanoparticle-coated titanium implant with improved antibacterial activity and osteogenesis. In *Colloids and surfaces. B, Biointerfaces* 202, p. 111699. DOI: 10.1016/j.colsurfb.2021.111699.

Buga, Csaba; Hunyadi, Mátyás; Gácsi, Zoltán; Hegedűs, Csaba; Hakl, József; Schmidt, Ute et al. (2019): Calcium silicate layer on titanium fabricated by electrospray deposition. In *Materials science & engineering. C, Materials for biological applications* 98, pp. 401–408. DOI: 10.1016/j.msec.2019.01.011.

Bulla, Soumya S.; Bhajantri, R. F.; Chavan, Chetan (2021): Optical and Structural Properties of Biosynthesized Silver Nanoparticle Encapsulated PVA (Ag–PVA) Films. In *J Inorg Organomet Polym* 31 (6), pp. 2368–2380. DOI: 10.1007/s10904-021-01909-2.

Burgaz, Engin; Lian, Huiqin; Alonso, Rafael Herrera; Estevez, Luis; Kelarakis, Antonios; Giannelis, Emmanuel P. (2009): Nafion–clay hybrids with a network structure. In *Polymer* 50 (11), pp. 2384–2392. DOI: 10.1016/j.polymer.2009.03.042.

Cappellini, Cristian; Malandruccolo, Alessio; Abeni, Andrea; Attanasio, Aldo (2023): A feasibility study of promoting osseointegration surface roughness by micro-milling of Ti-6Al-4V biomedical alloy. In *Int J Adv Manuf Technol* 5 (7), p. 371. DOI: 10.1007/s00170-023-11318-z.

Carrouel, Florence; Viennot, Stephane; Ottolenghi, Livia; Gaillard, Cedric; Bourgeois, Denis (2020): Nanoparticles as Anti-Microbial, Anti-Inflammatory, and Remineralizing Agents in Oral Care Cosmetics. A Review of the Current Situation. In *Nanomaterials (Basel, Switzerland)* 10 (1). DOI: 10.3390/nano10010140.

Chandhru, M.; Logesh, R.; Kutti Rani, S.; Ahmed, Neesar; Vasimalai, N. (2022): Green synthesis of silver nanoparticles from plant latex and their antibacterial and photocatalytic studies. In *Environmental technology* 43 (20), pp. 3064–3074. DOI: 10.1080/09593330.2021.1914181.

Chen, Qizhi; Thouas, George A. (2015): Metallic implant biomaterials. In *Materials Science and Engineering: R: Reports* 87 (Suppl), pp. 1–57. DOI: 10.1016/j.mser.2014.10.001.

Chen, Xionggang; Zhou, Jianhong; Qian, Yu; Zhao, LingZhou (2023): Antibacterial coatings on orthopedic implants. In *Materials today. Bio* 19, p. 100586. DOI: 10.1016/j.mtbio.2023.100586.

Chien, Chi-Sheng; Lin, Chao-Jen; Ko, Chih-Jung; Tseng, Sung-Pin; Shih, Chi-Jen (2018): Antibacterial activity of silver nanoparticles (AgNP) confined to mesostructured silica against methicillin-resistant Staphylococcus aureus (MRSA). In *Journal of Alloys and Compounds* 747 (16), pp. 1–7. DOI: 10.1016/j.jallcom.2018.02.334.

Csakvari, Adriana Cecilia; Moisa, Cristian; Radu, Dana G.; Olariu, Leonard M.; Lupitu, Andreea I.; Panda, Anca Ofelia et al. (2021a): Green Synthesis, Characterization, and Antibacterial Properties of Silver Nanoparticles Obtained by Using Diverse Varieties of Cannabis sativa Leaf Extracts. In *Molecules (Basel, Switzerland)* 26 (13). DOI: 10.3390/molecules26134041.

Csakvari, Adriana Cecilia; Moisa, Cristian; Radu, Dana G.; Olariu, Leonard M.; Lupitu, Andreea I.; Panda, Anca Ofelia et al. (2021b): Green Synthesis, Characterization, and Antibacterial Properties of Silver Nanoparticles Obtained by Using Diverse Varieties of Cannabis sativa Leaf Extracts. In *Molecules (Basel, Switzerland)* 26 (13). DOI: 10.3390/molecules26134041.

Darie-Niţă, Raluca Nicoleta; Vasile, Cornelia; Stoleru, Elena; Pamfil, Daniela; Zaharescu, Traian; Tarţău, Liliana et al. (2018): Evaluation of the Rosemary Extract Effect on the Properties of Polylactic Acid-Based Materials. In *Materials (Basel, Switzerland)* 11 (10). DOI: 10.3390/ma11101825.

Darwish, Moustafa A.; Zubar, Tatiana I.; Kanafyev, Oleg D.; Di Zhou; Trukhanova, Ekaterina L.; Trukhanov, Sergei V. et al. (2022): Combined Effect of Microstructure, Surface Energy, and Adhesion Force on the Friction of PVA/Ferrite Spinel Nanocomposites. In *Nanomaterials (Basel, Switzerland)* 12 (12). DOI: 10.3390/nano12121998.

Del Olmo, Jon Andrade; Pérez-Álvarez, Leyre; Pacha-Olivenza, Miguel Ángel; Ruiz-Rubio, Leire; Gartziandia, Oihane; Vilas-Vilela, José Luis; Alonso, José Maria (2021): Antibacterial catechol-based hyaluronic acid, chitosan and poly (N-vinyl pyrrolidone) coatings onto Ti6Al4V surfaces for application as biomedical implant. In *International journal of biological macromolecules* 183, pp. 1222–1235. DOI: 10.1016/j.ijbiomac.2021.05.034.

Delgado-Rangel, Luis Humberto; Hernández-Vargas, Julia; Becerra-González, Marymar; Martínez-Torres, Ataúlfo; Prokhorov, Evgen; González Campos, J. Betzabe (2019): Development of Collagen/Poly(vinyl alcohol)/Chondroitin Sulfate and Collagen/Poly(vinyl alcohol)/HA Electrospun Scaffolds for Tissue Engineering. In *Fibers Polym* 20 (12), pp. 2470–2484. DOI: 10.1007/s12221-019-9341-x.

Dikshit, Pritam; Kumar, Jatin; Das, Amit; Sadhu, Soumi; Sharma, Sunita; Singh, Swati et al. (2021): Green Synthesis of Metallic Nanoparticles. Applications and Limitations. In *Catalysts* 11 (8), p. 902. DOI: 10.3390/catal11080902.

Ding, Mingchao; Shi, Jin; Wang, Weiqi; Li, Dechao; Tian, Lei (2022): Early osseointegration of micro-arc oxidation coated titanium alloy implants containing Ag. A histomorphometric study. In *BMC oral health* 22 (1), p. 628. DOI: 10.1186/s12903-022-02673-6.

Dolabella, Simone; Borzì, Aurelio; Dommann, Alex; Neels, Antonia (2022): Lattice Strain and Defects Analysis in Nanostructured Semiconductor Materials and Devices by High-Resolution X-Ray Diffraction. Theoretical and Practical Aspects. In *Small methods* 6 (2), e2100932. DOI: 10.1002/smtd.202100932.

Donya, Hossam; Taha, T. A.; Alruwaili, A.; Tomsah, I.B.I.; Ibrahim, M. (2020): Micro-structure and optical spectroscopy of PVA/iron oxide polymer nanocomposites. In *Journal of Materials Research and Technology* 9 (4), pp. 9189–9194. DOI: 10.1016/j.jmrt.2020.06.040.

Drummer, Sean; Madzimbamuto, Tafirenyika; Chowdhury, Mahabubur (2021): Green Synthesis of Transition-Metal Nanoparticles and Their Oxides. A Review. In *Materials (Basel, Switzerland)* 14 (11). DOI: 10.3390/ma14112700.

Dwivedi, Poushpi; Narvi, Shahid S.; Tewari, Ravi P. (2013): Application of polymer nanocomposites in the nanomedicine landscape. Envisaging strategies to combat implant associated infections. In *Journal of applied biomaterials & functional materials* 11 (3), e129-42. DOI: 10.5301/JABFM.2013.11544.

Elangovan, Dhivya; Rahman, Haajira Beevi Habeeb; Dhandapani, Ranjithkumar; Palanivel, Velmurugan; Thangavelu, Sathiamoorthi; Paramasivam, Ragul; Muthupandian, Saravanan (2022): Coating of wallpaper with green synthesized silver nanoparticles from Passiflora foetida fruit and its illustrated antifungal mechanism. In *Process Biochemistry* 112 (16), pp. 177–182. DOI: 10.1016/j.procbio.2021.11.027.

El-Deeb, A. S.; Kader, M. M. Abdel; Nasr, G. M.; Ahmed, M. A.; Taha, Eman O. (2022): Modification of structural, thermal, dielectric and dynamic mechanical properties of PVA using lead (II) titanate. In *Bull Mater Sci* 45 (2), p. 229. DOI: 10.1007/s12034-022-02658-9.

Elias, C. N.; Lima, J. H. C.; Valiev, R.; Meyers, M. A. (2008): Biomedical applications of titanium and its alloys. In *JOM* 60 (3), pp. 46–49. DOI: 10.1007/s11837-008-0031-1.

Eskandari Azar, Behzad; Ramazani, Ali; Taghavi Fardood, Saeid; Morsali, Ali (2020): Green synthesis and characterization of ZnAl2O4@ZnO nanocomposite and its environmental applications in rapid dye degradation. In *Optik* 208, p. 164129. DOI: 10.1016/j.ijleo.2019.164129.

Farinon, Barbara; Molinari, Romina; Costantini, Lara; Merendino, Nicolò (2020): The seed of industrial hemp (Cannabis sativa L.). Nutritional Quality and Potential Functionality for Human Health and Nutrition. In *Nutrients* 12 (7). DOI: 10.3390/nu12071935.

Fayet, Catherine M.J.; Reilly, Kate H.; van Ham, Chantal; Verburg, Peter H. (2022): The potential of European abandoned agricultural lands to contribute to the Green Deal objectives. Policy perspectives. In *Environmental Science & Policy* 133 (4), pp. 44–53. DOI: 10.1016/j.envsci.2022.03.007.

Feldman, Dorel (2016): Polymer nanocomposites in medicine. In *Journal of Macromolecular Science, Part A* 53 (1), pp. 55–62. DOI: 10.1080/10601325.2016.1110459.

García-Galdeano, José María; Villalón-Mir, Marina; Medina-Martínez, José; Vázquez-Foronda, Lydia María; Zamora-Bustillos, Jessandra Gabriela; Agil, Ahmad et al. (2020): Zn, Cu, and Fe Concentrations in Dehydrated Herbs (Thyme, Rosemary, Cloves, Oregano, and Basil) and the Correlation with the Microbial Counts of Listeria monocytogenes and Other Foodborne Pathogens. In *Foods (Basel, Switzerland)* 9 (11). DOI: 10.3390/foods9111658.

Garg, Rajni; Rani, Priya; Garg, Rishav; Khan, Mohammad Amir; Khan, Nadeem Ahmad; Khan, Afzal Husain; Américo-Pinheiro, Juliana Heloisa Pinê (2022): Biomedical and catalytic applications of agri-based biosynthesized silver nanoparticles. In *Environmental pollution (Barking, Essex : 1987)* 310, p. 119830. DOI: 10.1016/j.envpol.2022.119830.

Gautam, Anurag; Ram, S. (2010): Preparation and thermomechanical properties of Ag-PVA nanocomposite films. In *Materials Chemistry and Physics* 119 (1-2), pp. 266–271. DOI: 10.1016/j.matchemphys.2009.08.050.

Ghanipour, Mahshad; Dorranian, Davoud (2013): Effect of Ag-Nanoparticles Doped in Polyvinyl Alcohol on the Structural and Optical Properties of PVA Films. In *Journal of Nanomaterials* 2013 (5), pp. 1–10. DOI: 10.1155/2013/897043.

González-Campos, J. Betzabe; Prokhorov, Evgen; Sanchez, Isaac C.; Luna-Bárcenas, J. Gabriel; Manzano-Ramírez, Alejandro; González-Hernández, Jesús et al. (2012): Molecular Dynamics Analysis of PVA- AgnP Composites by Dielectric Spectroscopy. In *Journal of Nanomaterials* 2012 (8), pp. 1–11. DOI: 10.1155/2012/925750.

Gour, Aman; Jain, Narendra Kumar (2019): Advances in green synthesis of nanoparticles. In *Artificial cells, nanomedicine, and biotechnology* 47 (1), pp. 844–851. DOI: 10.1080/21691401.2019.1577878.

Hadzhieva, Zoya; Boccaccini, Aldo R. (2022): Recent developments in electrophoretic deposition (EPD) of antibacterial coatings for biomedical applications - A review. In *Current Opinion in Biomedical Engineering* 21, p. 100367. DOI: 10.1016/j.cobme.2021.100367.

Hairom, Nur Hanis Hayati; Mohammad, Abdul Wahab; Ng, Law Yong; Kadhum, Abdul Amir Hassan (2015): Utilization of self-synthesized ZnO nanoparticles in MPR for industrial dye wastewater treatment using NF and UF membrane. In *Desalination and Water Treatment* 54 (4-5), pp. 944–955. DOI: 10.1080/19443994.2014.917988.

Hajinaebi, Melika; Ganjali, Monireh; Nasab, Navid Ahmadi (2022): Antibacterial Activity and Drug Release of Ciprofloxacin Loaded PVA-nHAp Nanocomposite Coating on Ti-6Al-4 V. In *J Inorg Organomet Polym* 32 (9), pp. 3521–3532. DOI: 10.1007/s10904-022-02361-6.

Hamid, Hazrulrizawati Abd; Anuar, Muhamad Zubbair Ammar Khairul; Zulkifli, Farah Hanani (2022): Preparation and characterization of deer velvet antler/polyvinyl alcohol (DVA/PVA) scaffold for bone tissue engineering. In *Materials Today: Proceedings* 51 (2), pp. 1332–1337. DOI: 10.1016/j.matpr.2021.11.377.

Hanawa, Takao (1999): In vivo metallic biomaterials and surface modification. In *Materials Science and Engineering: A* 267 (2), pp. 260–266. DOI: 10.1016/S0921-5093(99)00101-X.

He, Pan Yang; Zhang, Yao Jun; Chen, Hao; Liu, Li Cai (2019): Development of an eco-efficient CaMoO4/electroconductive geopolymer composite for recycling silicomanganese slag and degradation of dye wastewater. In *Journal of Cleaner Production* 208 (2), pp. 1476–1487. DOI: 10.1016/j.jclepro.2018.10.176.

Hebeish, Ali; Sharaf, S. (2015): Novel nanocomposite hydrogel for wound dressing and other medical applications. In *RSC Adv.* 5 (125), pp. 103036–103046. DOI: 10.1039/C5RA07076G.

Hermani, Milad; Etemadi, Habib; Khezraqa, Homayun (2022): Polycarbonate/polyvinyl alcohol thin film nanocomposite membrane incorporated with silver nanoparticles for water treatment. In *Braz. J. Chem. Eng.* 306, p. 2000767. DOI: 10.1007/s43153-022-00273-z.

Htwe, Y. Z. N.; Mariatti, M. (2020): Fabrication and characterization of silver nanoparticles/PVA composites for flexible electronic application. In. 3RD INTERNATIONAL POSTGRADUATE CONFERENCE ON MATERIALS, MINERALS & POLYMER (MAMIP) 2019. Penang, Malaysia, 31 October–1 November 2019: AIP Publishing (AIP Conference Proceedings), p. 20046.

Huq, Md Amdadul; Ashrafudoulla, Md; Rahman, M. Mizanur; Balusamy, Sri Renukadevi; Akter, Shahina (2022): Green Synthesis and Potential Antibacterial Applications of Bioactive Silver Nanoparticles. A Review. In *Polymers* 14 (4). DOI: 10.3390/polym14040742.

Ivanets, Andrei; Prozorovich, Vladimir; Roshchina, Marina; Kouznetsova, Tatyana; Budeiko, Nikolai; Kulbitskaya, Lyudmila et al. (2021): A comparative study on the synthesis of

magnesium ferrite for the adsorption of metal ions. Insights into the essential role of crystallite size and surface hydroxyl groups. In *Chemical Engineering Journal* 411, p. 128523. DOI: 10.1016/j.cej.2021.128523.

Jadoun, Sapana; Arif, Rizwan; Jangid, Nirmala Kumari; Meena, Rajesh Kumar (2021): Green synthesis of nanoparticles using plant extracts. A review. In *Environ Chem Lett* 19 (1), pp. 355–374. DOI: 10.1007/s10311-020-01074-x.

Jalilian, Fereshteh; Chahardoli, Azam; Sadrjavadi, Komail; Fattahi, Ali; Shokoohinia, Yalda (2020): Green synthesized silver nanoparticle from Allium ampeloprasum aqueous extract. Characterization, antioxidant activities, antibacterial and cytotoxicity effects. In *Advanced Powder Technology* 31 (3), pp. 1323–1332. DOI: 10.1016/j.apt.2020.01.011.

Januariyasa, I. Komang; Ana, Ika Dewi; Yusuf, Yusril (2020): Nanofibrous poly(vinyl alcohol)/chitosan contained carbonated hydroxyapatite nanoparticles scaffold for bone tissue engineering. In *Materials science & engineering. C, Materials for biological applications* 107, p. 110347. DOI: 10.1016/j.msec.2019.110347.

Jarzębski, Maciej; Smułek, Wojciech; Baranowska, Hanna Maria; Masewicz, Łukasz; Kobus-Cisowska, Joanna; Ligaj, Marta; Kaczorek, Ewa (2020): Characterization of St. John's wort (Hypericum perforatum L.) and the impact of filtration process on bioactive extracts incorporated into carbohydrate-based hydrogels. In *Food Hydrocolloids* 104 (1), p. 105748. DOI: 10.1016/j.foodhyd.2020.105748.

Jiang, Yaqi; Zhou, Pingfan; Zhang, Peng; Adeel, Muhammad; Shakoor, Noman; Li, Yuanbo et al. (2022): Green synthesis of metal-based nanoparticles for sustainable agriculture. In *Environmental pollution (Barking, Essex : 1987)* 309, p. 119755. DOI: 10.1016/j.envpol.2022.119755.

Jouyandeh, Maryam; Tavakoli, Omid; Sarkhanpour, Reza; Sajadi, S. Mohammad; Zarrintaj, Payam; Rabiee, Navid et al. (2022): Green products from herbal medicine wastes by subcritical water treatment. In *Journal of hazardous materials* 424 (Pt A), p. 127294. DOI: 10.1016/j.jhazmat.2021.127294.

Karabegović, Ivana T.; Stojičević, Saša S.; Veličković, Dragan T.; Todorović, Zoran B.; Nikolić, Nada Č.; Lazić, Miodrag L. (2014): The effect of different extraction techniques on the composition and antioxidant activity of cherry laurel (Prunus laurocerasus) leaf and fruit extracts. In *Industrial Crops and Products* 54 (1), pp. 142–148. DOI: 10.1016/j.indcrop.2013.12.047.

Karan, Tunay; Erenler, Ramazan; Moran Bozer, Busra (2022): Synthesis and characterization of silver nanoparticles using curcumin. Cytotoxic, apoptotic, and necrotic effects on various cell lines. In *Zeitschrift fur Naturforschung. C, Journal of biosciences* 77 (7-8), pp. 343–350. DOI: 10.1515/znc-2021-0298.

Karki, Sandeep; Kim, Hyeongmin; Na, Seon-Jeong; Shin, Dohyun; Jo, Kanghee; Lee, Jaehwi (2016): Thin films as an emerging platform for drug delivery. In *Asian Journal of Pharmaceutical Sciences* 11 (5), pp. 559–574. DOI: 10.1016/j.ajps.2016.05.004.

Kawaguchi, Minoru; Fukushima, Tadao; Hayakawa, Toru; Nakashima, Naotoshi; Inoue, Yusuke; Takeda, Shoji et al. (2006): Preparation of carbon nanotube-alginate nanocomposite gel for tissue engineering. In *Dental materials journal* 25 (4), pp. 719–725. DOI: 10.4012/dmj.25.719.

Khatoon, Nafeesa; Alam, Hammad; Khan, Afreen; Raza, Khalid; Sardar, Meryam (2019): Ampicillin Silver Nanoformulations against Multidrug resistant bacteria. In *Scientific reports* 9 (1), p. 6848. DOI: 10.1038/s41598-019-43309-0.

Kravanja, Katja Andrina; Finšgar, Matjaž (2021): Analytical Techniques for the Characterization of Bioactive Coatings for Orthopaedic Implants. In *Biomedicines* 9 (12). DOI: 10.3390/biomedicines9121936.

Kurakula, Mallesh; Raghavendra Naveen, N. (2021): Electrospraying. A facile technology unfolding the chitosan based drug delivery and biomedical applications. In *European Polymer Journal* 147 (50), p. 110326. DOI: 10.1016/j.eurpolymj.2021.110326.

Lee, Donggeun; Cho, Jinhan; Son, Jeong Gon; Yeom, Bongjun (2022): Highly aligned aramid nanofibrillar nanocomposites for enhanced dynamic mechanical properties. In *Composites Part B: Engineering* 229, p. 109467. DOI: 10.1016/j.compositesb.2021.109467.

Lee, Seong Jin; Park, Sang Min; Han, Seon Jin; Kim, Dong Sung (2020): Electrolyte solution-assisted electrospray deposition for direct coating and patterning of polymeric nanoparticles on non-conductive surfaces. In *Chemical Engineering Journal* 379, p. 122318. DOI: 10.1016/j.cej.2019.122318.

Lešnik, Samo; Furlan, Veronika; Bren, Urban (2021a): Rosemary (Rosmarinus officinalis L.). Extraction techniques, analytical methods and health-promoting biological effects. In *Phytochem Rev* 20 (6), pp. 1273–1328. DOI: 10.1007/s11101-021-09745-5.

Lešnik, Samo; Furlan, Veronika; Bren, Urban (2021b): Rosemary (Rosmarinus officinalis L.). Extraction techniques, analytical methods and health-promoting biological effects. In *Phytochem Rev* 20 (6), pp. 1273–1328. DOI: 10.1007/s11101-021-09745-5.

Levana, Odelia; Hong, Soonkook; Kim, Se Hyun; Jeong, Ji Hoon; Hur, Sung Sik; Lee, Jin Woo et al. (2022): A Novel Strategy for Creating an Antibacterial Surface Using a Highly Efficient Electrospray-Based Method for Silica Deposition. In *International journal of molecular sciences* 23 (1). DOI: 10.3390/ijms23010513.

Li, Chunquan; Huang, Ying; Dong, Xiongbo; Sun, Zhiming; Duan, Xiaodi; Ren, Bangxing et al. (2019a): Highly efficient activation of peroxymonosulfate by natural negatively-charged kaolinite with abundant hydroxyl groups for the degradation of atrazine. In *Applied Catalysis B: Environmental* 247, pp. 10–23. DOI: 10.1016/j.apcatb.2019.01.079.

Li, Rufen; Chen, Zhenmin; Ren, Na; Wang, Yixuan; Wang, Yujia; Yu, Fengye (2019b): Biosynthesis of silver oxide nanoparticles and their photocatalytic and antimicrobial activity evaluation for wound healing applications in nursing care. In *Journal of photochemistry and photobiology. B, Biology* 199, p. 111593. DOI: 10.1016/j.jphotobiol.2019.111593.

Li, Xianyu; Hu, Anyang; Ye, Lin (2011): Structure and Property of Porous Polyvinylalcohol Hydrogels for Microorganism Immobilization. In *J Polym Environ* 19 (2), pp. 398–404. DOI: 10.1007/s10924-011-0289-1.

Li, Yuhang; Luan, Yunhao; Liu, Wanyi; Wang, Cong; Cao, Hui; Liu, Pengtao (2022): Cellulose nanofibrils/polyvinyl alcohol/silver nanoparticles composite hydrogel. Preparation and its catalyst degradation performance of cationic dye. In *J. Appl. Polym. Sci.* 139 (22), p. 52246. DOI: 10.1002/app.52246.

Lin, Ming-Hong; Wang, Yan-Hsiung; Kuo, Cheng-Hsien; Ou, Shih-Fu; Huang, Pin-Zhen; Song, Tzu-Yu et al. (2021): Hybrid ZnO/chitosan antimicrobial coatings with enhanced mechanical and bioactive properties for titanium implants. In *Carbohydrate polymers* 257, p. 117639. DOI: 10.1016/j.carbpol.2021.117639.

Listgarten, M. A.; Lang, N. P.; Schroeder, H. E.; Schroeder, A. (1991): Periodontal tissues and their counterparts around endosseous implants corrected and republished with original paging, article orginally printed in Clin Oral Implants Res 1991 Jan-Mar;2(1):1-19. In *Clinical oral implants research* 2 (3), pp. 1–19. DOI: 10.1034/j.1600-0501.1991.020309.x.

Lomelí-Rosales, Diego Alberto; Zamudio-Ojeda, Adalberto; Reyes-Maldonado, Oscar Kevin; López-Reyes, Morelia Eunice; Basulto-Padilla, Georgina Cristina; Lopez-Naranjo, Edgar José et al. (2022): Green Synthesis of Gold and Silver Nanoparticles Using Leaf Extract of Capsicum chinense Plant. In *Molecules (Basel, Switzerland)* 27 (5). DOI: 10.3390/molecules27051692.

Luchina, K. I.; Tserkovnyĭ, G. F.; Chernaenko, T. D.; Iasneva, I. E. (1975): K voprosu o rol kadrov v spetsializatsii gosudarstvennogo sanitarnogo nadzora v SSSR. In *Gigiena i sanitariia* (9), pp. 67–70.

Macit, İdris (2021): Evaluation of agronomic, bioactive and element status of promising cherry laurel (P. laurocerasus) accessions in the genetic collection by multivariate analysis. In *Scientia Horticulturae* 287 (4), p. 110253. DOI: 10.1016/j.scienta.2021.110253.

Madian, Noha G.; Mohamed, Noha (2020): Enhancement of the dynamic mechanical properties of chitosan thin films by crosslinking with greenly synthesized silver nanoparticles. In *Journal of Materials Research and Technology* 9 (6), pp. 12970–12975. DOI: 10.1016/j.jmrt.2020.09.028.

Mahanty, Anuradha; Shikha, Deep (2022): Changes in the morphology, mechanical strength and biocompatibility of polymer and metal/polymer fabricated hydroxyapatite for orthopaedic implants. A review. In *Journal of Polymer Engineering* 42 (4), pp. 298–322. DOI: 10.1515/polyeng-2021-0171.

Makvandi, Pooyan; Josic, Uros; Delfi, Masoud; Pinelli, Filippo; Jahed, Vahid; Kaya, Emine et al. (2021): Drug Delivery (Nano)Platforms for Oral and Dental Applications. Tissue Regeneration, Infection Control, and Cancer Management. In *Advanced science (Weinheim, Baden-Wurttemberg, Germany)* 8 (8), p. 2004014. DOI: 10.1002/advs.202004014.

Martínez-Cabanas, María; López-García, Marta; Rodríguez-Barro, Pilar; Vilariño, Teresa; Lodeiro, Pablo; Herrero, Roberto et al. (2021): Antioxidant Capacity Assessment of Plant Extracts for Green Synthesis of Nanoparticles. In *Nanomaterials (Basel, Switzerland)* 11 (7). DOI: 10.3390/nano11071679.

Martínez-Molina, Esther Candelaria; Freile-Pelegrín, Yolanda; Ovando-Chacón, Sandy Luz; Gutiérrez-Miceli, Federico Antonio; Ruiz-Cabrera, Miguel Ángel; Grajales-Lagunes, Alicia et al. (2022): Development and characterization of alginate-based edible film from Sargassum fluitans incorporated with silver nanoparticles obtained by green synthesis. In *Food Measure* 16 (1), pp. 126–136. DOI: 10.1007/s11694-021-01156-6.

Martorana, Annalisa; Pitarresi, Giovanna; Palumbo, Fabio Salvatore; Catania, Valentina; Schillaci, Domenico; Mauro, Nicolò et al. (2022): Fabrication of silver nanoparticles by a diethylene triamine-hyaluronic acid derivative and use as antibacterial coating. In *Carbohydrate polymers* 295, p. 119861. DOI: 10.1016/j.carbpol.2022.119861.

Mat Yazik, Muhamad Hasfanizam; Sultan, Mohamed Thariq Hameed; Jawaid, Mohammad; Abu Talib, Abd Rahim; Mazlan, Norkhairunnisa; Md Shah, Ain Umaira; Safri, Syafiqah Nur Azrie (2021): Effect of Nanofiller Content on Dynamic Mechanical and Thermal Properties of Multi-Walled Carbon Nanotube and Montmorillonite Nanoclay Filler Hybrid Shape Memory Epoxy Composites. In *Polymers* 13 (5). DOI: 10.3390/polym13050700.

Mathew, Shiji; Mathew, Jyothis; Radhakrishnan, E. K. (2019): Polyvinyl alcohol/silver nanocomposite films fabricated under the influence of solar radiation as effective antimicrobial food packaging material. In *J Polym Res* 26 (9), p. 273. DOI: 10.1007/s10965-019-1888-0.

Miłek, Dorota; Nowak, Paulina; Latosińska, Jolanta (2022): The Development of Renewable Energy Sources in the European Union in the Light of the European Green Deal. In *Energies* 15 (15), p. 5576. DOI: 10.3390/en15155576.

Mohammed, Mohsin Talib; Khan, Zahid A.; Siddiquee, Arshad Noor (2014): Surface Modifications of Titanium Materials for developing Corrosion Behavior in Human Body Environment. A Review. In *Procedia Materials Science* 6, pp. 1610–1618. DOI: 10.1016/j.mspro.2014.07.144.

Mokhtari-Hosseini, Zahra-Beagom; Hatamian-Zarmi, Ashrafalsadat; Mahdizadeh, Soheila; Ebrahimi-Hosseinzadeh, Bahman; Alvandi, Hale; Kianirad, Soheil (2022a): Environmentally-Friendly Synthesis of Ag Nanoparticles by Fusarium sporotrichioides for the Production of

PVA/Bentonite/Ag Composite Nanofibers. In *J Polym Environ* 8 (1), p. 1. DOI: 10.1007/s10924-022-02509-y.

Mokhtari-Hosseini, Zahra-Beagom; Hatamian-Zarmi, Ashrafalsadat; Mahdizadeh, Soheila; Ebrahimi-Hosseinzadeh, Bahman; Alvandi, Hale; Kianirad, Soheil (2022b): Environmentally-Friendly Synthesis of Ag Nanoparticles by Fusarium sporotrichioides for the Production of PVA/Bentonite/Ag Composite Nanofibers. In *J Polym Environ* 30 (10), pp. 4146–4156. DOI: 10.1007/s10924-022-02509-y.

Momeni, Sina; Safder, Muhammad; Khondoker, Mohammad Abu Hasan; Elias, Anastasia Leila (2021): Valorization of Hemp Hurds as Bio-Sourced Additives in PLA-Based Biocomposites. In *Polymers* 13 (21). DOI: 10.3390/polym13213786.

Montano, Elena; Vivo, Maria; Guarino, Andrea Maria; Di Martino, Orsola; Di Luccia, Blanda; Calabrò, Viola et al. (2019): Colloidal Silver Induces Cytoskeleton Reorganization and E-Cadherin Recruitment at Cell-Cell Contacts in HaCaT Cells. In *Pharmaceuticals (Basel, Switzerland)* 12 (2). DOI: 10.3390/ph12020072.

Morad, Ibrahim; Alshehri, A. M.; Mansour, A. F.; Wasfy, M. H.; El-Desoky, M. M. (2020): Facile synthesis and comparative study for the optical performance of different TiO2 phases doped PVA nanocomposite films. In *Physica B: Condensed Matter* 597, p. 412415. DOI: 10.1016/j.physb.2020.412415.

Moshood, Taofeeq D.; Nawanir, Gusman; Mahmud, Fatimah; Mohamad, Fazeeda; Ahmad, Mohd Hanafiah; AbdulGhani, Airin (2022a): Biodegradable plastic applications towards sustainability. A recent innovations in the green product. In *Cleaner Engineering and Technology* 6 (1), p. 100404. DOI: 10.1016/j.clet.2022.100404.

Moshood, Taofeeq D.; Nawanir, Gusman; Mahmud, Fatimah; Mohamad, Fazeeda; Ahmad, Mohd Hanafiah; AbdulGhani, Airin (2022b): Sustainability of biodegradable plastics. New problem or solution to solve the global plastic pollution? In *Current Research in Green and Sustainable Chemistry* 5 (80-), p. 100273. DOI: 10.1016/j.crgsc.2022.100273.

Mudhafar, Mustafa; Zainol, Ismail; Alsailawi, H. A.; Aiza Jaafar, C. N. (2022): Synthesis and characterization of fish scales of hydroxyapatite/ collagen–silver nanoparticles composites for the applications of bone filler. In *J. Korean Ceram. Soc.* 59 (2), pp. 229–239. DOI: 10.1007/s43207-021-00154-0.

Müller, V.; Jobbagy, M.; Djurado, E. (2021): Coupling sol-gel with electrospray deposition. Towards nanotextured bioactive glass coatings. In *Journal of the European Ceramic Society* 41 (14), pp. 7288–7300. DOI: 10.1016/j.jeurceramsoc.2021.07.041.

Nicolae-Maranciuc, Alexandra; Chicea, Dan; Chicea, Liana Maria (2022): Ag Nanoparticles for Biomedical Applications-Synthesis and Characterization-A Review. In *International journal of molecular sciences* 23 (10). DOI: 10.3390/ijms23105778.

Nieto-Maldonado, Alejandra; Bustos-Guadarrama, Sayra; Espinoza-Gomez, Heriberto; Z. Flores-López, Lucía; Ramirez-Acosta, Kendra; Alonso-Nuñez, Gabriel; Cadena-Nava, Ruben D. (2022): Green synthesis of copper nanoparticles using different plant extracts and their antibacterial activity. In *Journal of Environmental Chemical Engineering* 10 (2), p. 107130. DOI: 10.1016/j.jece.2022.107130.

Ong, Wei Ting Jess; Nyam, Kar Lin (2022): Evaluation of silver nanoparticles in cosmeceutical and potential biosafety complications. In *Saudi journal of biological sciences* 29 (4), pp. 2085–2094. DOI: 10.1016/j.sjbs.2022.01.035.

Ostovan, Abbas; Ghaedi, Mehrorang; Arabi, Maryam; Yang, Qian; Li, Jinhua; Chen, Lingxin (2018): Hydrophilic Multitemplate Molecularly Imprinted Biopolymers Based on a Green Synthesis Strategy for Determination of B-Family Vitamins. In *ACS applied materials & interfaces* 10 (4), pp. 4140–4150. DOI: 10.1021/acsami.7b17500.

Ounkaew, Artjima; Kasemsiri, Pornnapa; Jetsrisuparb, Kaewta; Uyama, Hiroshi; Hsu, Yu-I; Boonmars, Thidarut et al. (2020): Synthesis of nanocomposite hydrogel based carboxymethyl starch/polyvinyl alcohol/nanosilver for biomedical materials. In *Carbohydrate polymers* 248, p. 116767. DOI: 10.1016/j.carbpol.2020.116767.

Oves, Mohammad; Ahmar Rauf, Mohd; Aslam, Mohammad; Qari, Huda A.; Sonbol, Hana; Ahmad, Irfan et al. (2022): Green synthesis of silver nanoparticles by Conocarpus Lancifolius plant extract and their antimicrobial and anticancer activities. In *Saudi journal of biological sciences* 29 (1), pp. 460–471. DOI: 10.1016/j.sjbs.2021.09.007.

Oza, Goldie; Reyes-Calderón, Almendra; Mewada, Ashmi; Arriaga, Luis Gerardo; Cabrera, Gabriel Betanzos; Luna, Diego Estrada et al. (2020): Plant-based metal and metal alloy nanoparticle synthesis. A comprehensive mechanistic approach. In *J Mater Sci* 55 (4), pp. 1309–1330. DOI: 10.1007/s10853-019-04121-3.

Pandey, Pradeep Kumar; Gangwar, Chinky; Yaseen, Bushra; Kumar, Indresh; Nayak, Rashmi; Kumar, Saurabh et al. (2023): Anticancerous and antioxidant properties of fabricated silver nanoparticles involving bio-organic framework using medicinal plant Blumea lacera. In *Chem. Pap.* 18 (11), p. 356. DOI: 10.1007/s11696-023-02723-5.

Park, Kyuhyun; Kang, Sangmo; Park, Ji-Woon; Hwang, Jungho (2021): Fabrication of silver nanowire coated fibrous air filter medium via a two-step process of electrospinning and electrospray for anti-bioaerosol treatment. In *Journal of hazardous materials* 411, p. 125043. DOI: 10.1016/j.jhazmat.2021.125043.

Parmar, Mrinalini; Sanyal, Mallika (2022): Extensive study on plant mediated green synthesis of metal nanoparticles and their application for degradation of cationic and anionic dyes. In *Environmental Nanotechnology, Monitoring & Management* 17, p. 100624. DOI: 10.1016/j.enmm.2021.100624.

Pei, Chun; Zhu, Ji-Hua; Xing, Feng (2021): Photocatalytic property of cement mortars coated with graphene/TiO2 nanocomposites synthesized via sol–gel assisted electrospray method. In *Journal of Cleaner Production* 279 (1), p. 123590. DOI: 10.1016/j.jclepro.2020.123590.

Perveen, Rehana; Shujaat, Shahida; Naz, Misbah; Qureshi, Muhammad Zahid; Nawaz, Shaista; Shahzad, Khurram; Ikram, Muhammad (2021): Green synthesis of antimicrobial silver nanoparticles with Brassicaceae seeds. In *Mater. Res. Express* 8 (5), p. 55007. DOI: 10.1088/2053-1591/ac006b.

Prakash, M.; Kavitha, Helen P.; Abinaya, S.; Vennila, Jasmine P.; Lohita, D. (2022): Green synthesis of bismuth based nanoparticles and its applications - A review. In *Sustainable Chemistry and Pharmacy* 25 (4), p. 100547. DOI: 10.1016/j.scp.2021.100547.

Prasad, Soni; Ehrensberger, Mark; Gibson, Monica Prasad; Kim, Hyeongil; Monaco, Edward A. (2015): Biomaterial properties of titanium in dentistry. In *Journal of Oral Biosciences* 57 (4), pp. 192–199. DOI: 10.1016/j.job.2015.08.001.

Prathipkumar, S.; Vijayakumar, S.; Alsalhi, Mohamad S.; Devanesan, Sandhanasamy; Nilavukkarasi, M.; Sangeetha, R.; Kim, Woong (2023): Biogenic-mediated silver nanoparticles using heneicosane and their enhanced antimicrobial, antiproliferative, sensing capability and photocatalytic potential. In *Appl Nanosci* 308 (10), p. 136274. DOI: 10.1007/s13204-023-02787-5.

Qin, Yan; Xu, Fengfeng; Yuan, Limin; Hu, Huixia; Yao, Xiyu; Liu, Jun (2020): Comparison of the physical and functional properties of starch/polyvinyl alcohol films containing anthocyanins and/or betacyanins. In *International journal of biological macromolecules* 163, pp. 898–909. DOI: 10.1016/j.ijbiomac.2020.07.065.

Rafique, Muhammad; Sadaf, Iqra; Rafique, M. Shahid; Tahir, M. Bilal (2017): A review on green synthesis of silver nanoparticles and their applications. In *Artificial cells, nanomedicine, and biotechnology* 45 (7), pp. 1272–1291. DOI: 10.1080/21691401.2016.1241792.

Ragab, H. M.; Rajeh, A. (2020): Structural, thermal, optical and conductive properties of PAM/PVA polymer composite doped with Ag nanoparticles for electrochemical application. In *J Mater Sci: Mater Electron* 31 (19), pp. 16780–16792. DOI: 10.1007/s10854-020-04233-6.

Raja, T.; Mohanavel, V.; Ravichandran, M.; Kumar, S. Suresh; Albaqami, Munirah D.; Alotabi, Reham Ghazi et al. (2022): Dynamic Mechanical Analysis of Banyan/Ramie Fibers Reinforced with Nanoparticle Hybrid Polymer Composite. In *Advances in Polymer Technology* 2022, pp. 1–10. DOI: 10.1155/2022/1560330.

Rajati, Hajar; Alvandi, Hosna; Rahmatabadi, Seyyed Soheil; Hosseinzadeh, Leila; Arkan, Elham (2022): A nanofiber-hydrogel composite from green synthesized AgNPs embedded to PEBAX/PVA hydrogel and PA/Pistacia atlantica gum nanofiber for wound dressing. In *International journal of biological macromolecules. DOI:* 10.1016/j.ijbiomac.2022.11.255.

Rana, V. K.; Pandey, Asutosh K.; Singh, Raj Pal; Kumar, B.; Mishra, Satyendra; Ha, Chang-Sik (2010): Enhancement of thermal stability and phase relaxation behavior of chitosan dissolved in aqueous l-lactic acid. Using 'silver nanoparticles' as nano filler. In *Macromol. Res.* 18 (8), pp. 713–720. DOI: 10.1007/s13233-010-0801-9.

Rani, Santoshi; Chandra, Rampalli Viswa; Reddy, Aileni Amarender; Reddy, Bavigadda Harish; Nagarajan, Sripriya; Naveen, Anumala (2015): Evaluation of the Antibacterial Effect of Silver Nanoparticles on Guided Tissue Regeneration Membrane Colonization--An in Vitro Study. In *Journal of the International Academy of Periodontology* 17 (3), pp. 66–76.

Ranjit, Eliza; Hamlet, Stephen; Love, Robert M. (2023): Keratin coated titanium as an aid to osseointegration. Physicochemical and mechanical properties. In *Surface and Coatings Technology* 462 (7), p. 129457. DOI: 10.1016/j.surfcoat.2023.129457.

Reinhold, Catherine (2007): Greener nanostructures. In *Materials Today* 10 (5), p. 9. DOI: 10.1016/S1369-7021(07)70060-3.

Rezayan, Ali Hossein; Firoozi, Negar; Kheirjou, Somayyeh; Tabatabaei Rezaei, Seyed Jamal; Nabid, Mohammad Reza (2017): Synthesis and Characterization of Biodegradable Semi-Interpenetrating Polymer Networks Based on Star-Shaped Copolymers of ε-Caprolactone and Lactide. In *Iranian journal of pharmaceutical research : IJPR* 16 (1), pp. 63–73.

Rolim, Wallace R.; Pelegrino, Milena T.; Araújo Lima, Bruna de; Ferraz, Letícia S.; Costa, Fanny N.; Bernardes, Juliana S. et al. (2019): Green tea extract mediated biogenic synthesis of silver nanoparticles. Characterization, cytotoxicity evaluation and antibacterial activity. In *Applied Surface Science* 463, pp. 66–74. DOI: 10.1016/j.apsusc.2018.08.203.

S R, Pavan; Venkatesan, Jayachandran; Prabhu, Ashwini (2022): Anticancer activity of silver nanoparticles from the aqueous extract of Dictyota ciliolata on non-small cell lung cancer cells. In *Journal of Drug Delivery Science and Technology* 74, p. 103525. DOI: 10.1016/j.jddst.2022.103525.

Sadeghi-Kiakhani, Mousa; Tehrani-Bagha, Ali Reza; Miri, Fateme Sadat; Hashemi, Elaheh; Safi, Mahdi (2022): Application of Achillea millefolium extract as a reducing agent for synthesis of silver nanoparticles (AgNPs) on the cotton. Antibacterial, antioxidant and dyeing studies. In *Biometals : an international journal on the role of metal ions in biology, biochemistry, and medicine* 35 (2), pp. 313–327. DOI: 10.1007/s10534-022-00366-9.

Safaee-Ardakani, Mohammad Reza; Hatamian-Zarmi, Ashrafalsadat; Sadat, Seyedeh Mahdieh; Mokhtari-Hosseini, Zahra Beagom; Ebrahimi-Hosseinzadeh, Bahman; Rashidiani, Jamal; Kooshki, Hamid (2019): Electrospun Schizophyllan/polyvinyl alcohol blend nanofibrous scaffold as potential wound healing. In *International journal of biological macromolecules* 127, pp. 27–38. DOI: 10.1016/j.ijbiomac.2018.12.256.

Salević, Ana; Stojanović, Dušica; Lević, Steva; Pantić, Milena; Đorđević, Verica; Pešić, Radojica et al. (2022): The Structuring of Sage (Salvia officinalis L.) Extract-Incorporating Edible Zein-

Based Materials with Antioxidant and Antibacterial Functionality by Solvent Casting versus Electrospinning. In *Foods (Basel, Switzerland)* 11 (3). DOI: 10.3390/foods11030390.

Samide, Adriana; Iacobescu, Gabriela Eugenia; Tutunaru, Bogdan; Iordache, Simona (2022): Silver nanoparticles/polyvinyl alcohol film. Studies of thermal characterization, AFM and corrosion protection by electrodeposition on 304L stainless steel. In *J Therm Anal Calorim* 147 (2), pp. 1041–1051. DOI: 10.1007/s10973-020-10444-0.

Sarkhel, Rwiddhi; Ganguly, Preetha; Das, Papita; Bhowal, Avijit; Sengupta, Shubhalakshmi (2023): Synthesis of biodegradable PVA/cellulose polymer composites and their application in dye removal. In *Environmental Quality Mgmt* 32 (3), pp. 313–323. DOI: 10.1002/tqem.21920.

Satarkar, Nitin S.; Zach Hilt, J. (2008): Hydrogel nanocomposites as remote-controlled biomaterials. In *Acta biomaterialia* 4 (1), pp. 11–16. DOI: 10.1016/j.actbio.2007.07.009.

Schenk, R. K.; Buser, D. (1998): Osseointegration. A reality. In *Periodontology 2000* 17, pp. 22–35. DOI: 10.1111/j.1600-0757.1998.tb00120.x.

Sealy, Cordelia (2020): Naturally inspired 'green' membranes clean up. In *Materials Today* 35, p. 8. DOI: 10.1016/j.mattod.2020.03.007.

Selvamani, Vidhya; Kadian, Sachin; Detwiler, David A.; Zareei, Amin; Woodhouse, Ian; Qi, Zhimin et al. (2022): Laser-Assisted Nanotexturing and Silver Immobilization on Titanium Implant Surfaces to Enhance Bone Cell Mineralization and Antimicrobial Properties. In *Langmuir : the ACS journal of surfaces and colloids* 38 (13), pp. 4014–4027. DOI: 10.1021/acs.langmuir.2c00008.

Senthamarai Kannan, Monika; Hari Haran, Ponlakshmi S.; Sundar, Krishnan; Kunjiappan, Selvaraj; Balakrishnan, Vanavil (2022): Fabrication of anti-bacterial cotton bandage using biologically synthesized nanoparticles for medical applications. In *Progress in biomaterials* 11 (2), pp. 229–241. DOI: 10.1007/s40204-022-00190-x.

Shaaban, E. R.; Afify, N.; El-Taher, A. (2009): Effect of film thickness on microstructure parameters and optical constants of CdTe thin films. In *Journal of Alloys and Compounds* 482 (1-2), pp. 400–404. DOI: 10.1016/j.jallcom.2009.04.033.

Sharif, Adnan; Mustaqeem, Mujahid; Saleh, Tawfik A.; ur Rehman, Aziz; Ahmad, Muhammad; Warsi, Muhammad Farooq (2022): Synthesis, structural and dielectric properties of Mg/Zn ferrites -PVA nanocomposites. In *Materials Science and Engineering: B* 280 (3), p. 115689. DOI: 10.1016/j.mseb.2022.115689.

Shin, Munju; Yang, Sejun; Kwak, Hyo Won; Lee, Ki Hoon (2022): Synthesis of gold nanoparticles using silk sericin as a green reducing and capping agent. In *European Polymer Journal* 164 (1), p. 110960. DOI: 10.1016/j.eurpolymj.2021.110960.

Shume, Workneh M.; Murthy, H. C. Ananda; Zereffa, Enyew Amare (2020): A Review on Synthesis and Characterization of Ag 2 O Nanoparticles for Photocatalytic Applications. In *Journal of Chemistry* 2020 (5), pp. 1–15. DOI: 10.1155/2020/5039479.

Sidambe, Alfred T. (2014): Biocompatibility of Advanced Manufactured Titanium Implants-A Review. In *Materials (Basel, Switzerland)* 7 (12), pp. 8168–8188. DOI: 10.3390/ma7128168.

Skóra, Bartosz; Krajewska, Urszula; Nowak, Anna; Dziedzic, Andrzej; Barylyak, Adriana; Kus-Liśkiewicz, Małgorzata (2021): Noncytotoxic silver nanoparticles as a new antimicrobial strategy. In *Scientific reports* 11 (1), p. 13451. DOI: 10.1038/s41598-021-92812-w.

Srichiangsa, Natnaree; Ounkaew, Artjima; Kasemsiri, Pornnapa; Okhawilai, Manunya; Hiziroglu, Salim; Theerakulpisut, Somnuk; Chindaprasirt, Prinya (2022): Facile fabrication of green synthesized silver-decorated magnetic particles for coating of bioactive packaging. In *Cellulose (London, England)* 29 (10), pp. 5853–5868. DOI: 10.1007/s10570-022-04636-0.

Srikhao, Natwat; Kasemsiri, Pornnapa; Ounkaew, Artjima; Lorwanishpaisarn, Narubeth; Okhawilai, Manunya; Pongsa, Uraiwan et al. (2021): Bioactive Nanocomposite Film Based on Cassava

Starch/Polyvinyl Alcohol Containing Green Synthesized Silver Nanoparticles. In *J Polym Environ* 29 (2), pp. 672–684. DOI: 10.1007/s10924-020-01909-2.

Stojkovska, Jasmina; Zvicer, Jovana; Obradovic, Bojana (2020): Preclinical functional characterization methods of nanocomposite hydrogels containing silver nanoparticles for biomedical applications. In *Applied microbiology and biotechnology* 104 (11), pp. 4643–4658. DOI: 10.1007/s00253-020-10521-2.

Subha, Veeramani; Ranu, Ashok; Shankar, Anitha; Kirubanandan, Shanmugam; Satheeshkumar, Ellappan; Suresh, Subramaniyam et al. (2022): Functionalization of spray coated cellulose nanofiber sheet with montmorillonite (MMT) and silver nanoparticles (AgNPs) to biomedical nanocomposite as wound regeneration scaffold. In *Progress in Organic Coatings* 166 (3), p. 106782. DOI: 10.1016/j.porgcoat.2022.106782.

Sudha, Kattakgoundar Govindaraj; Ali, Saheb; Karunakaran, Gopalu; Kowsalya, Mariyappan; Kolesnikov, Evgeny; Rajeshkumar, Mohan Prasanna (2020): Eco-friendly synthesis of ZnO nanorods using Cycas pschannae plant extract with excellent photocatalytic, antioxidant, and anticancer nanomedicine for lung cancer treatment. In *Appl Organometal Chem* 34 (4), p. 33. DOI: 10.1002/aoc.5511.

Sun, Jeong-Yun; Zhao, Xuanhe; Illeperuma, Widusha R. K.; Chaudhuri, Ovijit; Oh, Kyu Hwan; Mooney, David J. et al. (2012): Highly stretchable and tough hydrogels. In *Nature* 489 (7414), pp. 133–136. DOI: 10.1038/nature11409.

Sykaras, N.; Iacopino, A. M.; Marker, V. A.; Triplett, R. G.; Woody, R. D. (2000): Implant materials, designs, and surface topographies. Their effect on osseointegration. A literature review. In *The International journal of oral & maxillofacial implants* 15 (5), pp. 675–690.

Tahir, Muhammad Farrukh; Khan, Muhammad Zaman; Attacha, Safira; Asim, Noreen; Tayyab, Muhammad; Ali, Azam et al. (2022): The Comparative Performance of Phytochemicals, Green Synthesised Silver Nanoparticles, and Green Synthesised Copper Nanoparticles-Loaded Textiles to Avoid Nosocomial Infections. In *Nanomaterials (Basel, Switzerland)* 12 (20). DOI: 10.3390/nano12203629.

Tan, Yujie; Zhao, Weixuan; Sun, Luying; Zhang, Renxi; Hou, Jianyuan; Fu, Shaoxiang et al. (2022): Photocatalytic abatement of formaldehyde under visible light irradiation via bamboo carbon/TiO2 modified by plasma at low temperature. In *Journal of Cleaner Production* 369 (Pt 2), p. 133280. DOI: 10.1016/j.jclepro.2022.133280.

Thompson, Audie K.; Hackett, Cannon; Grady, Tony L.; Enyinnia, Silver; Moore, Quincy C.; Nave, Felecia M. (2020): Development and Characterization of Membranes with PVA Containing Silver Particles. A Study of the Addition and Stability. In *Polymers* 12 (9). DOI: 10.3390/polym12091937.

Tjong, S. C. (2006): Structural and mechanical properties of polymer nanocomposites. In *Materials Science and Engineering: R: Reports* 53 (3-4), pp. 73–197. DOI: 10.1016/j.mser.2006.06.001.

Torricelli, Fabrizio; Alessandri, Ivano; Macchia, Eleonora; Vassalini, Irene; Maddaloni, Marina; Torsi, Luisa (2022): Green Materials and Technologies for Sustainable Organic Transistors. In *Adv Materials Technologies* 7 (2), p. 2100445. DOI: 10.1002/admt.202100445.

Uzunoğlu, Deniz; Ergüt, Memduha; Kodaman, Cemile Gamze; Özer, Ayla (2020): Biosynthesized Silver Nanoparticles for Colorimetric Detection of Fe3+ Ions. In *Arab J Sci Eng* 5 (3), p. 2782. DOI: 10.1007/s13369-020-04760-8.

van Noort, R. (1987): Titanium. The implant material of today. In *J Mater Sci* 22 (11), pp. 3801–3811. DOI: 10.1007/BF01133326.

Varadavenkatesan, T.; Selvaraj, R.; Vinayagam, R. (2019): Dye degradation and antibacterial activity of green synthesized silver nanoparticles using Ipomoea digitata Linn. flower extract. In *Int. J. Environ. Sci. Technol.* 16 (5), pp. 2395–2404. DOI: 10.1007/s13762-018-1850-4.

Varshney, Lalit (2007): Role of natural polysaccharides in radiation formation of PVA–hydrogel wound dressing. In *Nuclear Instruments and Methods in Physics Research Section B: Beam Interactions with Materials and Atoms* 255 (2), pp. 343–349. DOI: 10.1016/j.nimb.2006.11.101.

Vega, Clara; Valbuena-Carabaña, María; Gil, Luis; Fernández, Victoria (2021): Water Sorption and Desorption of Isolated Cuticles From Three Woody Species With Focus on Ilex aquifolium. In *Frontiers in plant science* 12, p. 728627. DOI: 10.3389/fpls.2021.728627.

Venkategowda, T.; Manjunatha, L. H.; Anilkumar, P. R. (2022): Dynamic mechanical behavior of natural fibers reinforced polymer matrix composites – A review. In *Materials Today: Proceedings* 54 (2), pp. 395–401. DOI: 10.1016/j.matpr.2021.09.465.

Vidal, Oscar Lombo; Barros Santos, Millena Cristina; Batista, Ana Paula; Andrigo, Fernanda Franceschi; Baréa, Bruno; Lecomte, Jérôme et al. (2022): Active packaging films containing antioxidant extracts from green coffee oil by-products to prevent lipid oxidation. In *Journal of Food Engineering* 312, p. 110744. DOI: 10.1016/j.jfoodeng.2021.110744.

Viswanathan, Sandhiya; Palaniyandi, Thirunavukkarasu; Shanmugam, Rajeshkumar; Karunakaran, Suganya; Pandi, Marimuthu; Wahab, Mugip Rahaman Abdul et al. (2023): Synthesis, characterization, cytotoxicity, and antimicrobial studies of green synthesized silver nanoparticles using red seaweed Champia parvula. In *Biomass Conv. Bioref.* 204 (1), p. 111786. DOI: 10.1007/s13399-023-03775-z.

Walter, Nike; Stich, Theresia; Docheva, Denitsa; Alt, Volker; Rupp, Markus (2022): Evolution of implants and advancements for osseointegration. A narrative review. In *Injury* 53 Suppl 3, S69-S73. DOI: 10.1016/j.injury.2022.05.057.

Wan, Rongxin; Wang, Xiaojuan; Lei, Li; Hu, Guoying; Tang, Huiqing; Gu, Hanqing (2022): Enhanced anti-microbial activity and osseointegration of Ta/Cu co-implanted polyetheretherketone. In *Colloids and surfaces. B, Biointerfaces* 218, p. 112719. DOI: 10.1016/j.colsurfb.2022.112719.

Wang, Qian; Wang, Peizhuang; Kou, Lvheng; Wei, Hongyuan; Zhou, Jiang (2022): Fabrication and characterization of transparent underwater superoleophobic coatings based chitin nanofibers and polyvinyl alcohol. In *J of Applied Polymer Sci* 139 (21), p. 52205. DOI: 10.1002/app.52205.

Wataha, J. C. (2000): Biocompatibility of dental casting alloys. A review. In *The Journal of prosthetic dentistry* 83 (2), pp. 223–234. DOI: 10.1016/s0022-3913(00)80016-5.

Winey, Karen I.; Vaia, Richard A. (2007): Polymer Nanocomposites. In *MRS Bull.* 32 (4), pp. 314–322. DOI: 10.1557/mrs2007.229.

Wu, Xiaofang; Liu, Siyu; Chen, Kai; Wang, Fengyan; Feng, Cunao; Xu, Linmin; Zhang, Dekun (2021): 3D printed chitosan-gelatine hydrogel coating on titanium alloy surface as biological fixation interface of artificial joint prosthesis. In *International journal of biological macromolecules* 182, pp. 669–679. DOI: 10.1016/j.ijbiomac.2021.04.046.

Wu, Yanan; Lyu, Defu; Chen, Lichao; Ren, Haohao; Yan, Yonggang (2023): High-strength/high-modulus polyvinyl alcohol fiber reinforced poly(amino acid)/hydroxyapatite composite for load-bearing orthopedics applications. In *Polymer Composites* 28, p. 1054. DOI: 10.1002/pc.27250.

Wunnoo, Suttiwan; Paosen, Supakit; Lethongkam, Sakkarin; Sukkurd, Rattanavadee; Waen-Ngoen, Tassanai; Nuidate, Taiyeebah et al. (2021): Biologically rapid synthesized silver nanoparticles from aqueous Eucalyptus camaldulensis leaf extract. Effects on hyphal growth, hydrolytic enzymes, and biofilm formation in Candida albicans. In *Biotechnology and bioengineering* 118 (4), pp. 1597–1611. DOI: 10.1002/bit.27675.

Xu, Zhiqiang; Huang, Junhui; He, Yuqi; Su, Jingjing; Xu, Lin; Zeng, Xiuxia (2022): Fabrication of an ordered micro-/nanotextured titanium surface to improve osseointegration. In *Colloids and surfaces. B, Biointerfaces* 214, p. 112446. DOI: 10.1016/j.colsurfb.2022.112446.

Yahya Rahnamaee, Seyed; Bagheri, Reza; Vossoughi, Manouchehr; khafaji, Mona; Asadian, Elham; Ahmadi Seyedkhani, Shahab; Samadikuchaksaraei, Ali (2022): A new approach for simultaneously improved osseointegration and antibacterial activity by electrochemical deposition of graphene nanolayers over titania nanotubes. In *Applied Surface Science* 580 (4), p. 152263. DOI: 10.1016/j.apsusc.2021.152263.

Ying, Shuaixuan; Guan, Zhenru; Ofoegbu, Polycarp C.; Clubb, Preston; Rico, Cyren; He, Feng; Hong, Jie (2022): Green synthesis of nanoparticles. Current developments and limitations. In *Environmental Technology & Innovation* 26 (1), p. 102336. DOI: 10.1016/j.eti.2022.102336.

Yontar, Arife Kübra; Avcioğlu, Suna; Çevik, Sinem (2022): Nature-based nanocomposites for adsorption and visible light photocatalytic degradation of methylene blue dye. In *Journal of Cleaner Production* 380, p. 135070. DOI: 10.1016/j.jclepro.2022.135070.

Yontar, Arife Kübra; Çevik, Sinem (2023): Effects of Plant Extracts and Green-Synthesized Silver Nanoparticles on the Polyvinyl Alcohol (PVA) Nanocomposite Films. In *Arab J Sci Eng* 5 (1), p. 1. DOI: 10.1007/s13369-023-07643-w.

Yoshida, Ryo; Sakai, Kiyotaka; Okano, Teruo; Sakurai, Yasuhisa (1993): Pulsatile drug delivery systems using hydrogels. In *Advanced Drug Delivery Reviews* 11 (1-2), pp. 85–108. DOI: 10.1016/0169-409X(93)90028-3.

Zare, Yasser; Shabani, Iman (2016): Polymer/metal nanocomposites for biomedical applications. In *Materials science & engineering. C, Materials for biological applications* 60, pp. 195–203. DOI: 10.1016/j.msec.2015.11.023.

Zeng, Haojie; Sun, Feiyun; Zhang, Jianjun; Wang, Ying; Yang, Songwen; Xing, Dingyu (2023): Gradient crosslinking optimization for the selective layer to prepare polyvinyl alcohol (PVA) nanofiltration (NF) membrane. The enhanced filtration performance and potential rejection for EDCs. In *Journal of Membrane Science* 675, p. 121548. DOI: 10.1016/j.memsci.2023.121548.

Zepon, Karine Modolon; Amaral Fetzner Pucci, Caroline do; Hansen, Alana Witt; Moraes, Fernanda Mendes de; Jose Heriberto Oliveria, do Nascimento; Morisso, Fernando Dal Pont et al. (2023): Using sugars as both reducing and cryoprotectants of freeze-dried silver nanoparticles for improving long-term stability. In *Industrial Crops and Products* 197, p. 116519. DOI: 10.1016/j.indcrop.2023.116519.

Zhang, Boxue; Cao, Shengxin; Du, Meiqi; Ye, Xiaozhou; Wang, Yun; Ye, Jianfeng (2019): Titanium Dioxide (TiO2) Mesocrystals. Synthesis, Growth Mechanisms and Photocatalytic Properties. In *Catalysts* 9 (1), p. 91. DOI: 10.3390/catal9010091.

Zhang, J.; Wang, Q.; Wang, A. (2010): In situ generation of sodium alginate/hydroxyapatite nanocomposite beads as drug-controlled release matrices. In *Acta biomaterialia* 6 (2), pp. 445–454. DOI: 10.1016/j.actbio.2009.07.001.

Zhang, Mingyue; Biesold, Gill M.; Choi, Woosung; Yu, Jiwoo; Deng, Yulin; Silvestre, Clara; Lin, Zhiqun (2022): Recent advances in polymers and polymer composites for food packaging. In *Materials Today* 53 (11), pp. 134–161. DOI: 10.1016/j.mattod.2022.01.022.

Zhang, Zhijie; Wu, Yunping; Wang, Zhihua; Zou, Xueyan; Zhao, Yanbao; Sun, Lei (2016): Fabrication of silver nanoparticles embedded into polyvinyl alcohol (Ag/PVA) composite nanofibrous films through electrospinning for antibacterial and surface-enhanced Raman scattering (SERS) activities. In *Materials science & engineering. C, Materials for biological applications* 69, pp. 462–469. DOI: 10.1016/j.msec.2016.07.015.

Zhao, Zhi-Yuan; Li, Pei-Jun; Xie, Run-Sheng; Cao, Xing-Ye; Su, Dong-Lin; Shan, Yang (2022): Biosynthesis of silver nanoparticle composites based on hesperidin and pectin and their

synergistic antibacterial mechanism. In *International journal of biological macromolecules* 214, pp. 220–229. DOI: 10.1016/j.ijbiomac.2022.06.048.

Zhu, Guang; Wang, Guocheng; Li, Jiao Jiao (2021): Advances in implant surface modifications to improve osseointegration. In *Mater. Adv.* 2 (21), pp. 6901–6927. DOI: 10.1039/D1MA00675D.

Zvezdanović, Jelena; Petrović, Sanja; Savić, Saša; Cvetković, Dragan; Stanojević, Ljiljana; Stanojević, Jelena; Lazarević, Aleksandar (2021): Phenolics and mineral content in St. John's wort infusions from Serbia origin. An HPLC and ICP-OES study. In *Chem. Pap.* 75 (6), pp. 2807–2817. DOI: 10.1007/s11696-021-01521-1.

CURRICULUM VITEA

Arife Kübra YONTAR received her BE and ME degrees in Materials Science and Engineering from Ondokuzmayıs University in 2015 and 2018, respectively. She worked as a research assistant at Ondokuz Mayıs University, Department of Metallurgical and Materials Engineering between 2017-2020. She has been working as a Lecturer at Ondokuzmayıs University Yeşilyurt Demir Vocational School since 2020. Her current research interests include the green synthesis of inorganic nanoparticles and fabrication of nanocomposite systems for a wide range of application areas such as biomaterials, green photocatalytic materials, biocompatible coating, thin films and renewable energy. During her graduate and undergraduate education, she worked on the welding applications and corrosion behavior of Ti-6Al-4V, aluminum and steel metal materials, as well as the production of ceramic materials and waste management.

Contact Information :

ORCID ID : 0000-0003-1486-9332

Publications:

1. Arife Kübra Yontar and Sinem Çevik, Effects of Plant Extracts and Green-Synthesized Silver Nanoparticles on the Polyvinyl Alcohol (PVA) Nanocomposite Films. *Arab J Sci Eng* (2023). https://doi.org/10.1007/s13369-023-07643-w .
2. Arife Kübra Yontar, Sinem Çevik and Onur Yontar, Green production of plant/collagen-based antibacterial polyvinyl alcohol (PVA) nanocomposite films. *Sustainable Chemistry and Pharmacy* Volume 33, (2023), https://doi.org/10.1016/j.scp.2023.101119 .
3. Arife Kübra Yontar, Suna Avcıoğlu, Sinem Çevik, Nature-based nanocomposites for adsorption and visible light photocatalytic degradation of methylene blue dye, *Journal of Cleaner Production*, Volume 380, Part 2, (2022), 135070, ISSN 0959-6526, https://doi.org/10.1016/j.jclepro.2022.135070 .
4. Çevik, S., Mutuk, T., Oktay, B.M. et al. Mechanical and microstructural characterization of cement mortars prepared by waste foundry sand (WFS). *J Aust Ceram Soc* 53, 829–837 (2017). https://doi.org/10.1007/s41779-017-0096-9
5. Mutuk, T, Demirbaş, AK, Çevik, S, Mesci Oktay, B. The effects of casting ındustry waste of scale ınstead of cement on the mechanical and microstructure properties. *Int J Appl Ceram Technol.* (2019); 17: 197– 204. https://doi.org/10.1111/ijac.13400
6. Arife Kübra Demirbaş and Sinem Çevik, S. Regulatory Policies For Safety Of Nanomaterials . *Open Journal of Nano* 5 (2020): 1-16 https://dergipark.org.tr/en/pub/ojn/issue/52691/637652

7. Arife Kübra Demirbaş and Sinem Çevik, TİG Kaynak Yöntemiyle Birleştirilmiş Alüminyum 1050 Alaşımının Mekanik Ve Mikroyapı Özellikleri, *Academic Platform - Journal of Engineering and Science*, vol. 8, no. 3, pp. 471-477, Sep. (2020), https://doi.org/10.21541/apjes.644267
8. Arife Kübra Demirbaş and Sinem Çevik, Eco-Friendly And Nature-Based Polymer Composites , *September 2022, Cooperation for Climate and Green Deal Symposium*, (Samsun), (Oral Presentation-Abstract Paper).
9. Arife Kübra Demirbaş and Sinem Çevik , Structural Analysis Of Carbon Steels Joined Withdifferent Welding Methods By Ultrasonic Testing, *September 2019, 4.The International Porous and Powder Materials Symposium and Exhibition*, (Marmaris), (Oral Presentation-Full Text Paper).
10. Arife Kübra Demirbaş, Sinem Çevik, Tuğba Mutuk and Suna Avcıoğlu, The Effect Of Waste Foundry Sand On The Densificatıon Of Cement Mortars, *September 2018, II. International Congress on New Trends in Science, Engineering and Technology*, (Roma), (Oral Presentation-Full Text Paper).
11. Arife Kübra Demirbaş and Sinem Çevik, Investigation Of Laser Welding Application Of Ti-6al-4v Alloy Used In Dental Applications, *September 2018, II. International Congress on New Trends in Science, Engineering and Technology*, (Roma), (Oral Presentation-Abstract Paper).
12. Arife Kübra Demirbaş and Sinem Çevik, Ultrasonic Testing Of Aluminum Alloys Joined With Different Welding Methods, *September 2018, II. International Congress on New Trends in Science, Engineering and Technology*, (Roma), (Oral Presentation-Abstract Paper).
13. Effects Of Steel Sector Wastes To Cement Production," *September 2017, 3rd International Porous and Powder MaterialsSymposium and Exhibition* , (Marmaris), (Oral Presentation-Full Text Paper).
14. Arife Kübra Demirbaş and Sinem Çevik, Laser Welding of Ti Alloys for Dental Applications MicrostructuralCharacterization, *September 2017, 1st International Symposium on Multidisciplinary Studies and Innovative Technologies*, (Tokat), (Oral Presentation-Abstract Paper).
15. Arife Kübra Demirbaş and Sinem Çevik, Demir Ve Demir Dişi Metal Döküm Endüstrisi İçin Atik Yönetimi, September 2017, 1st International Symposium on Multidisciplinary Studies and Innovative Technologies Proceedings (Tokat), (Oral Presentation-Full Text Paper).
16. Dental Uygulamalarda Kullanilan Ti-6al-4v Alaşiminin Lazer Kaynak Uygulamasinin İncelenmesi, November 2017, *1 International Academicresearch Congress*, (Antalya), (Oral Presentation-Full Text Paper).

Patents

1. Arife Kübra YONTAR and Sinem ÇEVİK, Production of Biopolymer Materials Containing Nanoparticles and Plant Extracts Produced by Green Synthesis for Health Field, 2021/020092, (30.12.2022).(Patented).
2. Arife Kübra YONTAR and Sinem ÇEVİK, Photocatalytic Plant Extracts-Containing Polymer Composite Material, 2022/012579, (09/08/2022), (Applied).
3. Sinem ÇEVİK, Arife Kübra YONTAR, Büşra BİRATEŞ and Suna AVCIOĞLU, An Environmentally Friendly Flexible And High Strength Ceramic Composite Material And Its Production Method, 2022/020555, (26.12.2022), (Applied).

Projects

1. Sinem ÇEVİK and Arife Kübra YONTAR, 1904- B- Doctoral Thesis Projects-OMÜ, Coating of Dental Metallic Materials with Plant Extract Added Biocompatible Polymers, PYO.MUH.1904.22.028, (2023-2025).
2. Sinem ÇEVİK and Arife Kübra YONTAR, 1908 Scientific R&D Support Program Projects, Sağlık alanı için yeşil sentezle üretilen nanopartikül ve bitki özü içeren biyopolimer film malzemesi üretimi, PYO.MUH.1908.21.00, (2022-2023).
3. Sinem ÇEVİK and Arife Kübra YONTAR , 1908 Scientific R&D Support Program Projects, Bitki özleri ve kolajen içeren yeşil içerikli gıda ambalaj film üretimi, PYO.MUH.1908.22.024, (2022-2023).
4. Onur YONTAR, Sinem ÇEVİK, Arife Kübra YONTAR and Murat AYDIN, 1908 Scientific R&D Support Program Projects, Polivinil Alkol(PVA)-Yeşil Sentezlenmiş Nano Gümüş katkılı, doğal içerikli filtre kağıdı üretimi, PYO.MUH.1908.22.037, (2022-2023).
5. Sinem ÇEVİK, Arife Kübra YONTAR, Büşra BİATEŞ and Suna AVCIOĞLU, 1908 Scientific R&D Support Program Projects, Medikal sektörü için doğal içerikli paketleme malzemelerinin üretimi ve karakterizasyonu, PYO.MUH.1908.22.074, (2022-2024).
6. Özgür DEMİRCAN, Mevlüt GÜRBÜZ, Suna AVCIOĞLU, Abdurrahman YILDIZ, Arife Kübra YONTAR and Naser REZAEİ, 1901-Scientific R&D Support Program Projects, Karbon Nano Tüp-Grafen Nano Parçacıklı (CNT-GNP) elyaf takviyeli termoplastik kompozitlerin arayüzey özelliklerinin iyileştirilmesi ve otomotiv ve havacılık sektörlerinde uygulamalarının araştırılması, PYO.MUH.1901.18.008, (2018-2022).
7. Sinem ÇEVİK, Pınar UYAN, Suna AVCIOĞLU, Arife Kübra DEMİRBAŞ, Ömer ANDAÇ and Mevlüt GÜRBÜZ, 1901-Scientific R&D Support Program Projects, LED Paketleme Sistemleri için AlN İnce Film Kaplamaların Elektro-sprey Biriktirme Yöntemi ile Üretimi ve Isıl Özelliklerinin İyileştirilmesi, PYO.MUH.1901.18.006, (2018-2021).
8. 1906-Research Infrastructure Support Program Projects, Improvement of Materials Science and Engineering Laboratories, PYO.MUH.1906.19.001, (2019-2020).

Won Awards, Incentives and Scholarships

1. Arge Maraton Project Ideas Contest, 2nd place award, YEDAŞ and Ondokuz Mayıs University Technology Transfer Office, 2023.
2. ISIF 23 International Invention Fair / Silver Medal, Turkish Patent and Trademark Authority, TURKEY.
3. ISIF 22 International Invention Fair / Silver Medal, Turkish Patent and Trademark Authority, TURKEY.
4. Graduation with the First Place in the Department of Materials Science and Engineering, 2015, Ondokuz Mayıs University, TURKEY.
5. Ondokuz Mayıs University, Faculty of Engineering, Honors Degree, TURKEY.